University of Alberta

The role of mitochondria in cancer development and hypoxia adaptation

by

Nicole Salloum

A thesis submitted to the Faculty of Graduate Studies and Research in partial fulfillment of the

requirements for the degree of *Master of Science*

Department of *Oncology*

Edmonton, Alberta
Fall 2005

Your file Votre référence
ISBN: 0-494-09278-5
Our file Notre référence
ISBN: 0-494-09278-5

DEDICATION

For my Mom

Diane Salloum
1942-1999

In loving memory

ABSTRACT

The focus of this thesis was on the role of mitochondria in tumorigenesis. The first project involved the development of a rapid screening method for the detection of mtDNA mutations in Complex I of the electron transport chain (ETC), in order to study the correlation between Complex I mtDNA mutation and prognosis of cervical cancer patients. The second project involved studying hypoxia adaptation in malignant glioma cell lines. According to Hochachka's model of hypoxia tolerance, normal cells adapt to low oxygen conditions in two phases: metabolic depression followed by the induction of hypoxia-responsive gene expression. We postulated that in cancer cells cytochrome *c* oxidase could play a role in metabolic adaptation to hypoxia, and proceeded to look for differences in enzyme activity and subunit expression levels among previously characterized hypoxia-tolerant and hypoxia-sensitive glioblastoma cell lines. The final project involved a preliminary study of neuroglobin expression in malignant glioma cell lines.

ACKNOWLEDGEMENTS

I would like to thank my supervisor, Dr. Joan Turner, for being an exceptional role model. Some day I hope to be as knowledgeable and well-respected in my chosen field of study. I also hope to have as many interests outside of that field.

Thank you also to the members of my supervisory committee, Dr. Moira Glerum and Dr. Matthew Parliament, for helping to guide me on this journey.

The collaborative spirit of this department means I have many people to thank. First and foremost, thank you to the members of the Turner lab, past and present (Brent Altheim, Bonnie Andrais, Ivy Ma, Jason Han, Jason Wong, Katherine Leung, and Carrie DeHaan). You made coming to work a joy, even on the most challenging days. Thank you also to Roseline Godbout for all your advice and encouragement, and to the Godbout and Spencer labs for your answers to my many technical questions.

I owe a special debt of gratitude to Tanya Gillan and Anne Galloway: thank you for your friendship, advice, and laughter.

Finally, thank you to my (growing!) family: Dad, Kathi, Simone and Erin. I couldn't have done this without your love and support.

TABLE OF CONTENTS

LIST OF TABLES

LIST OF FIGURES

LIST OF ABBREVIATIONS

(H)	heart
(L)	liver
°C	degrees Celsius
6-FAM	6-carboxyl fluorescein
A_{260}	absorbance at 260 nm
ADP	adenosine diphosphate
AICA	5-aminoimidazole-4-carboxamide
AMP	adenosine monophosphate
AP-2	activator protein-2
ARNT	aryl hydrocarbon receptor nuclear translocator
ATP	adenosine triphosphate
BCA	bicinchoninic acid
BNIP-3	BCL2/adenovirus E1B 19kDa interacting protein 3
bp	base pair
BSA	bovine serum albumin
CBP	CREB binding protein
cDNA	complementary deoxyribonucleic acid
$CoCl_2$	cobalt chloride
Cox	cytochrome *c* oxidase
C_T	threshold cycle
Cu	copper

Cy	cyanine dye
Dfx	Deferoxamine
DHPLC	denaturing high performance liquid chromatography
D-loop	displacement loop
DMEM/F12	Dulbecco's modified minimum essential medium plus Ham's F12 medium
DNA	deoxyribonucleic acid
dNTP	deoxynucleoside triphosphate
dsDNA	Double stranded deoxyribonucleic acid
e^-	electron
EF5	2-(2-nitro-1H-imidazol-1-y1)-N-(2,2,3,3,3-pentafluoropropyl)acetamide
EGFR	epidermal growth factor receptor
ETC	electron transport chain
FBS	fetal bovine serum
FGF2	fibroblast growth factor 2
g	gram
GABP	GA binding protein
GAPDH	glyceraldehyde-3-phosphate dehydrogenase
GBM	glioblastoma multiforme
Glut-1	glucose transporter 1
H^+	proton
H2B	histone 2B

Hb	hemoglobin
HGF	hepatocyte growth factor
HIF-1	hypoxia inducible factor 1
His	Histidine
HRE	hypoxia response element
IAZA	iodoazomycin arabinoside
IPTG	isopropylthiogalactoside
K^+	potassium
kb	kilobase pair
kDa	kilodalton
kV	kilovolt
LB	Luria-Bertani media
Mb	myoglobin
MEF2	myocyte-specific enhancer-binding factor-2
min	minute
mL	milliliter
mol	mole
MOPS	4-Morpholinopropanesulphonic acid
mtDNA	mitochondrial DNA
Na^+	sodium
SSC	sodium chloride/sodium citrate buffer
NADH	nicotinamide adenine dinucleotide hydride
ng	nanogram

Ngb	neuroglobin
nm	nanometer
NRF	nuclear respiratory factor
O/N	overnight
pO_2	partial pressure, oxygen
ODN	oligodeoxynucleotide
OXPHOS	oxidative phosphorylation
PBS	phosphate buffered saline
PCR	polymerase chain reaction
PDGF	platelet derived growth factor
pH	log of $[H^+]$
pRb	retinoblastoma protein
PTEN	Phosphatase and Tensin homolog deleted on chromosome Ten
Redox	oxidation-reduction reactions
RF	replicative form
RNA	ribonucleic acid
ROS	reactive oxygen species
RPS27A	ribosomal protein S27a
SCID	severe combined immunodeficiency
SNP	sodium nitroprusside
Sp1	specificity protein 1
ssDNA	single stranded deoxyribonucleic acid
SURE	Stop unwanted rearrangement events

Tet	tetracycline
TN	turnover number
UTR	untranslated region
VEGF-A	vascular endothelial growth factor A
VHL	von Hippel-Lindau
WBC	white blood cell
X-gal	5-bromo-4-chloro-3-indolyl-bD-galactoside
$\Delta\psi$	membrane potential
µFD	microfaraday
mg	microgram
µL	microliter
µm	micrometer

CHAPTER 1: INTRODUCTION

1.1 Malignant Gliomas

1-1.1. Classification of Gliomas

Primary malignant brain tumors occur at an incidence of approximately 15 per 100,000 (Jansen *et al.,* 2004). Malignant gliomas are the most common type of brain tumor among adults. They are classified according to their hypothesized cell type of origin, either as astrocytomas, oligodendrogliomas, or oligoastrocytomas. Within the astrocytoma family, tumors are further categorized based on their histology and prognosis. Patients with low-grade astrocytomas (grade II) can survive for as long as 10-15 years (Holland, 2001). Patients with higher grade anaplastic astrocytomas (grade III) typically survive for 2-3 years (Holland, 2001). The most prevalent and aggressive astrocytoma is glioblastoma multiforme (GBM) (grade IV) (Jansen *et al.,* 2004). Median survival time for patients with this tumor type is less than one year.

Histologically, GBM is characterized by vascular proliferation and regional necrosis (Holland, 2001). The tumor cells invade the adjacent normal brain tissue and migrate through the white matter to collect around blood vessels and neurons (Holland, 2001). The highly invasive nature of GBM makes it very difficult to treat. After more than 30 years of research, standard treatment for this tumor is still macroscopic resection, followed by radiotherapy and chemotherapy (Jansen *et al.,* 2004). Despite aggressive therapy, there has been almost no significant improvement in survival time (Jansen *et al.,* 2004).

1-1.2. Gliomagenesis

Much work has been devoted to understanding the biology of gliomagenesis so that more effective adjuvant treatments can be designed. Genetic and biochemical studies have indicated that gliomas arise via a multi-step pathogenic process. GBM can either arise from a lesser-grade astrocytoma or *de novo* (Ichimura *et al.,* 2004). The inactivation of cell cycle checkpoint pathways, such as the p53 and pRb pathways, is common in astrocytomas (Ichimura *et al.,* 2004). Disruption of the PI3/Akt pathway is also common. Growth factors, such as PDGF and FGF2, and receptor tyrosine kinases, such as EGFR, are often over-expressed, resulting in the disruption of downstream signal transduction pathways. Allelic loss of the PTEN tumor suppressor seems to be a critical step in the progression from astrocytoma to glioblastoma (Jansen *et al.*, 2004). Inactivation of PTEN results in elevated Akt activity and increased VEGF-A expression.

Deregulated control of angiogenesis is one of the hallmarks of GBM, and signals the beginning of an aggressive growth phase (Brat and Mapstone, 2003). As mentioned above, genetic mutations such as PTEN inactivation can result in increased angiogenesis. The hypoxic tumor microenvironment of GBM has been suggested to promote an angiogenic switch. Hypoxia is a potent stimulator of VEGF expression via the hypoxia-regulated transcription factor, HIF-1. Hypoxia also promotes increased stability of the VEGF mRNA. It has been observed in some studies that the tumor cells surrounding regions of necrosis in GBM express levels of VEGF two hundred to three hundred times that of serum concentrations (Takano *et al.,* 1996). Interestingly, a recent study using EF5 binding to measure hypoxia found a positive correlation between tumor hypoxia and

clinical outcome, with the more aggressive GBM tumors showing more severe hypoxia (Evans *et al.,* 2004).

However, not all studies indicate extensive hypoxia in GBM. For example, Urtasun *et al.* (1996), using the hypoxia imaging agent iodoazomycin arabinoside (IAZA), showed no uptake of the marker in 11 patients with GBM. This was in contrast to other tumor types, including small cell lung cancer and squamous cell carcinoma of the head and neck, which were positive for the marker (Urtasun *et al.*, 1996). These observations led to further studies using human glioma cell lines grown as tumor xenografts in nude mice and rats, where hypoxic regions of the tumors were labeled with [3H]misonidazole (Parliament *et al.,* 1997). The binding pattern of the misonidazole varied among the xenografts, with some xenograft sections showing large regions of necrosis surrounded by cells heavily labeled with the hypoxia marker, while other xenografts had large regions of necrosis surrounded by cells only lightly labeled (Parliament *et al.*, 1997). Such clinical and experimental data raise the possibility that at least a subset of GBM cells possess the ability to adapt to hypoxia.

1-2 Oxygen Tension and Normal Physiology

Oxygen homeostasis is important for the normal functioning of tissues and organs (Michiels, 2004). The optimal oxygen tension for different tissues varies depending on the tissue in question; for example, lung tissue is normally exposed to atmospheric oxygen concentrations (20.9%), while the liver is exposed to much lower oxygen concentrations (2-8%) (Papandreou *et al.,* 2005). Precise control of oxygen tension within a narrow range can be vital for proper fetal development and tissue differentiation

(Graham *et al.,* 2000). For example, a low oxygen environment is necessary for the proper functioning of trophoblast cells in developing placenta (Graham *et al.,* 2000). The role of trophoblasts is to penetrate the placenta and invade the mother's uterus in order to modify the uterine blood vessels so that maternal blood flow is increased to the placenta (Graham *et al.,* 2000). *In vitro* experiments by Graham and colleagues (2000) demonstrated that cultured trophoblast cells showed increased invasiveness through reconstituted basement membrane under low oxygen conditions that mimicked the placental environment (1% O_2) in comparison to normal culture conditions (21% O_2). This suggests that low oxygen levels in the placenta during the first trimester are essential for normal placental invasion and development (Graham *et al.*, 2000).

The maintenance of proper oxygen levels is also important for tissue differentiation. For example, a recent study of retinal blood vessel development in newborn mice suggested that moderate hypoxia (10% O_2) reversibly disrupts artery-vein differentiation (Claxton and Fruttiger, 2005). Hypoxia was shown to prevent the expression of several artery-specific genes in the retinal vessels, as well as to increase the expression of venous endothelial cells (Claxton and Fruttiger, 2005). In turn, this resulted in the disruption of the vascular morphology, as seen by the reduction of capillary-free zones around arteries, the presence of double-layered capillary networks, and the crossing of capillaries over veins (Claxton and Fruttiger, 2005).

Since physiological oxygen tensions vary widely depending on the developmental state and type of tissue in question, hypoxia cannot be defined by a single value (Papandreou *et al.,* 2005). Instead, hypoxia is defined as an inadequate supply of oxygen that compromises normal biological processes (Shannon *et al.,* 2003). Hypoxia can arise

as a result of physiological conditions such as exercise or high altitude, or it can result from pathophysiological conditions such as disrupted vasculature in solid tumors (Papandreou *et al.,* 2005).

1-3 Hypoxia and Cancer

1-3.1. The Tumor Microenvironment

The tumor microenvironment is often considered hostile, being characterized by regions of transient or chronic hypoxia, low extracellular pH and nutrient deprivation (Raghunand *et al.,* 2003). Hypoxia develops in a tumor when rapidly growing tumor cells outstrip their oxygen supply. Most tumors larger than 1 mm^3 in volume contain regions of hypoxia (Shannon *et al.,* 2003). Hypoxia in tumors can arise from several different mechanisms. Diffusion-related or chronic hypoxia occurs when tumor cells grow beyond the oxygen diffusion limit of the nearest blood vessel (Vaupel and Harrison, 2004) (Figure 1-3.1). Recent measurements suggest that the diffusion distance of O_2 in tumors is approximately 80 μm (Raghunand *et al.,* 2003). In contrast, perfusion-related or acute hypoxia is caused by inadequate blood flow to the tumor (Vaupel and Harrison, 2004) (Figure 1-3.1). This is common in solid tumors as their blood vasculature is often disorganized and unevenly distributed, resulting in blood flow that is sluggish and intermittent (Siemann, 1998). Anemia-related hypoxia is the result of the blood's reduced capacity to carry oxygen due to treatment or tumor related anemia (Vaupel and Harrison, 2004). In reality, the reason for a tumor's hypoxic status is not due solely to one of the three scenarios listed above. The tumor microenvironment is complex and

varied, and there are regions of both chronic and acute hypoxia that can change due to tumor growth and the behavior of the tumor vasculature (Bussink *et al.,* 2003).

As a result of their disorganized vasculature, tumors generally have lower oxygen tensions than normal tissue (Vaupel and Harrison, 2004). A study measuring oxygen concentrations in head and neck tumors and adjacent normal tissue with polarographic oxygen electrodes showed that the median pO_2 of normal subcutaneous tissue adjacent to a tumor is approximately 7.0%, with no part of the tissue being below 1.4% O_2 (Brown, 1999). The median pO_2 of a head and neck tumor is much lower at approximately 1.4%, with half the regions of the tumor exhibiting a pO_2 less than 1.4% (Brown, 1999). Under physiological conditions, arterial pO_2 is approximately 13% and venous pO_2 is approximately 5% (Erecinska and Silver, 2001).

Studies of cervical cancer show that the extent of hypoxia within a tumor is independent of tumor size, stage, histopathological type, or grade of malignancy (Vaupel and Harrison, 2004). This does not seem to hold true for all cancers as recent studies of gliomas demonstrated a correlation between tumor grade and degree of hypoxia (Evans *et al.,* 2004).

The tumor microenvironment is acidic for several reasons. Hypoxic tumors produce greater amounts of lactic acid as a result of increased glycolysis (Raghunand *et al.,* 2003). The chaotic nature of the tumor vasculature prevents the effective removal of lactic acid and of protons that have been exported from tumor cells that are trying to maintain intracellular pH levels (Raghunand *et al.,* 2003). Also, hypoxia leads to the increased expression of carbonic anhydrases which catalyze the reversible hydration of CO_2 to carbonic acid (Shannon *et al.,* 2003).

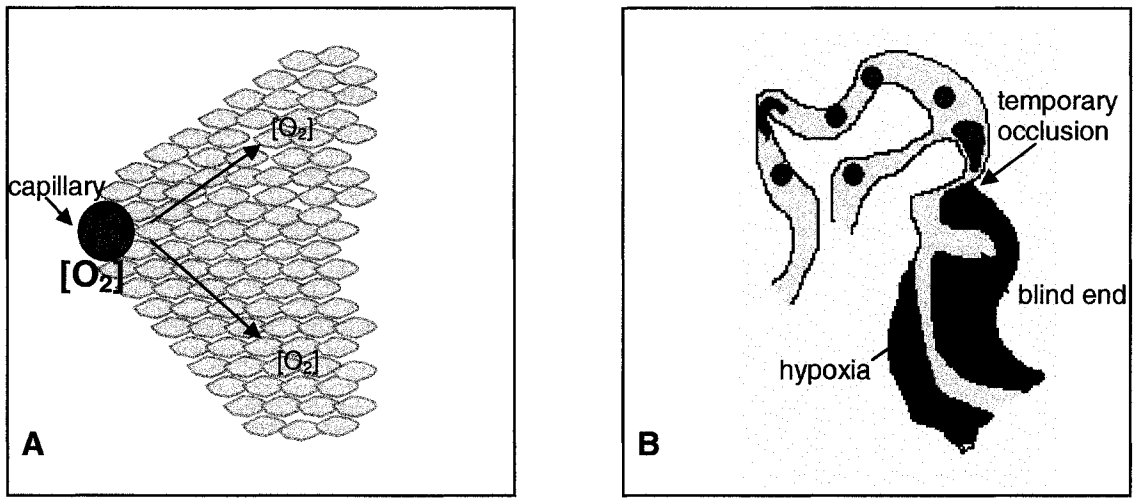

Diffusion-limited Perfusion-limited

Figure 1-3.1. Mechanisms for the development of tumor hypoxia. (**A**) Diffusion-limited hypoxia arises when tumor cells grow beyond the O_2 diffusion limit of the nearest capillary. (**B**) Perfusion-limited hypoxia is common in tumors because of their malformed and chaotic tumor vasculature. Blood flow is often sluggish or intermittent as a result of the formation of blind ends or temporary occlusions. This results in acute and/or chronic hypoxia. Adapted from Brown and Wilson (2004).

1-3.2. The effect of hypoxia on tumorigenesis

The malignant progression that is associated with tumor hypoxia is mediated by several mechanisms, including genomic instability, changes in gene expression, and clonal selection. Reynolds and colleagues (1996) used a tumorigenic cell line with a recoverable lambda-phage shuttle vector, which was designed to identify mutations without the need for a selection-based genetic assay, to study the effect of the tumor microenvironment on genomic instability. They compared the mutation frequency of cells grown either in culture or as tumors in nude mice, and found that the mutation frequency of the tumors was five times that of the cultured cells (Reynolds *et al.,* 1996). Further experiments showed that when the cultured cells were grown in hypoxic conditions their mutation rate became elevated and showed a similar pattern to that of the

tumor xenografts, thus demonstrating the mutagenic properties of the tumor microenvironment (Reynolds *et al.,* 1996).

It is estimated that approximately 1.5% of the genes in the human genome can respond to changes in oxygen tension via hypoxia-responsive transcription factors (Leo *et al.,* 2004). The cellular response can either hinder tumor growth through apoptosis or necrosis, or it can promote tumor growth through processes that allow the tumor to adapt to the hostile microenvironment, such as metabolic adaptation, angiogenesis, invasion, and oxygen delivery (Leo *et al.,* 2004; Hockel and Vaupel, 2001). Many different signal transduction cascades are initiated during both physiological and pathological hypoxia. The most well studied cascade involves the HIF-1 transcription factor.

HIF-1 is a heterodimer, consisting of an alpha- and a beta-subunit. The HIF-1β subunit, also known as aryl hydrocarbon receptor nuclear translocator (ARNT), is constitutively expressed. The HIF-1α subunit is stably expressed in the absence of oxygen. In the presence of oxygen, HIF-1α is hydroxylated at key proline residues by prolyl hydroxylases and as a result, targeted for ubiquitination via the von Hippel-Lindau (VHL) protein (Figure 1.3-2). Stabilization of the HIF-1 protein allows it to activate the expression of over thirty hypoxia-regulated genes. In order to activate gene expression, HIF-1 also interacts with the coactivator CBP/p300 in a hypoxia-dependent manner. HIF-1 binds to conserved gene sequences, termed hypoxia response elements (HREs) in the promoter regions of target genes. Increased HIF-1 protein levels are found in approximately half of malignant tumors, including colon, breast, glioblastoma, lung, and prostate, compared to the respective normal tissues (Acker and Plate, 2002). It is important to note that HIF-1 not only activates genes involved in the promotion of

tumorigenesis, such as VEGF and Glut-1, but also genes with anti-tumorigenic functions, such as BNIP-3, and cyclin G_2 (Acker and Plate, 2002). Thus, the role of HIF-1 in tumorigenesis is more complicated than is often suggested.

Many of the genes that are expressed under hypoxic conditions are those that are necessary for the promotion of a more malignant phenotype. This explains in part why studies of cervical cancer, head and neck cancer, and sarcomas have shown that tumor hypoxia is a negative prognostic indicator, regardless of treatment (Hockel *et al.,* 1996).

A recent study by Pennacchietti and colleagues (2003) focused on the expression and activity of c-Met, a receptor for hepatocyte growth factor (HGF) that is upregulated in response to hypoxia. c-Met is part of a signal transduction pathway that stimulates increased cell motility and production of proteases that destroy the extracellular matrix (Pennacchietti *et al.,* 2003). Both of these processes are necessary for metastasis. Studies such as these provide a mechanistic link between the expression of hypoxia-responsive genes and metastasis

Graeber and colleagues (1996) demonstrated that hypoxia could act as a physiological selective pressure for the survival of apoptosis-resistant, $p53^{-/-}$ cells in a tumor. They exposed a mixed population of transformed $p53^{+/+}$ and $p53^{-/-}$ cells to several rounds of hypoxia and aerobic recovery, and found that the percentage of $p53^{-/-}$ cells increased by 2.4 fold following each treatment (Graeber *et al.,* 1996). *In vivo,* hypoxia also selected for the survival of apoptotic resistant, p53 mutant cells, which led to a more malignant tumor phenotype (Graeber *et al.,* 1996). The selective pressure exerted by hypoxia leads to the clonal expansion of tumor cell variants with adaptations favorable to survival under hypoxic conditions (Vaupel and Harrison, 2004). The expansion of these

clones can, in turn, exacerbate tumor hypoxia; this leads to a vicious circle of increasing hypoxia and subsequent malignant progression (Vaupel and Harrison, 2004).

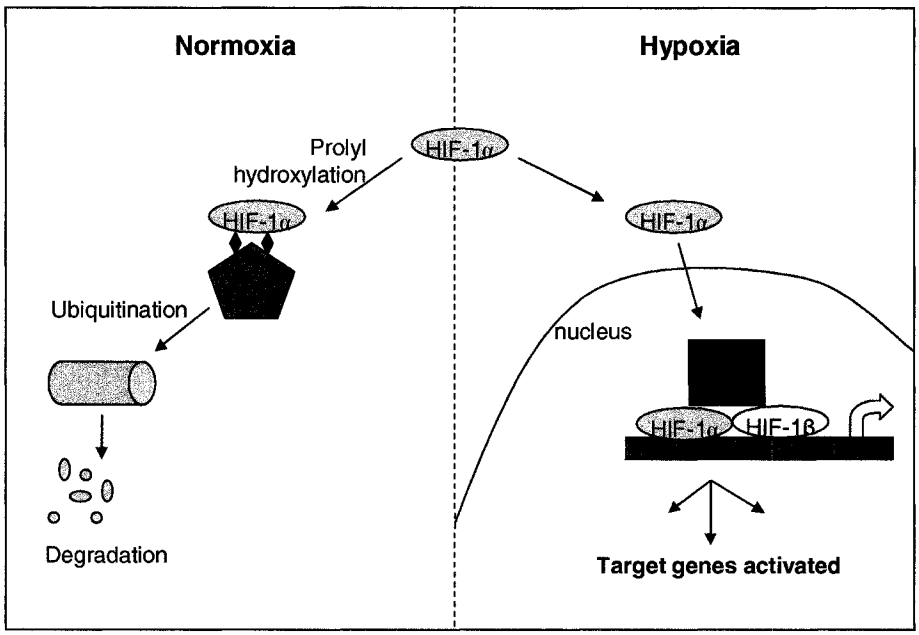

Figure 1-3.2. Oxygen-dependent control of the HIF-1 transcription factor. Adapted from Ratcliffe *et al.* (2000).

1-3.3. The effect of hypoxia on treatment

Hypoxia has been termed a double-edged sword in the battle against cancer. On the one hand, starving a tumor of oxygen and nutrients as a means of stopping its growth has won wide support and led to the development of antiangiogenic therapies (Bottaro and Liotta, 2003). On the other hand, the presence of hypoxic microregions in a tumor has been correlated to poor treatment outcome and increased risk of metastasis (Leo *et al.*, 2004).

Hypoxia can modify cellular response to radiotherapy and certain chemotherapies. It has been known for many years that hypoxic cells can be up to three

times less sensitive to the killing effects of ionizing radiation. Radiosensitivity is diminished under low oxygen conditions because oxygen serves to "fix" the DNA damage caused by free radicals, such as hydroxyl radicals (Brown, 1999). Since oxygen is extremely electrophilic, it is able to react with the DNA free radicals produced by the ionizing radiation to make them permanent (Brown, 1999). Without oxygen, much of the DNA damage can be repaired by the cell, in a process called restitution, whereby DNA free radicals are reduced by donation of H^+ from non-protein sulfhydryls, such as glutathione (Brown, 1999). Studies have suggested that resistance to radiotherapy occurs when the median pO_2 of the tumor is between 0.07 - 2.8%, an oxygen range that is very common in the hypoxic regions of solid tumors (Bussink *et al.*, 2003).

Chemotherapy resistance is a common feature of hypoxic tumors. This resistance occurs for a number of reasons: (1) The drug may not reach all areas of the tumor because of the poorly formed tumor vasculature or due to the diffusion limitations of the drug. (2) Chemotherapeutic drugs are often targeted towards rapidly proliferating cells as they act mainly during DNA synthesis to cause DNA damage; however, the cells in hypoxic tumor microregions divide more slowly and under severe hypoxia are arrested in the G_1/S phase so they may not be targeted by the drug (Shannon *et al.*, 2003). (3) Many chemotherapeutic agents, such as doxorubicin and carboplatin, require oxygen for activation (Hockel and Vaupel, 2001). (4) Tissue acidosis, which is quite common in hypoxic microregions, can impact drug efficacy. (5) Hypoxic tumor cells often express elevated levels of genes, such as dihydrofolate reductase, that confer drug resistance to agents such as adriamycin or cisplatin (Rice *et al.*, 1986). (6) Hypoxia selects for cells

with reduced apoptotic potential which can result in increased drug resistance (Shannon *et al.*, 2003).

Important studies done by Hockel and colleagues in the 1990s clearly showed that hypoxia affects both treatment and tumor progression (Hockel *et al.*, 1996). When treatment response was evaluated, they showed that patients with hypoxic cervical tumors had statistically significant lower overall and disease-free survival compared with patients with non-hypoxic tumors (Hockel *et al.*, 1996). Importantly, survival time of patients with hypoxic tumors was found to be independent of treatment: patients who received surgery alone fared just as badly as patients who received radiotherapy (Hockel *et al.*, 1996). Multiple studies, using various cancer types, have shown pre-oxygenation status of a tumor to be a prognostic indicator of patient outcome (reviewed by Hockel and Vaupel, 2001).

Although hypoxia exerts many negative effects on tumor progression and treatment, hypoxia can be exploited in an attempt to develop treatments that target cancers specifically. One such strategy involves the design of prodrugs that are activated specifically in the absence of oxygen. Tirapazamine is probably the best studied prodrug in this class, and it has been used in several clinical trials in concert with both radiotherapy and chemotherapy (Brown and Wilson, 2004). Under both aerobic and hypoxic conditions, tirapazamine is reduced by various cellular reductases from its non-toxic form to a highly reactive radical that is capable of forming single and double strand DNA breaks (Brown, 1999). In the presence of O_2, the oxygen cycles the electron donated by the reductase, thereby back-oxidizing tirapazamine to its original non-toxic form (Brown, 1999). Gene therapy is another treatment option that is being pursued

preclinically. In this case, a construct is created that has hypoxia-response elements (HREs) in the promoter region of a gene that encodes a prodrug-metabolizing enzyme (Brown and Wilson, 2004). This way the prodrug-metabolizing enzyme is transcribed, and goes on to activate the prodrug, only in hypoxic tissues expressing high levels of the HIF-1 transcription factor (Brown and Wilson, 2004). Another interesting potential therapy that has been studied in mice and humans is the use of genetically engineered *Clostridium*, a non-pathogenic, anaerobic bacterium, to selectively target prodrug-metabolizing enzymes to necrotic, hypoxic regions of tumors (Brown and Wilson, 2004). Most hypoxia targeted therapies are still in their infancy; however, evidence suggests that these strategies produce an additive effect when they are used in tandem with conventional therapies (Brown and Wilson, 2004). The use of hypoxia-targeted therapy will continue to increase as the therapies continue to be engineered to be more efficient and specific.

1-4 Hypoxia Adaptation

All cells in the body have the ability to sense and adapt to hypoxia to some degree. Systemically, the body is able to sense and respond to oxygen deficit through increased ventilation and cardiac output to ensure appropriate amounts of oxygen continue to be delivered to tissues (Michiels, 2004). Erythropoietin expression is increased in order to increase the production of red blood cells for O_2 delivery. Angiogenesis is also promoted in order to expand the vasculature and improve oxygen carrying capacity in the heart and brain (Poyton, 1999). At the cellular level, adaptation

to hypoxia is achieved by consolidating ATP supply and demand, and upregulating the expression of hypoxia-responsive genes. This is described in more detail below.

1.4-1. Hochachka Model of Hypoxia Adaptation

Comparative physiologists have been studying how animals adapt to conditions of low oxygen availability for many years. A common anoxia-tolerant model organism is the western painted turtle, or *Chrysemys picta.* These turtles are able to survive dives in anoxic water for up to 2 days at 25°C (Suarez *et al.,* 1989). By comparing the biochemical properties of the brains of these anoxia-tolerant turtles with anoxia-sensitive animals, such as rats, scientists gain a better understanding of the survival strategies used by anoxia-tolerant organisms (Suarez *et al.*, 1989). For example, it has been determined that anoxia-tolerant turtles use glucose at a rate six-fold lower than anoxia-sensitive rats (Suarez *et al.*, 1989). This implies that the ATP turnover in turtles is at least six fold lower than that in rats (Suarez *et al.*, 1989). Also, anoxia-tolerant turtles exhibit Na^+/K^+/ATPase activity that is at least two-fold lower compared to anoxia-sensitive rats (Suarez *et al.,* 1989). Suarez and colleagues (1989) postulated that the low metabolic rate and the reduced ion flux in the turtle brains could be mechanisms that allow anoxia-tolerant turtles to survive long periods without oxygen. Calorimetric studies done with hepatocytes from anoxia-tolerant turtles showed that the heat flux, and therefore metabolism, of the hepatocytes was rapidly suppressed by 76% under anoxic conditions (Buck *et al.,* 1993).

Studies of hibernating frogs have shown that an important strategy for surviving low oxygen (3% O_2) conditions is to reduce the activity of the electron transport chain and thereby reduce the amount of proton leak across the inner mitochondrial membrane

(St. Pierre *et al.,* 2000). A reduction in proton leak means that more protons are available for the generation of the proton gradient necessary for driving ATP synthase. This in turn means that oxygen is being used more efficiently (St. Pierre *et al.,* 2000). When the rate of proton leak was compared between hypoxia-tolerant frogs and hypoxia-sensitive rats, it was determined that frog skeletal muscle mitochondria exhibited three-fold less proton leak than comparable tissue in the rat (St. Pierre *et al.,* 2000).

The Unifying Theory of Hypoxia Tolerance is the culmination of many such studies (Figure 1-4.1) (Hochachka *et al.,* 1996). Here, Hochachka and his colleagues suggest that hypoxia-tolerant organisms, and specifically their cells, adapt to oxygen lack in two phases. The first phase, termed the defense phase, is one of metabolic adaptation, during which ATP supply and demand is suppressed to a new steady-state level (Hochachka *et al.,* 1996). The major ATP-demand pathways, such as protein synthesis, protein degradation, Na^+/K^+ pumps, and glucose biosynthesis are down-regulated. For example, the rate of proteolysis is reduced by 94% in turtle hepatocytes (Hochachka *et al.,* 1996). The relative importance of the down-regulation of ATPase ion pumps compared with other ATP-utilizing systems is related to the degree of sensitivity of a cell type to hypoxia (Michiels, 2004). Cells that rely heavily on ATPase pumps for normal functioning are less likely to meet energy demands under oxygen limiting conditions, resulting in cell death (Michiels, 2004). As ATP-demand pathways are down-regulated, ATP-supply pathways are made more efficient. The net result is that the yield of ATP per mol of oxygen is maximized (Hochachka *et al.,* 1996). In fact, it has been found that when hypoxia-tolerant cells encounter oxygen lack they are able to suppress their energy

turnover by a factor of almost 10-fold. In other words, one mole of ATP could sustain these cells for 10 times longer than under normal conditions (Hochachka *et al.,* 1996).

Metabolic adaptation is an important strategy for short-term survival; however, long-term survival requires the induction of a second phase of hypoxia-adaptation: the rescue phase, so termed because it involves the rescue of protein synthesis for a select group of proteins (Hochachka *et al.,* 1996). First, key transcription factors, such as HIF-1, are upregulated. As a result, hypoxia-sensitive genes involved in maintaining cellular processes under prolonged hypoxia are expressed (Hochachka *et al.,* 1996). These proteins are involved in such processes as glycolysis, glucose uptake, oxygen transport, and angiogenesis (Figure 1-4.1).

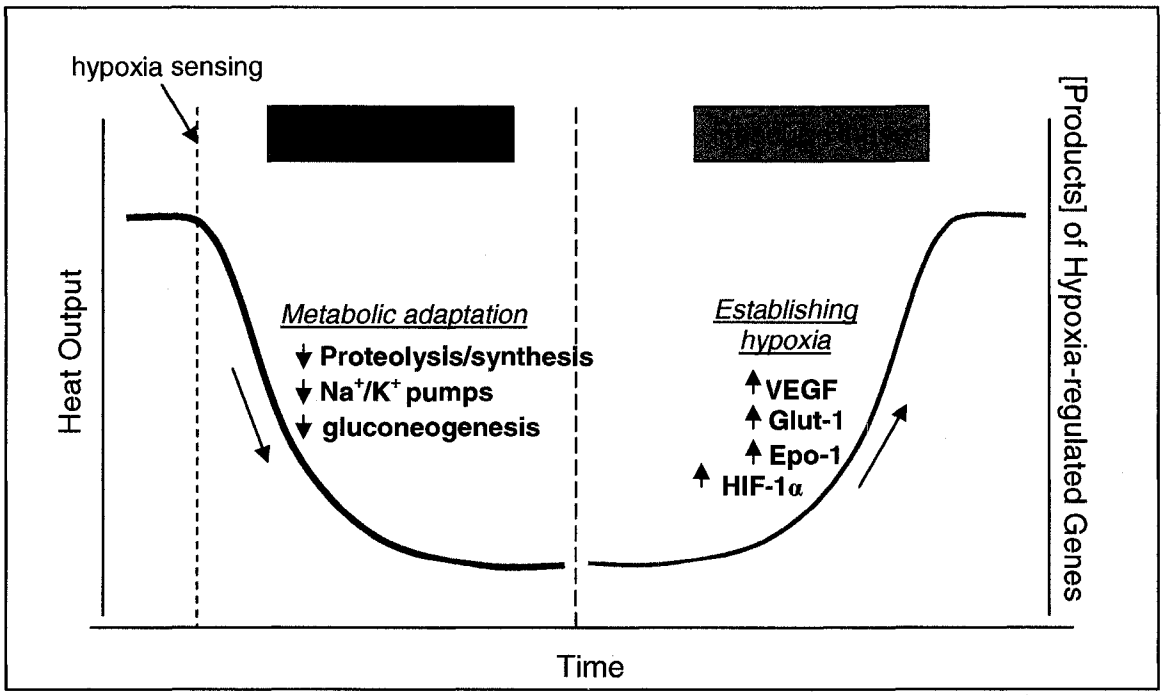

Figure 1-4.1. Hochachka's unifying theory of hypoxia tolerance. Adapted from Hochachka *et al.* (1996).

1-4.2. Tumor metabolic adaptation to hypoxia

Although the Hochachka model for hypoxia adaptation was developed by studying comparative physiology, it has great relevance to the study of tumor adaptation to hypoxia. The first step in the Hochachka model of hypoxia adaptation is metabolic adaptation, where ATP supply and demand are coordinately down-regulated. Increasing evidence suggests that tumors must undergo similar metabolic adaptation in order to continue their aggressive growth. A recent report by Swinnen *et al.* (2005) showed that the energy status of the cancer cell regulates its ability to proliferate, form colonies, invade, and migrate. Though this study does not deal with hypoxia directly, it illustrates the importance of metabolic regulation in cancer development. Since the energy status of a cell is reflected by the ratio of ATP/AMP, the researchers mimicked a low energy state in two cancer cell lines by adding 5-aminoimidazole-4-carboxamide (AICA), a nucleoside analog that mimics the effects of AMP (Swinnen *et al.,* 2005). Addition of the compound resulted in reduced levels of lipid, protein, and DNA synthesis (Swinnen *et al.,* 2005). Furthermore, when they tested downstream cell functions such as cell proliferation, cell survival, colony formation, migration, and matrix invasion, they found that these tumor-associated end-points were reduced in all treated cells (Swinnen *et al.,* 2005). When they looked at the effect of the low energy status *in vivo*, the group found that the AMP mimetic compound reduced tumor growth in nude mice compared to untreated controls (Swinnen *et al.,* 2005).

Since metabolic regulation is so important to cancer development, it is imperative that cancer cells be able to modulate their metabolism in response to stressful situations such as when nutrients or oxygen are limited. There is evidence to suggest that cancer

cells have a greater ability to respond and adapt to hypoxia compared with normal cells. A study of normal and transformed breast cancer cell lines demonstrated that transformed MCF-7 cells were able to down-regulate protein synthesis in response to severe hypoxia, and maintain viability, while normal HME breast cells were not (Guppy *et al.,* 2005). Clearly, metabolic adaptation is extremely important for cancer growth.

Tumor cells are most often characterized as being highly glycolytic. This observation was first made by Otto Warburg over fifty years ago (Warburg, 1956). He observed that mouse cancer cells produced more lactic acid than normal murine liver and kidney cells under air-saturated conditions (Zu and Guppy, 2004). He hypothesized that cancer cells generate a greater proportion of their ATP using aerobic glycolysis instead of oxidative phosphorylation, since lactic acid production is a hallmark of glycolysis (Zu and Guppy, 2004). Therefore, he suggested that tumors have an inherently glycolytic metabolism, and depend strongly on glucose and glutamine as fuels (Guppy *et al.*, 2002). This perception has played a strong role in guiding subsequent research; however new evidence suggests that tumors are not inherently glycolytic (Zu and Guppy, 2004).

A recent paper by Zu and Guppy (2004) challenges the idea of a Warburg effect in cancer cells. They suggest that many of the subsequent papers that supported Warburg's conclusions were misleading because the studies did not calculate a 'minimal energy budget' (Zu and Guppy, 2004). The minimal energy budget is a calculation of oxygen consumption and lactate production so that total oxidative ATP production and total glycolytic ATP production are determined (Zu and Guppy, 2004). They note that a common pitfall in many studies is to compare the rates of glycolysis between normal and cancer cells without measuring oxygen consumption, and therefore total oxidative ATP

production (Zu and Guppy, 2004). Without having a measure of total ATP production, it is impossible to know the contribution glycolytic ATP production makes to the generation of total ATP (Zu and Guppy, 2004). Another common mistake in many of the studies is to measure only glucose-based oxidative ATP production. This underestimates total oxidative ATP production because the contribution from other fuels, such as fatty acids, is not included (Zu and Guppy, 2004).

When Zu and Guppy (2004) compared the metabolism of normal and cancer cells from a set of previously published studies that calculated the minimal energy budget, they found that there was no significant difference in the glycolytic contribution to total ATP production between normal and cancer cells in room air. Furthermore, when Guppy and colleagues compared the contribution of aerobic glycolysis to oxidative phosphorylation in normal and MCF-7 breast cancer cells, they found that ATP production was 80% oxidative and 20% glycolytic for both cell types (Guppy *et al.,* 2002). Therefore, under aerobic conditions, tumor cells generate the same proportion of ATP from glycolysis as normal cells.

Even though tumors are not inherently glycolytic, there is evidence that under hypoxic conditions, tumor cells do increase their rate of anaerobic glycolysis (Zu and Guppy, 2004). This is known as the Pasteur Effect. It is important to note that although the Pasteur Effect is effective during short term hypoxia, the large quantities of fuel required to sustain this pathway make it impossible for long-term hypoxic survival (Guppy *et al.*, 2005).

1-4.3. Oxidative Metabolism and Hypoxia Adaptation

Although it is known that glycolysis is increased in hypoxic cancer cells, less is known about how oxidative phosphorylation (OXPHOS) is affected. High throughput screening of genes differentially expressed in normal and tumor gastric tissue has identified several OXPHOS genes that are upregulated in tumor tissue (Jung *et al.*, 2000). These genes include ATPase synthase subunit e, NADH-ubiquinone oxidoreductase, NADH dehydrogenase, and cytochrome *c* oxidase subunit II (Jung *et al.*, 2000). These findings mirror earlier work done with rat hepatoma cells that shows increased expression of genes coding for some subunits of ATP synthase and of cytochrome *c* oxidase (Capuano *et al.*, 1997). Genes involved in oxidative phosphorylation could be upregulated in order to meet the high metabolic demands of the tumor (Jung *et al.*, 2000). The role of cytochrome *c* oxidase in tumor metabolism is of particular interest because it plays a central role in oxidative phosphorylation. It has been hypothesized that increasing glycolytic flux and altering the kinetics of cytochrome *c* oxidase are two ways in which hypoxic cells could maintain adequate ATP levels during tumor growth (Vijayasarathy *et al.*, 2003).

Several studies suggest that an increase in the expression of genes involved in oxidative phosphorylation leads to increased tumor aggressiveness (Hermann *et al.*, 2003). For example, a study by Hermann *et al.* (2003) found a correlation between the malignancy of prostate cancer tissue specimens and the ratio of nuclear-encoded to mitochondrial-encoded subunits of cytochrome *c* oxidase. Specifically, there was an increase in the ratio of nuclear- to mitochondrial-encoded subunits in all prostate cancer specimens examined compared to matched normal cells (Hermann *et al.*, 2003).

Furthermore, the larger ratio appeared early in tumor progression, and increased with tumor progression (Hermann *et al.,* 2003). The authors hypothesized that increased expression of the nuclear-encoded subunits could affect cytochrome *c* oxidase activity, and alter oxidative metabolism (Hermann *et al.,* 2003). These observations have been recapitulated in other types of cancer, suggesting that changes in oxidative metabolism could be a feature common to many cancers.

A further study by this group correlated the increased ratio of nuclear-encoded to mitochondria-encoded Cox subunits to an increase in hexose monophosphate shunt metabolism relative to glycolytic metabolism passing through the Krebs cycle in several different cell lines (Kreig *et al.,* 2004). In other words, the shift in Cox subunit expression levels seems to correlate with changes in metabolic function that could be necessary for tumorigenesis (Kreig *et al.,* 2004).

A recent study by Vijayasarathy *et al.* (2003) looked specifically at how the expression of Cox subunits and the activity of the holoenzyme were affected by hypoxia in various mouse cell lines. They observed a decrease in subunit expression in both mitochondria- and nuclear- encoded subunits that appeared to be due to a decrease in the rate of transcription (Vijayasarathy *et al.,* 2003). The effect of hypoxia on enzyme efficiency was dependent on cell type (Vijayasarathy *et al.,* 2003). Under hypoxic conditions the PC12 cell line exhibited an increase in catalytic efficiency: the heme content of the enzyme dropped but its activity remained the same. Macrophages showed no change in enzyme efficiency in response to hypoxia (Vijayasarathy *et al.,* 2003). These results suggest that at least some cell lines were able to respond to the decrease in

oxygen availability by altering their Cox enzyme activity through changes in subunit expression.

Though the above mentioned studies seem to suggest that an increase in oxidative phosphorylation is a component of tumorigenesis, Simmonet and colleagues (2002) hypothesize the opposite: namely that a decrease in the OXPHOS capacity of tumors favors faster growth and increased invasiveness. This would occur because the substrates that are normally targeted for oxidation to CO_2 would instead be directed towards biosynthesis (Simonnet *et al.*, 2002). They studied several different grades of renal carcinoma taken from kidney biopsies, and showed that cytochrome *c* oxidase activity decreased with increasing tumor malignancy (Simonnet *et al.*, 2002). They suggest that the series of genetic events that occur during tumor progression could impart specific metabolic profiles on the tumors (Simonnet *et al.*, 2002). Specifically, they speculated that inactivation of the VHL tumor suppressor gene could cause the observed changes in tumor metabolism (Simonnet *et al.*, 2002). Clearly there is still much debate on the roles oxidative phosphorylation in general, and cytochrome *c* oxidase in particular, play in tumorigenesis.

One feature of cytochrome *c* oxidase that suggests it could adapt to changing oxygen availability is the presence of different Cox isozymes in tissues with different energy demands and substrate availabilities. These isozymes are comprised of subunits that are expressed as tissue- and development-specific isoforms, which change the catalytic properties of the holoenzyme. The structure and function of the Cox enzyme will be discussed in more detail in the following sections.

1-5 Cytochrome *c* oxidase

1-5.1. Cytochrome *c* oxidase structure and function

Cytochrome *c* oxidase plays a central role in oxidative phosphorylation. The low reserve of Cox capacity observed both *in vitro* and *in vivo* indicates that Cox exerts tight control of respiration (Villani and Attardi, 2000). This complex multi-subunit membrane protein is the terminal component of the electron transport chain. Its function is to catalyze the transfer of four electrons from ferrocytochrome *c* to oxygen, while at the same time pumping protons across the inner mitochondrial membrane, from the matrix to the cytoplasmic side. The enzyme has four redox-active metal centers (heme a, heme a_3, Cu_A, and Cu_B) that are involved in electron transfer. Electrons move from cytochrome *c* through Cu_A and heme a to the binuclear reaction center, comprised of heme a_3 and Cu_B, where oxygen is reduced to water (Burke and Poyton, 1998). It is not clear how electron transfer is coupled to proton pumping, though it has been suggested that the redox status of Cox confers different conformations to the binuclear reaction center, which allows the coupling of electron and proton movement (Burke and Poyton, 1998).

The Cox enzyme is of ancient origin, and is found in both prokaryotes and eukaryotes (Grossman and Lomax, 1997). In a subset of prokaryotes, the enzyme is made up of three major subunits and a fourth smaller subunit (Grossman and Lomax, 1997). In eukaryotes, the enzyme's subunits are encoded by both the mitochondrial and nuclear genomes (Grossman and Lomax, 1997). The three largest subunits are encoded by the mitochondrial DNA, and are homologous to the three largest prokaryotic Cox subunits (Grossman and Lomax, 1997). The remaining subunits are encoded by the

nuclear genome. The number of nuclear encoded subunits increases as the evolutionary complexity of the organism increases (Grossman and Lomax, 1997).

Most of the information on mammalian cytochrome *c* oxidase has come from studying the bovine enzyme. Mammalian Cox is assembled as a dimer, with each monomer composed of thirteen subunits (Figure 1-5.1). CoxI, CoxII, and CoxIII are encoded by the mitochondrial genome, while the other ten smaller subunits (CoxIV, CoxVa, CoxVb, CoxVIa, CoxVIb, CoxVIc, CoxVIIa, CoxVIIb, CoxVIIc, and CoxVIII) are encoded by the nuclear genome. The subunit nomenclature was established based on the order in which the subunits resolve on a gel, and is not meant to indicate any sort of relationship between the subunits (Grossman and Lomax, 1997). The mitochondria-encoded subunits form the catalytic core of the enzyme. CoxII binds cytochrome *c* and both CoxII and CoxI perform the electron transport function of the enzyme (Kadenbach *et al.,* 2000). CoxIII may play a role in proton pumping, or it may be involved in stabilizing the assembly of subunits I and II (Burke and Poyton, 1998). The functions of the individual nuclear-encoded subunits are not well understood. Generally, it is believed that the nuclear-encoded subunits play a role in assembly and modulation of the enzyme's kinetics. Some of the proposed functions of the nuclear-encoded subunits are outlined below. Subunit IV has been found to have an effect on enzyme kinetics via two ATP binding sites: when ATP interacts with the CoxIV subunit, the enzyme's affinity for cytochrome *c* is decreased (Kadenbach *et al.*, 2000). Subunit Va also affects enzyme kinetics: it has a binding site for the thyroid hormone 3,5-diodothyronine (Kadenbach *et al.*, 2000). Binding of the hormone results in increased enzyme activity (Kadenbach *et al.*, 2000). Subunit VIb may play an inhibitory role, as its removal from the holoenzyme

results in increased enzyme activity (Vijayasarathy *et al.*, 1998). It is not yet clear how the subunits functionally interact with one another to affect the overall enzyme activity.

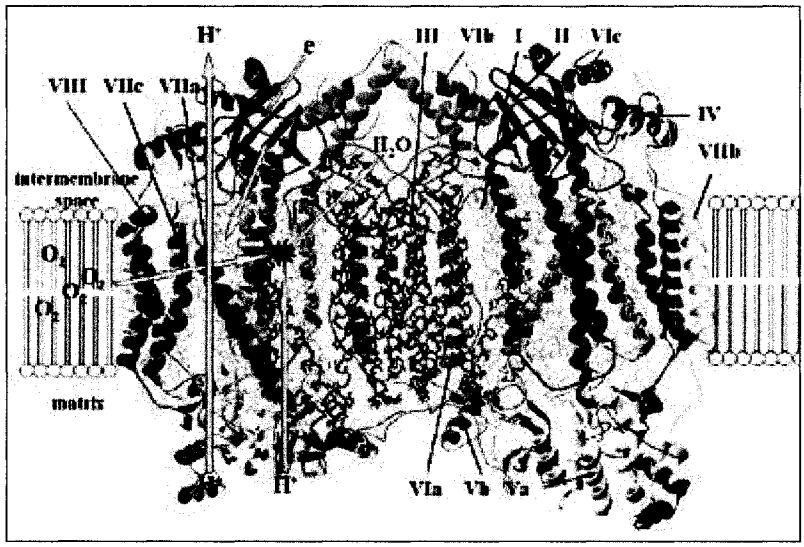

Figure 1-5.1. Bovine cytochrome *c* oxidase crystal structure, from Kadenbach *et al.* (2000).

1-5.2. Cytochrome *c* oxidase subunit isoforms

Additional complexity arises from the fact that several of the nuclear-encoded subunits have isoforms that are expressed in a tissue-specific manner, and are developmentally regulated. The isoforms are encoded by different genes, and arose as a result of gene duplication events. Different animal species possess different combinations of isoforms, and express them differently in various tissues (Grossman and Lomax, 1997). In humans, CoxIV, CoxVIa, and CoxVIIa are expressed in two forms, with CoxVIa and CoxVIIa exhibiting a slightly different pattern of expression than CoxIV. In the heart and skeletal muscle, the heart isoforms of CoxVIa and CoxVIIa (CoxVIaH, CoxVIIaH) are predominantly expressed. The liver isoforms (CoxVIaL, CoxVIIaL) are expressed in all tissues including the heart and skeletal muscle, albeit at

lower levels. For example, in the adult rat heart, Cox is made up of two thirds subunit VIa(H) and one third subunit VIa(L) (Kadenbach *et al.*, 2000). CoxIV-1 is expressed ubiquitously in all tissues, while CoxIV-2 is expressed predominantly in the adult lung, fetal lung and fetal muscle, and to a lesser extent in the adult brain and heart (Huttemann *et al.*, 2001).

The functions of the different isoforms have been studied extensively in both yeast and mammals. The fact that the isoforms have been retained through evolution suggests that the function they provide is advantageous to the organism (Grossman and Lomax, 1997). Since the developing fetus and the various tissues of the body have different energy requirements and oxygen availability, it has been postulated that the developmental and tissue-specific expression of the isoforms confers different enzyme kinetics to the holoenzyme so that Cox can meet the energy demands of a given tissue (Lenka *et al.*, 1998). Studies done in mice show a very clear 'isoform switch' from embryo to neonate. In the embryo the CoxVIa(L) isoform is expressed almost exclusively (Parsons *et al.*, 1996). As development continues into the late fetal stages expression of the heart isoform increases in heart and muscle, but the liver isoform remains the dominant form (Parsons *et al.*, 1996). After birth, CoxVIa(H) expression continues to increase while the liver isoform expression diminishes to nearly undetectable levels (Parsons *et al.*, 1996). It is interesting to note that during development the Cox isoform switch parallels the switch from the relatively hypoxic fetal environment (1.7-4.2% O_2) to the oxic neonatal environment (Land, 2004).

Isoform switching has also been observed *in vitro* during the development of cultured muscle cells (Parsons *et al.*, 1996). Undifferentiated myoblasts express only the

CoxVIa(L) isoform, but when the cells are grown to confluence and shifted to a differentiation medium, the cells form multinucleated myotubes and begin to express the CoxVIa(H) isoform (Parsons *et al.,* 1996). Then, as the myofibers continue to mature, CoxVIa(L) expression becomes downregulated (Parsons *et al.,* 1996). Parsons *et al.* hypothesize that isoform switching occurs during development so that the Cox enzyme is able to match its capacity to generate energy with changing metabolic demands and substrate availability during muscle development (Parsons *et al.,* 1996).

1-5.3. Changes in Cox Catalytic Activity

The presence of different Cox isozymes in tissues with different energy demands and substrate availabilities suggests that the Cox enzyme is capable of adapting to different environments by changing its catalytic properties via changes to the subunits that make up the holoenzyme. Differences in isoform expression are not the only way in which Cox can affect its catalytic activity. Studies have shown that the expression level of various Cox subunits can also impact the catalytic activity of the Cox enzyme (Vijayasarathy *et al.,* 1998). Vijayasarathy and colleagues found that tissues with high oxidative capacity, such as heart and brain, expressed higher levels of CoxIV-1 and CoxVb protein compared with tissues with lower oxidative capacity (Vijayasarathy *et al.,* 1998). They also observed that tissues with high oxidative capacity exhibited a high K_m for cytochrome *c* and a low turnover number (TN), while tissues with low oxidative capacity had lower K_m and higher TN (Vijayasarathy *et al.,* 1998). The TN is the number of molecules of reduced cytochrome *c* converted to oxidized cytochrome *c* by the enzyme per mole of catalytic sites per second.

Oxygen availability exerts a direct effect on the catalytic activity of cytochrome *c* oxidase whereby hypoxia inhibits Cox activity in cardiomyocytes. Chandel and coworkers found that lowering the oxygen concentration in isolated bovine Cox resulted in a decrease in V_{max} and a small increase in the apparent $K_{M,}$ for both cytochrome *c* and oxygen, compared with control enzyme incubated at higher oxygen concentrations (Chandel *et al.,* 1996). They noted that the inhibition of the enzyme occurred only after prolonged hypoxic exposure, and was rapidly reversed when the enzyme was exposed to higher O_2 concentrations (Chandel *et al.,* 1996). Experiments with isolated Cox enzymes are possible because of the long half-life of the enzyme and because the co-factors necessary for enzyme activity remain tightly associated with the enzyme during the purification process. Further experiments identified that the decrease in catalytic activity was due to inhibition of the electron transfer step between heme a_3 and oxygen (Chandel *et al.,* 1996). Chandel and coworkers hypothesize that oxygen regulates the catalytic activity of Cox directly by interacting with the enzyme at a second binding site that is distinct from the binuclear catalytic center (Chandel *et al.,* 1996). Lower oxygen concentrations would cause a slow dissociation of the O_2 from its putative binding site and would result in the enzyme moving towards an inhibited, or conformed, state (Chandel *et al.,* 1996).

Cox activity in osteoclasts has been shown to be controlled by the non-receptor tyrosine kinase c-Src, most likely via phosphorylation of key Cox subunits (Miyazaki *et al.*, 2003). Miyazaki and colleagues (2003) reported that c-Src deficiency resulted in decreased Cox activity in osteoclasts, and that Cox activity was correlated to c-Src kinase activity.

1-5.4. Hypoxia adaptation in yeast

Yeast is often used as a model for studying cytochrome *c* oxidase because it is amenable to both genetic and biochemical manipulation. Also, the yeast Cox is very similar to its mammalian counterpart. It is comprised of twelve subunits, three of which are encoded by the mitochondrial genome and perform the catalytic function of the enzyme (Taanman and Capaldi, 1992). The remaining nine subunits are encoded by the nuclear genome (Poyton, 1999). It has been much easier to determine the functions of the yeast Cox subunits because it is easy to generate mutant yeast strains that lack a particular subunit. The nuclear subunits modulate enzyme activity, and function in the assembly and stability of the holoenzyme (Poyton, 1999). Primary sequence identity shows that all of the yeast subunits have homologs in the mammalian enzyme (Burke and Poyton, 1998). In yeast, the nuclear-encoded subunit V is expressed as interchangeable isoforms Va and Vb, which are encoded by the *COX5a* and *COX5b* genes, respectively (Poyton, 1999). Subunit V is homologous to mammalian subunit IV. The yeast subunit V isoforms are regulated differentially by oxygen (Waterland *et al.,* 1991). Va is expressed under aerobic conditions while Vb is expressed under hypoxic conditions. Oxygen regulates the expression of both isoforms at the level of gene transcription (Burke and Poyton, 1998). When Vb is incorporated into the yeast holoenzyme, the enzyme has a higher turnover rate and faster, more efficient electron transfer within the enzyme (Waterland *et al.,* 1991). This suggests that the isoforms may function allosterically by changing the conformation of the proteins within the holoenzyme and thereby alter the accessibility of the heme moieties to electrons (Waterland *et al.,* 1991). This lends strong support to the hypothesis that the subunit isoforms function to regulate

holoenzyme activity (Waterland *et al.,* 1991). Based on structural models, it appears that the carboxy-terminal domains of both isoforms may be necessary for the transfer of electrons from cytochrome *c* to heme a and/or for the exit of protons from the enzyme (Burke and Poyton, 1998).

1-5.5. A closer look at mammalian CoxIV

Since the mammalian CoxIV subunit is homologous to the yeast subunit V, it is possible that the mammalian CoxIV isoform expression is also regulated by oxygen tension (Grossman and Lomax, 1997). The CoxIV-1 gene is located on chromosome 16 and the CoxIV-2 gene is located on chromosome 20 (Huttemann *et al.,* 2001). The gene structure of the isoforms is similar: both are approximately 8 kb in size, and have 5 exons (Huttemann *et al.,* 2001). The promoter regions of the two isoforms are slightly different in that the CoxIV-1 promoter contains an NRF-2 binding site that is absent in CoxIV-2 (Huttemann *et al.,* 2001). It is believed that there are other regulatory sites on CoxIV-2 that have yet to be identified (Huttemann *et al.,* 2001). The protein sequences also show some interesting differences. The N-termini, which project into the matrix, are highly divergent between CoxIV-1 and CoxIV-2, while the transmembrane region remains conserved (Huttemann *et al.,* 2001). Also, the CoxIV-1 subunit of human, mouse, rat, and cow lacks cysteine residues, while three conserved cysteine residues are present in all the mammalian CoxIV-2 subunits studied to date (Huttemann *et al.,* 2001). Two of the three cysteines are close enough to form a cysteine bond (Huttemann *et al.,* 2001). In the C-terminal domain, CoxIV-2 has a net positive charge that is lacking in the CoxIV-1 subunit (Huttemann *et al.,* 2001).

Several studies have provided clues to the possible function of the CoxIV subunit. The bovine crystal structure shows that CoxIV makes contact with the CoxI and CoxII catalytic subunits, suggesting that CoxIV may play a role in regulating catalytic function (Huttemann *et al.,* 2001). CoxIV is believed to play a role in proton pumping, as proteolysis experiments have shown that when CoxIV is digested with trypsin, there is a reduction in the H^+/e^- ratio (Grossman and Lomax, 1997). The presence of two cysteine residues capable of forming a disulfide bond in CoxIV-2 suggest that this isoform could be subject to conformational changes that could affect enzyme function (Huttemann *et al.,* 2001). For example, CoxI, II, and IV form an ATP binding pocket which ultimately allows the energy status of the cell to be coordinated with Cox activity (Huttemann *et al.,* 2001). This binding pocket could be altered due to a conformational change in the CoxIV subunit which would affect enzyme activity (Huttemann *et al.,* 2001). It is possible that the third conserved cysteine residue could serve as a sensor of the redox state of the cell (Huttemann *et al.,* 2001). Signal transduction based on redox state is well established in other systems (Huttemann *et al.,* 2001). Finally, it appears that CoxIV is important for assembly of the holoenzyme (Nijtmans *et al.,* 1998). Its binding to CoxI is the first step of holoenzyme assembly, and probably represents a rate-limiting step in the assembly of a functional enzyme (Nijtmans *et al.,* 1998).

1-5.6. Gene Structure of the Cox Subunits

CoxI, CoxII, and CoxIII are encoded by the mitochondrial genome. The mitochondrial genome is a double stranded, closed-circular molecule of approximately 16.5 kb. It encodes thirteen polypeptides involved in oxidative phosphorylation, as well as two rRNA genes and twenty two tRNA genes necessary for transcription and

translation of the mitochondrial-encoded proteins (Fernandez-Silva, 2003). mtDNA transcription is initiated at the D-loop, a non-coding control regions of the mtDNA. Transcription is controlled by the mitochondria RNA polymerase and at least three transcription factors, including mtTFA. mtDNA is transcribed as three large polycistronic transcripts that are later processed to yield the individual rRNAs, tRNAs, and mRNAs (Fernandez-Silva, 2003). Since all of the mRNAs are encoded on a polycistronic transcript, they are all made in equal amounts. At this point, it is not clear what effect mRNA turnover has on the steady state levels of mRNA in mammals (Scheffler, 1999). Furthermore, very little is known about the translational regulation of these genes. The mammalian mitochondrial mRNAs lack 5′ or 3′ UTR, and translation factors that could control protein expression have yet to be detected (Scheffler, 1999).

The nuclear-encoded Cox genes range in size from 2 to 10 kb (Lenka *et al.*, 1998). The gene structure of the nuclear encoded Cox subunits is conserved among species (Grossman and Lomax, 1997). All of the nuclear encoded subunits, except for *Cox7a(H)* and *Cox8*, have coding regions that are divided into three exons: one exon encodes the transmembrane domain, and the two remaining exons encode the flanking hydrophilic domains (Grossman and Lomax, 1997). Most of the nuclear encoded subunits have a cleavable presequence for importation into the mitochondria on exon I (Fabrizi *et al.*, 1992). The *Cox7a* liver and heart isoforms have a low level (60%) of sequence homology; however, they show high interspecies homology (80-90%), again suggesting different tissue-specific roles for the isoforms (Lenka *et al.*, 1998).

1-5.7. Control of Cox subunit expression

Much work has gone into understanding how coordinate expression of the Cox genes is controlled. Since the holoenzyme is composed of both mitochondria- and nuclear-encoded subunits, the two genomes must coordinate their expression. Most likely, nuclear genes are responsible for controlling the expression of the mitochondria-encoded genes since they contribute the proteins that are necessary for mitochondrial DNA replication, transcription, and translation (Lenka *et al.,* 1998).

Transcriptional Level

In terms of the individual nuclear-encoded subunits, not all subunit promoter regions have been studied in detail. However, it is apparent that the regulatory pathways are complicated, with each subunit controlled by a unique complement of transcription factors (Table 1-5.7). Almost all of the nuclear-encoded Cox subunits have promoter regions much like housekeeping genes. Instead of having the TATAA element required for tissue-specific transcription, they have GC-rich elements for the binding of such transcription factors as Sp1 and AP-2 (Grossman and Lomax, 1997). Many of the Cox subunits are controlled in part by the same transcription factors, including NRF-1 and NRF-2 (Grossman and Lomax, 1997). NRF-1 binding sites are found in the CoxVb, CoxVIc, and CoxVIIa(L) promoter regions, as well as other OXPHOS genes such as cytochrome *c* and ATP synthase γ subunit (Yu *et al.,* 2002). NRF-1 binding is believed to be regulated by a phosphorylation- dependent pathway (Scarpulla, 1997). Such a pathway could be used to regulate the transcription of target genes in response to the availability of ATP (Scarpulla, 1997). NRF-2, also known as GABP in the mouse, helps activate CoxIV-1, CoxVb, CoxVIIa(L), and CoxVIIc (Grossman and Lomax, 1997).

NRF-2 binding affinity is affected by the redox state of the cell, so it may act as a sensor to alter the expression of its target genes in response to the redox state of the cell (Scarpulla, 1997). Because NRF-1 and NRF-2 can control directly the expression of nuclear genes, and indirectly the expression of mitochondrial genes, it has been suggested that these transcription factors are major integrators of nuclear-mitochondrial interactions (Yu *et al.*, 2002). Some subunits also have thyroid hormone response elements (TREs) in their promoter regions which may mediate hormonal or other physiological control of subunit expression (Bachman *et al.*, 1997). Mutagenesis studies have indicated that promoter activity depends on the interaction of several transcription factors (Yu *et al.*, 2002). The expression of the Cox isoforms is controlled in part by tissue- and development-specific transcription factors (Grossman and Lomax, 1997). For example, CoxVIa(H) is expressed in skeletal muscle because it has three copies of the E-box and a MEF2 enhancer element in its promoter region for the binding of myogenic transcription factors (Grossman and Lomax, 1997). The CoxVIa(L) isoform does not possess such enhancer elements.

Table 1-5.7. Promoter elements of the human nuclear-encoded Cox subunits.

Cox Subunit	Sp1	AP2	NRF1	NRF2	YY1	MyoD	MEF2
IV-1	X			X			
IV-2	X						
Va							
Vb	X	X	X	X			
VIa(L)	X		X	X	X		
VIa(H)	X	X		X		X	X
VIb							
Vic			X				
VIIa(L)			X	X			
VIIa(H)	X			X		X	X
VIIb	X						
VIIc				X			
VIII							

Post-transcriptional Level

CoxVIa isoform expression seems to be controlled post-transcriptionally in different tissues (Thames *et al.,* 2000). As mentioned above, the CoxVIa(H) isoform is predominantly expressed over CoxVIa(L) in the heart and striated muscle. This seems to occur because of tissue-specific differences in mRNA stability between the two isoforms (Thames *et al.,* 2000). In the liver, CoxVIa(L) mRNA has a half-life of approximately twelve hours (Thames *et al.,* 2000). In striated muscle, CoxVIa(L) mRNA has a half-life of 5-6 hours, compared to a half-life of more than 15-20 hours for the CoxVIa(H) mRNA (Thames *et al.,* 2000). The differences in CoxVIa(L) half-lives seem to be due to the presence of tissue-specific destabilization element in the 3′ UTR of CoxVIa(L) mRNA (Thames *et al.,* 2000).

1-6 Cox and the Regulation of Cellular Respiration

As previously mentioned, one of the most important steps during tumorigenesis, particularly in response to hypoxia, is metabolic adaptation. Tumor cells must balance their ATP supply and demand in the face of reduced oxygen availability in order to continue growing. Indirect and direct evidence shows that the Cox enzyme is able to respond and adapt to changing energy demands and substrate availability. This suggests that its expression could have important consequences for tumorigenesis. In this section, the role Cox plays in controlling respiration will be discussed. An emerging model pioneered by Kadenbach and colleagues suggests that cytochrome *c* oxidase per se controls respiration in response to the metabolic demands of the cell. This would make Cox *the* pivotal enzyme of the respiratory chain, and make any changes to the enzyme even more important.

However, first it is necessary to review features of the classic model of respiratory control, the chemiosmotic theory. According to this model, respiration rate is controlled by the electrochemical proton gradient ($\Delta\psi$) across the mitochondrial membrane (Kadenbach *et al.,* 2000). In this model, uptake of ADP into the mitochondria stimulates the ATP synthase. This results in a decrease of $\Delta\psi$, which stimulates the activity of the proton pumps (including Cox), and hence, respiration (Kadenbach *et al.,* 2000) (Figure 1-6).

A second mechanism of respiratory control was recently postulated by Kadenbach and co-workers. Their model suggests that respiration rate can be controlled by the allosteric inhibition of cytochrome *c* oxidase in response to high intramitochondrial ATP/ADP ratios (Kadenbach *et al.,* 2000). Since the energy status of the cell is reflected

by the ATP/ADP ratio, this mechanism effectively couples ATP demand and supply (Kadenbach *et al.,* 2000). Structural studies of bovine Cox confirmed the presence of seven high affinity binding sites for ATP or ADP, and three binding sites for ADP alone (Kadenbach *et al.,* 2000). When the ratio of ATP/ADP rises above a certain level, ATP replaces bound ADP on subunit IV of the enzyme (Kadenbach *et al.,* 2000). This leads to an allosteric change in the enzyme which decreases the efficiency of Cox proton pumping relative to electron transport such that the H^+/e^- stoichiometry is decreased from 1.0 to 0.5 (Ludwig *et al.,* 2001) (Figure 1-6).

The allosteric inhibition of cytochrome *c* oxidase may be regulated by hormones through cAMP-dependent phosphorylation of the enzyme (Kadenbach *et al.,* 2000). In the bovine heart, consensus sequences for cAMP-dependent phosphorylation have been found on subunits I, III, and Vb (Lee *et al.,* 2002). Hormone signaling can also turn off the allosteric inhibition by dephosphorylating the enzyme. The hormone signals come from the thyroid in the form of Ca^{+2} second messengers that activate Ca^{+2} dependent phosphatases (Kadenbach *et al.,* 2000).

Physiologically, this second mechanism of control would be beneficial to the organism (Kadenbach and Arnold, 1999). Since respiration would not be dependent on $\Delta\psi$, the mitochondrial membrane potential could remain at a low and steady state (Kadenbach and Arnold, 1999). This would result in the production of fewer reactive oxygen species (ROS), and as a result less DNA damage (Kadenbach and Arnold, 1999). For the reasons listed above, there is growing evidence that Cox plays an important role in controlling the cell's energy production. Especially important is the realization that the function of the nuclear-encoded subunits could be to act as receptors for nucleotides and

hormones and to respond to such signals with conformational changes that would change the catalytic activity of the holoenzyme (Kadenbach and Arnold, 1999). Indeed, studies have shown enzymes that incorporate the VIa(H) isoform, which has an ATP/ADP binding site, exhibit a decrease in H^+/e^- stoichiometry from 1.0 to 0.5 in response to high intramitochondrial ATP/ADP ratios (Ludwig *et al.*, 2001). This decrease in stoichiometry in response to ATP/ADP ratios is not seen in enzymes with the VIa(L) subunit as it lacks an ATP/ADP binding site (Ludwig *et al.*, 2001).

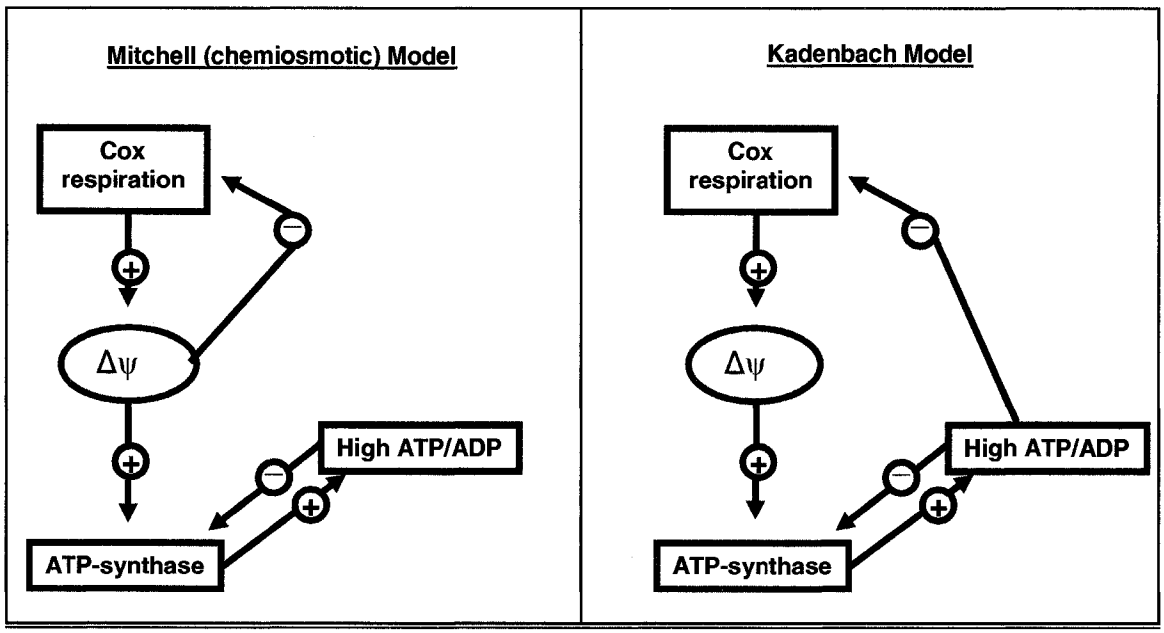

Figure 1-6. Comparison of the Mitchell and Kadenbach models of respiration control. Adapted from Kadenbach, 2003.

1-7 Neuroglobin

A few years ago a new member of the globin superfamily was discovered (Burmester *et al.*, 2000). Neuroglobin (Ngb), so named because it is expressed almost

exclusively in vertebrate brain, appears to be structurally and functionally unique among previously characterized vertebrate globins. Much recent work has gone into characterizing Ngb structure and function, and exciting preliminary data indicates that Ngb is able to protect the brain from experimental stroke *in vivo*.

Ngb is a newly discovered protein localized predominantly in the nerve cells of the vertebrate brain and peripheral nervous system. Ngb is a member of the globin super-family, along with such well-characterized proteins as hemoglobin (Hb) and myoglobin (Mb). It was discovered by screening the databases of anonymous mouse and human complementary DNAs for globin-like sequences (Burmester *et al.*, 2000). Globins are small respiratory proteins, capable of reversibly binding O_2 by means of an Fe-containing porphyrin ring (Pesce *et al.*, 2002). They are an important part in the respiratory systems of a wide variety of taxa, including bacteria, plants, fungi, and animals (Burmester *et al.*, 2000). Though these proteins all possess the classic 'globin fold', they differ widely in structure, tissue distribution and function (Pesce *et al.*, 2002). Hemoglobin is the most well-characterized protein of the globin family; it assembles as a heterodimer and is found in red blood cells. Hb functions to transport oxygen from the lungs to the tissues (Pesce *et al.*, 2002). Mb is a monomer; it is located in cardiac and striated muscle cells and functions to facilitate the delivery of oxygen to the mitochondria and to remove toxic NO (Pesce *et al.*, 2002). Cytoglobin, another newly discovered globin protein, is found in all cell types, and is localized in the nucleus. In mice and rats, Ngb has been identified in nerve cells as well as in non-neuronal cells of the endocrine system and testis (Pesce *et al.*, 2002). It is particularly concentrated in the oxygen rich environment of the retina (Schmidt *et al.*, 2003). *In situ* hybridization studies have localized Ngb specifically to the

cytoplasm (Geuens *et al.*, 2003). Interestingly, Ngb is not the first nerve-based globin to be identified, as annelids, molluscs, and other members of the invertebrate taxa also possess nerve globins (Burmester *et al.*, 2000). Phylogenetic analyses indicate a common ancient evolutionary origin among verterbrate Ngb and invertebrate nerve globins (Pesce *et al.*, 2003). In fact, the closest relative of Ngb today appears to be the globins of the annelid, *Aphrodite* (Couture *et al.*, 2001).

The 5800 bp Ngb gene is located on chromosome 14q24 (Pesce *et al.*, 2002). The gene structure of Ngb is different from other globins in that it is comprised of four exons and three introns, while Hbs and Mbs are comprised of only three exons and two introns in their coding regions (Zhang *et al.*, 2002). The Ngb promoter region contains several putative Sp1-binding sites, but lacks a TATAA box motif (Burmester *et al.*, 2000). The 5′ untranslated region of Ngb contains several copies of the HIF-1 consensus binding sequence (Sun *et al.*, 2001). Ngb is assembled as a monomer of 151 amino acids and is approximately 17 kDa in size (Burmester *et al.*, 2000). The structure of Ngb is unique in vertebrates. It possesses only 25% homology with Hb and Mb at the amino acid level, yet still retains key amino acid residues necessary for globin function (Burmester *et al.*, 2000). Sequence conservation between human and mouse Ngb is more conserved than between Ngb and orthologous hemoglobin and myoglobin of the same species (Burmester *et al.*, 2000). All globin proteins are assembled in a classic 'globin fold'; however, coordination of the heme moiety in Ngb is very different from that of Hb or Mb. In general, the globin fold is characterized by a three over three alpha-helix pattern where the heme group is buried in a deep pocket in the protein (Pesce *et al.*, 2002) (Figure 1-7A). The heme is held in place by non-covalent interactions with nearby

protein residues and by a coordination bond between the heme-Fe atom and the 'proximal His' residue. The heme-Fe atom is pentacoordinated in Hb and Mb by four pyrrole N atoms and by the proximal His NE2 atom. Oxygen binds Hb and Mb by forming a sixth coordination bond with the heme Fe. The interaction is stabilized by other interactions with distal protein residues. Ngb is unique in that its heme-Fe atom is hexacoordinated, with the final interaction coming from the 'distal' HisE7 residue (Pesce *et al.*, 2002) (Figure 1-7B). Therefore, O_2 or CO must displace the endogenous protein ligand in order to bind. This affects the affinity of oxygen binding, as O_2 must compete with the distal HisE7 ligand (Hamdane *et al.,* 2003). Another structural difference of Ngb is its large protein matrix cavity (Pesce *et al.*, 2003). Because the free energy requirements of maintaining such a large cavity are high, researchers believe it may have a functional role, such as providing a facilitated O_2 diffusion pathway (Pesce *et al.*, 2003). Alternatively, it may act as a docking/storage station for oxygen during the protein functional cycle, when heme is in the hexacoordinated state (Pesce *et al.*, 2003). Work done by Hamdane and co-workers (2003) indicates that Ngb possesses three cysteine residues, two of which are close enough to form an internal disulfide bond. When the sulfide bonds are broken by mutation or the use of reducing agents, a decrease in oxygen affinity by one order of magnitude is observed in Ngb (Hamdane *et al.*, 2003). It appears that breaking the disulfide bond causes a shift in the position of the neighbouring E-helix, which favourably alters the availability of the endogenous HisE7 ligand for heme hexacoordination (Hamdane *et al.,* 2003).

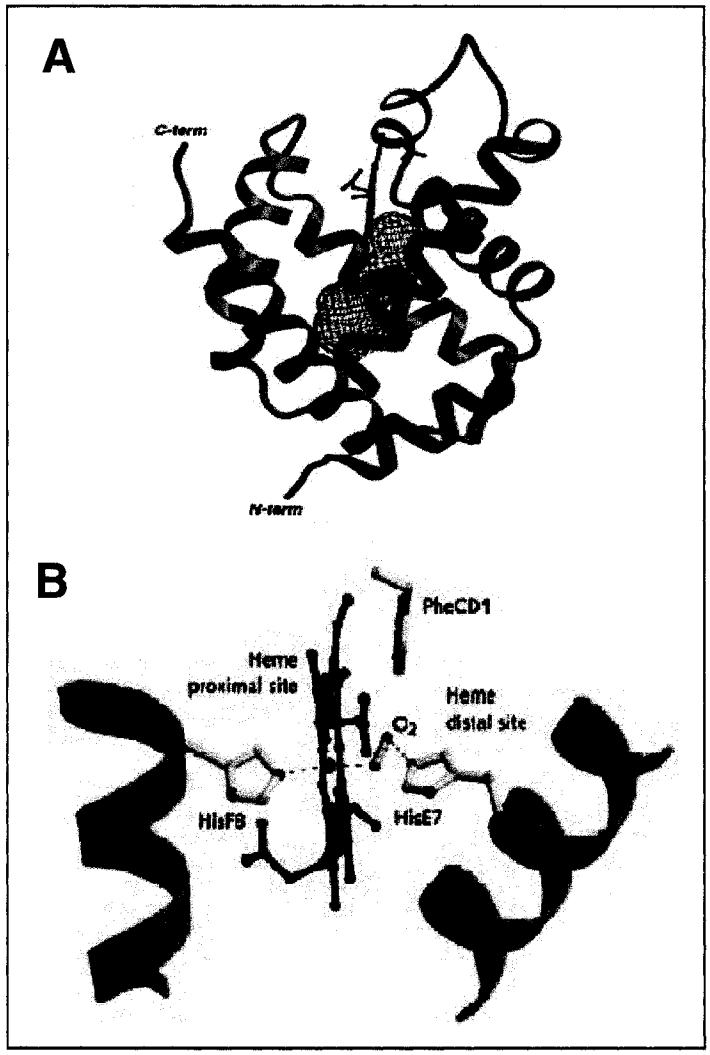

Figure 1-7. Ngb Structure. (**A**) The Ngb schematic fold, showing the large protein matrix cavity (black mesh) (Pesce *et al.,* 2004); (**B**) O_2 must compete with the distal HisE7 to bind the heme-Fe atom (Pesce *et al.,* 2002).

Though Ngb's physiological function is not completely understood, its high affinity for O_2 suggests that it may act as a vehicle for oxygen delivery. Sun *et al.* (2001, 2003) have conducted several interesting *in vitro* and *in vivo* experiments that suggest Ngb acts as a neuroprotective agent during hypoxic stress. They have shown that Ngb expression increases under hypoxic conditions both *in vitro* in cultured neuronal cells and *in vivo* in mouse brain (Sun *et al.,* 2001). They have also shown that Ngb induction is

regulated specifically by hypoxia-signaling pathways. For example, both the deprivation of oxygen and the addition of $CoCl_2$, which acts to mimic hypoxia, resulted in an increase in Ngb expression (Sun *et al.*, 2001). Similarly, the addition of deferoxamine (Dfx), a chemical that acts to increase HIF-1α expression, resulted in higher levels of Ngb. Other stressors such as staurosporine and sodium nitroprusside, a nitric oxide (NO) donor, did not change Ngb expression (Sun *et al.*, 2001). Further proof that Ngb is involved in the protection of neurons was generated when Sun and colleagues blocked Ngb expression with an antisense oligodeoxynucleotide (ODN) and showed that neuronal cell death was increased *in vitro* (Sun *et al.*, 2001). Similarly, when they overexpressed Ngb protein in a neuronal cell line, the result was increased cell viability under hypoxic conditions (Sun *et al.*, 2001). Their work was carried a step further when they proceeded to test the neuroprotective function of Ngb *in vivo*. When Ngb expression in rat brain was reduced by the administration of a Ngb antisense ODN and the rat brains were subjected to focal cerebral ischemia (stroke), there was a 60% increase in infarct volume and neurological deficit in the rats treated with the antisense ODN compared to control rats (Sun *et al.*, 2003). Conversely, rats treated with excess Ngb showed a decrease of 50% in the size of cerebral infarcts compared with control rats (Sun *et al.*, 2003). In this case, Ngb was cloned into an adeno-associated virus (AAV) vector and injected directly into the left cerebral cortex of the rat brains (Sun *et al.*, 2003).

The specific pathways for Ngb induction are not known. However, the presence of several HIF-1 binding sites in the 5′ UTR of the gene, and the increase in Ngb expression in the presence of Dfx suggests that hypoxia may induce Ngb expression through the HIF-1 pathway (Sun *et al.*, 2001).

The manner in which Ngb exerts its neuroprotective effect is also uncertain (Sun *et al.*, 2001). Clues gained from the structural analysis of Ngb may explain its involvement in hypoxia. Ngb may act like Mb and facilitate O_2 delivery to the mitochondria (Pesce *et al.*, 2002). As mentioned above, Ngb possesses two cysteine residues capable of forming a disulfide bond. Under hypoxic conditions, where the cell is accumulating reducing equivalents, the disulfide bond would be reduced and broken (Hamdane *et al.*, 2003). As a result, the distal E7 histidine dissociation rate would lower and oxygen would be released to counteract the hypoxia (Hamdane *et al.*, 2003). Under normoxic conditions, the free cysteines would be oxidized into an intramolecular disulfide bond (Hamdane *et al.*, 2003). This would result in an increase in O_2 affinity and O_2 storage. Although this is only a hypothetical model, it provides a nice link between observed function and structure. Brunori and others (2005) argue that it is unlikely that Ngb plays a role in oxygen storage and transport given its low average concentration. Ngb may alternatively exert its neuroprotective effect by acting as an NADH oxidase to facilitate the glycolytic production of ATP under semi-anaerobic conditions (Pesce *et al.*, 2002), or in NO detoxification (Brunori *et al.*, 2005). It could also be that Ngb is able to sense hypoxia and trigger downstream protective cellular responses (Sun *et al.*, 2001). Indeed, it has been postulated that the large conformational changes that occur in the heme pocket of hexacoordinated globins as a result of ligand binding may trigger signals in downstream regulators (Pesce *et al.*, 2004).

Continued study of Ngb is important because it might represent a target for the development of new treatments for stroke (Sun *et al.*, 2003). Insights into the Ngb's

structural and functional properties might offer hints for developing new therapeutics by either enhancing its activity or regulating its expression (Pesce *et al.*, 2003).

1-8 Research Objectives

In broad terms, our objective was to study the role of mitochondria in tumor cell adaptation to hypoxia. This theme was explored in three independent projects. The first project was focused on the development of an efficient, high throughput mutation screening protocol for the screening of mtDNA Complex I mutations, with the ultimate goal of correlating mtDNA mutation with prognosis in cervical cancer patients. The second project, which comprises the bulk of this work, focused on studying the role of metabolism, and specifically cytochrome *c* oxidase (Cox), in hypoxia adaptation. The third, and smallest, project focused on studying the expression pattern of neuroglobin (Ngb), a newly discovered protein believed to function as a neuro-protective agent in response to ischemia or hypoxia, in malignant glioma and neuroblastoma cell lines.

CHAPTER 2: MATERIALS AND METHODS

2-1 Cell Culture Conditions

The glioma cell lines M010b, M059K, and M006 were derived directly from tumor resections obtained from patients with glioblastoma (Parliament *et al.*, 1997). The M010b cell line was derived from an anaplastic astrocytoma. The M059K cell line was derived from a grade IV astrocytoma. The M006x cell line is a subline of M006, a cell line derived from a grade IV astrocytoma. M006x was established by passaging M006 cells as xenografts in SCID mice, then disaggregating the cells and culturing them as a monolayer (Parliament *et al.*, 1997). The M006xLo subline was derived to be adapted to growth under low oxygen conditions (Franko *et al.*, 1998). It was established from small M006 spheroids that had been exposed continuously to 0.6% O_2 for thirteen days (Franko *et al.*, 1998). The spheroids were disaggregated and the cells were grown as a monolayer for four passages, and then injected subcutaneously in SCID mice. The resultant tumor was disaggregated to yield the M006xLo cell line, which continued to be grown in monolayer culture (Franko *et al.*, 1998). The malignant glioma cell line U87 was a kind gift from the Godbout lab. The human embryonic kidney cell line, EcR293, and the hepatocarcinoma cell line, HepG2, were obtained from the ATCC. All cell lines, except EcR293, were cultured under standard tissue culture conditions in DMEM/F12 media supplemented with 10% FBS and 1% L-glutamine. EcR293 was cultured in DMEM media supplemented with 10% FBS and 1% L-glutamine. All cells were grown in a humidified incubator with 5% CO_2 at 37°C.

The GBM cell lines have been well-characterized in their responses to low oxygen conditions. The M059K, M006x, and M006xLo cell lines are hypoxia-tolerant:

they are able to decrease their oxygen consumption in response to decreasing oxygen availability without the occurrence of significant cell death (Allalunis-Turner *et al.*, 1999). Also, these cell lines retain stable mitochondrial membrane potential and stable intracellular ATP concentrations after three days in hypoxic (0.6% O_2) conditions (Turcotte *et al.*, 2002). The M010b cell line, on the other hand, is hypoxia-sensitive. M010b is unable to modulate its oxygen consumption in response to decreasing oxygen availability (Allalunis-Turner *et al.*, 1999). Furthermore, M010b cells show significant cell death under prolonged hypoxia (Allalunis-Turner *et al.*, 1999). M010b cells exhibited substantial and consistent increases in mitochondrial membrane potential and significantly reduced levels of ATP after three days in hypoxic (0.6% O_2) conditions (Turcotte *et al.*, 2002).

2-2 Creating hypoxic environments

Both a glove box and specially designed aluminum canisters were used to generate hypoxic conditions. Whenever possible, the canisters were used because they were more economical and O_2 concentration could be more precisely regulated. If large numbers of cells were required for a particular experiment, the glove box was used. 0.6% O_2, 5% CO_2, 95% N_2, and 0.01% O_2, 5% CO_2, 95% N_2 were used to mimic mild and severe hypoxia, respectively.

2-2.1. Glove box, Model 818-GB (PLAS Labs):

The glove box replaces a proportion of ambient room atmosphere with 5% CO_2, 95% N_2 to maintain a constant, predetermined O_2 concentration within the chamber (Figure 2-2.1). To operate, the desired O_2 percentage was entered on the control touch pad, and the

N_2 flow turned on. The glove box was used to maintain cells at 0.6% O_2 for 12 hours at 37°C.

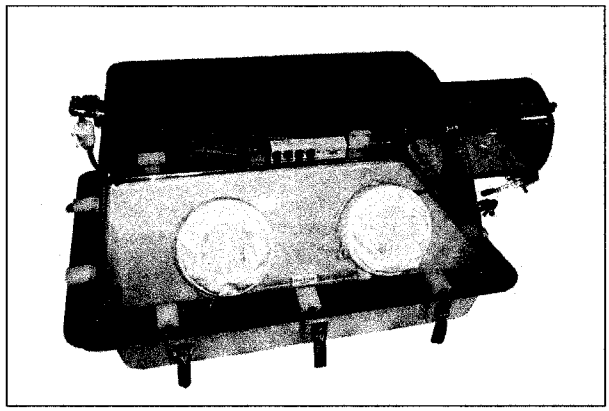

Figure 2-2.1. Glove box, model 818-GB.
From www.geneq.com/catalog/en/bgb.html

2-2.2. Aluminum Gas Canisters

Cells were seeded on glass dishes because unlike plastic, glass does not contain oxygen that could leach back into the overlying medium. The dishes were transferred to the airtight aluminum canisters specially designed to maintain precisely regulated O_2 tension within the chamber (Koch, 1984). The oxygen concentration was decreased by sequentially replacing a proportion of the gas within the canisters with 5% CO_2, 95% N_2 using a precision vacuum gauge and a gas-exchange manifold system. In this way, the O_2 concentration was reduced from 20.9% to 2.5% then to 0.6% or 0.01%. The sealed canisters were then incubated at 37°C for 6 or 12 hours.

2-2.3. Preparation of cells for hypoxic incubation

Glove Box: Briefly, cells were seeded on plastic culture plates and allowed to grow for 48 hours before being placed in the pre-warmed (37°C) glove box. The cells were covered with foil to prevent light from oxidizing the media.

Aluminum canister: Cells were seeded on 60 mm glass dishes and grown for 48 hours at 37°C before being transferred to the canisters.

2-3 Nucleic Acid and Protein Isolation

2-3.1. DNA Isolation

Whole blood from two normal donors was obtained for mtDNA sequencing. The white blood cells were isolated by Ficoll separation. DNA from white blood cells and cell lines was isolated using the Dneasy Kit from Qiagen.

2-3.2. RNA Isolation

Total RNA from cell lines was isolated using the Rneasy Kit from Qiagen. When plastic culture dishes were used for hypoxic incubations, 1 x 10^6 cells/plate x 3 plates were used per cell line. When glass dishes were used for hypoxic incubations, 2 x 10^5 cells/dish x 3 dishes were used per cell line.

2-3.3. Nucleic Acid Quantitation

Nucleic acids were quantified using a DU 7400 spectrophotometer (Beckman). For dsDNA, concentration was calculated by multiplying the A_{260} x 50 μg/mL x the dilution factor. For ssDNA, concentration was calculated by multiplying the A_{260} x 33μg/mL x the dilution factor. For RNA, concentration was calculated by multiplying the A_{260} x 40 μg/mL x the dilution factor.

2-3.4. Protein Quantification

Protein was quantified using the colorimetric BCA Protein Assay Kit (Pierce), according to the manufacturer's protocol. Briefly, 2 μL of cell extract and 98 μL of dH_2O were

added to 2 mL BCA reagent and incubated at 60°C for 30 min. Absorbance readings were measured at OD_{562} and plotted against a BSA standard curve.

2-4 Polymerase Chain Reaction (PCR)

mtDNA fragments were amplified as follows: 20 ng of DNA was amplified in 1X buffer (50 mM KCl, 1.5 mM $MgCl_2$, 10 mM Tris-HCl) (Amersham Biosciences), 400 μM dNTPs, 0.37 mM $MgCl_2$, 0.1 pmol of each forward and reverse primer (Table 2-4), and 1.0 U *Taq* polymerase (Amersham Biosciences). Thermocycling conditions were as follows: 94 °C for 2 min, followed by 35 cycles of 94 °C for 1 min, 55 °C for 1 min, and 1 min at 72 °C, with a final extension at 72 °C for 5 min. All PCR reactions were performed using the 9600 and 2400 GeneAmp PCR System (Applied Biosystems). PCR products were electrophoresed on 1% agarose gels, stained with ethidium bromide, and viewed using a Dual Light Transilluminator.

2-5 Automated DNA Sequencing

The entire mtDNA genomes from two normal WBC samples were sequenced to be used as normal controls during heteroduplex analysis. Table 2-4 lists the primers used to generate the 15 overlapping fragments that make up the mitochondrial genome. Table 2-5 lists the primers used to sequence the individual fragments. The following general sequencing procedure was performed:

DNA fragments were amplified by PCR and purified using the QIAquick PCR purification kit (Qiagen). Purified DNA was quantified and 100 ng was used for the sequencing reaction, along with 12.8 pmol PCR primer and 8.0 μL Big Dye Terminator

Ready Reaction Mix (Applied Biosystems) in a final volume of 20 µL. Reactions were overlaid with mineral oil. Cycle sequencing was performed using the following conditions: 96°C for 46 sec, 50°C for 51 sec, 60°C for 250 sec, for 25 cycles using the RoboCycler 40 (Stratagene). DNA was transferred to a new tube and ethanol precipitated with 80 µL of 60% ethanol. Samples were incubated at room temperature for 15 min, then centrifuged at 14000 rpm for 20 min at room temperature. The supernatant was aspirated and the pellets washed with 250 µL of 70% ethanol. Again the samples were centrifuged at 14000 rpm for 10 min at room temperature, and the supernatant was aspirated. The pellets were dried for 4 min at 90°C on a heating block, then resuspended carefully in 25 µL Template Suppression Reagent (TSR) and incubated at room temperature for 30 min. Samples were heated to 95°C for 5 minutes, placed on ice to cool, vortexed briefly, then returned to ice for 10 minutes. The samples were transferred to 310 septa tubes and placed in the 310 ABI Prism Genetic Analyzer (Applied Biosystems) for analysis.

2-6 Reverse Transcription (RT)-PCR

Reverse transcription was used to generate cDNA probes and during gene expression analysis. Each reaction was performed in duplicate, except that one sample acted as a control for DNA contamination and did not receive the reverse transcriptase enzyme. For each reaction, 1 µg of RNA was mixed with 1 µL of 250 ng/µL random hexamer primer, 1 µL of 10 mM dNTPs, and ddH_2O to a final volume of 13 µL. The mixture was heated at 65°C for 5 min, and then quickly chilled on ice. 4 µL of First-Strand buffer (50 mM Tris-HCl, pH 8.3, 75 mM KCl, 3 mM $MgCl_2$) and 10 mM DTT were added, and the

mixture was incubated at room temperature for 2 min. Two hundred units of SuperScript II reverse transcriptase (Invitrogen) were added and the mixture was incubated for an additional 10 min at room temperature. The reverse transcription was allowed to proceed for 50 min at 42°C. Heating the mixture to 70°C for 15 min subsequently inactivated the enzyme. First strand cDNA was then amplified using the following reaction mixture: 1 μL of cDNA was mixed with 2.5 pmol forward primer and 2.5 pmol reverse primer, 1x PCR buffer, 0.4 mM dNTPs, 1.5 mM $MgCl_2$, 0.5 U *Taq* DNA polymerase (Amersham Biosciences) and ddH_2O to 25 μL. Table 2-6 lists the primers used to amplify first strand cDNA. The contents of the tubes were overlaid with mineral oil. PCR was carried out in the Robocycler 40 (Stratagene) under the following conditions: 94°C for 1 min, 40 sec; 55°C for 1 min, 20 sec; 72°C for 2 min, 20 sec, for 40 cycles. The quality of the cDNA and the presence of DNA contamination were monitored on 1% agarose gels.

2-7 Detecting Mutations using Heteroduplex Analysis

The WAVE™ DNA Fragment Analysis System is a DHPLC column that allows for the rapid screening of mutations and/or polymorphisms in a particular DNA fragment. Equal amounts of control and sample DNA are mixed together and allowed to form duplexes. If the sample DNA is different from the control DNA by even a single base pair, the two DNA populations will form both homo- and hetero-duplexes (Figure 2-7). Under denaturing conditions, heteroduplexes denature into single strands faster than homoduplexes due to the presence of the base pair mismatch. The heteroduplexes are therefore eluted first from the column, ahead of the still intact homoduplexes. Mutations are identified on the WAVE by the distinct pattern of peaks or 'waves' on a

chromatograph which are the result of the differences in elution time of the homo- and hetero-duplex DNA.

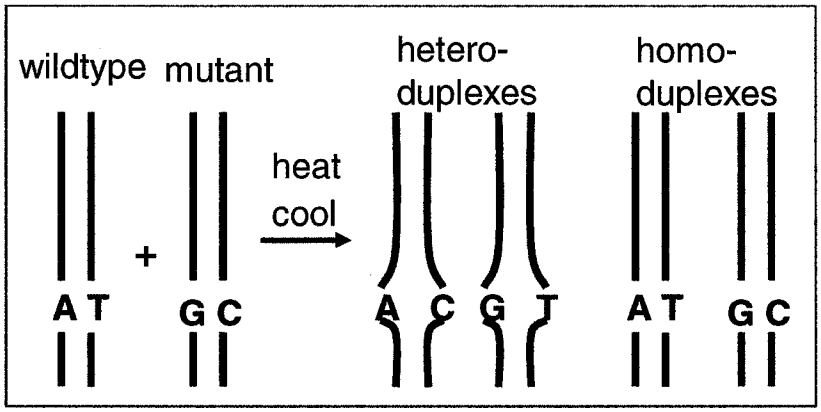

Figure 2-7. The formation of heteroduplexes and homoduplexes during heteroduplex analysis.

2-7.1. Heteroduplex Analysis

mtDNA encoding Complex I of the electron transport chain was amplified from the two previously sequenced control samples using standard conditions and the primers listed in Table 2-7. The quality of the PCR products was verified on 1% agarose gels. Equal amounts of the control DNA were combined in a final volume of 28 μL and allowed to hybridize under the following conditions: DNA was denatured at 95°C for 5 min, then allowed to hybridize by slowly cooling to 25°C over 45 min in the 9600 thermocycler (Applied Biosystems). WAVE software was used to determine the appropriate melting temperature and denaturing conditions for each fragment analyzed (Table 2-7). The DNA was loaded onto the WAVE for analysis. Chromatographs were analysed for the presence of mutations in one of the two samples. The results of the chromatographs were then compared with the sequence information of the two samples.

2-8 Microarray Analysis

Microarray analysis was used to study global changes in gene expression of cell lines exposed to mild hypoxia (0.6% O_2) for 12 hours. RNA was isolated from M006x, M006xLo, and M010b cells that had been cultured in either atmospheric air or hypoxia. In the PolyomX lab (Cross Cancer Institute) cDNA was prepared from 30 μg of the total RNA. Using an indirect amino allyl technique, cDNA from cells cultured in atmospheric air was labeled with Cy5, while cDNA from cells cultured in hypoxic conditions was labeled with Cy3. The microarray slides were of the Operon Human 70-mer oligonucleotide set, version 1.1, which represents 13,971 unique genes. Each oligo was printed in duplicate so that the median fluorescent values for a spot could be calculated. The Cy3 and Cy5 labeled cDNA from each cell line was mixed and allowed to hybridize to the microarray slide. The slides were then scanned with an Axon 4000B using GenePix 3.0 software. The data for each spot was expressed as a ratio of Cy5/Cy3, so that ratios less than one indicated that the gene expression was higher in hypoxic (Cy3) samples, whereas ratios greater than one indicated that the gene expression was higher in aerobic (Cy5) samples.

2-9 Quantitative real-time RT-PCR

The expression patterns of several nuclear-encoded cytochrome *c* oxidase subunits and isoforms were studied using Assays-on-Demand™ gene expression products (Applied Biosystems) and real-time quantitative RT-PCR. 18S rRNA was used as an endogenous control. RNA from M006x, M006xLo, and M010b cell lines was isolated under both normoxic and hypoxic conditions (0.6% O_2, 0.01% O_2, 100 μM $CoCl_2$). Forward and

reverse primers and probes against the Cox subunits of interest (Table 2-9) were purchased as 20x Target Assay mixes (Applied Biosystems), with forward primer concentrations of 18 μM, reverse primer concentrations of 18 μM, and probe concentrations of 5 μM. Probes contained a reporter dye (6-FAM) linked to the 5′ end, and a non-fluorescent quencher at the 3′ end. Q-RT-PCR was performed in two steps. The first step involved the reverse transcription of RNA to cDNA, which was performed using previously described methodology. The second step involved PCR and fluorescent analysis using the Assay-on-Demand reagents. Each sample was analyzed in triplicate on a 96 well plate. A single reaction mixture included 11.25 μL cDNA (diluted 1:100), 1x Target Assay Mix, and 1x Taqman Universal PCR Master Mix to a final volume of 25 μL. Samples were loaded onto the ABI Prism 7700 Sequence Detector, and the following thermocycling parameters were used: 95°C for 10 min (to activate the AmpliTaq Gold enzyme), and 40 cycles of 95°C for 15 sec, 60°C for 1 min. Amplification plots of normalized fluorescent signal versus cycle number were generated by the Sequence Detector software. After the baseline cycle numbers were manually adjusted, the threshold cycle values (C_T) were determined. C_T is the cycle at which a statistically significant increase in fluorescence is first detected.

2-10 Northern Blot Analysis

2-10.1. RNA Separation and Blotting

The gel apparatus was cleaned with Rnase*Zap* (Ambion) before being assembled. 10-20 μg of total RNA were mixed with equal parts RNA loading buffer [5.3 M formaldehyde, 43% deionized formamide, 7.7% bromphenol blue, 1.4 mM EDTA, 0.48x MOPS buffer

(20 mM MOPS, 5 mM sodium acetate)] and denatured by heating to 70°C for 10 min. The RNA samples were quickly chilled on ice, then loaded onto an agarose-formaldehyde gel (1% agarose, 1x MOPS buffer, 1 M formaldehyde); electrophoresis was performed for 2-3 hours at 110 V in 1x MOPS buffer. RNA was blotted onto a Hybond-XL nylon membrane (Amersham Biosciences) O/N, using the methodology of Brown and Mackey (1997). Membranes were baked at 80°C for 2 hours in a DP32 vacuum drying oven to immobilize the RNA. Membranes were then sealed in polyethylene bags and prehybridized in prehybridization buffer (49% formamide, 5x SSC, 7x Denhardt solution, 70 mM NaH_2PO_4, pH 6.5, along with 10 mg/mL freshly denatured salmon sperm DNA) for at least 4 hours at 42°C. DNA probes were labeled with [^{32}P] dCTP (description to follow) and mixed thoroughly with hybridization solution. The hybridization solution was made of 30% hybridization cocktail (18x SSC, 3.5x Denhardt solution, 70 mM NaH_2PO_4, 60 µmol dextran sulphate), 50% formamide, 20% ddH_2O and 1.25 mg of freshly denatured salmon sperm DNA. Hybridization occurred in polyethylene bags at 42°C, O/N. Membranes were washed twice for 5 min at room temperature in Wash 1 (2x SSC, 0.1% SDS), then twice for 1 hour at 65°C in Wash 2 (0.1x SSC, 0.1% SDS), before being exposed to Kodak XAR-5 X-ray film for 1-14 days at -80°C. Blots were stripped in stripping buffer (5 mM Tris pH 8.0, 2 mM EDTA, 0.1x Denhardt solution) at 65°C for 1 hour.

2-10.2. DNA probe labeling

Probes for Ngb, CoxIV-1, CoxIV-2, RPS27A, and β-actin were amplified from cDNA templates, under standard conditions, and using the primers listed in Table 2-10. The resulting DNA was sequenced to verify that the correct sequence had been amplified.

The Rediprime™ II random prime labeling system (Amersham Biosciences) was used to label 2.5-25 ng of cDNA with [^{32}P] dCTP. The probes were cleaned of unincorporated nucleotides using the QIAquick nucleotide removal kit (Qiagen), and eluted in a final volume of 200 µL. One µL was added to 5 mL of scintillation fluid so that probe activity could be measured using the LS 6500 or LS 5801 scintillation counters (Beckman). Activities of 10^8-10^{10} cpm/µg were obtained.

2-11 Transcription Run-offs

2-11.1. Glycerol Stocks

A single colony of *E. coli* SURE® cells was inoculated with 3 mL of LB supplemented with the antibiotic tetracycline (tet) (10 µg/mL) and grown O/N at 37°C. Equal volumes of the bacteria and glycerol stock solution (65% glycerol, 100 mM $MgSO_4$, and 25 mM Tris pH 8.0) were mixed gently, aliquoted, and stored at -80°C.

2-11.2. Harvesting Competent SURE Cells

Competent cells were harvested for use in the cloning procedure. Two 3 mL LB + tet (10 µg/mL) cultures were inoculated with SURE® cells from frozen glycerol stocks, and grown O/N in a shaking 37°C incubator. Both cultures were diluted in 250 mL LB broth and allowed to grow to log phase (OD_{590}= 0.5 – 0.6) at 37°C. The cells were then chilled on ice for 20 min and centrifuged at 4°C for 20 min at 3200 rpm in acid-washed, pre-chilled centrifuge bottles in a Sorvall RC5C Plus centrifuge. The cell pellets were gently resuspended in 250 mL cold, sterile dH_2O. The cells were centrifuged using the same conditions, and the pellets were resuspended in 125 mL cold, sterile dH_2O. Again the cells were centrifuged, and the pellets were pooled in 10 mL cold, sterile dH_2O + 10%

glycerol. A final spin pelleted the cells so that they could be resuspended in 1.5 mL cold, sterile dH_2O + 10% glycerol, and aliquoted into pre-chilled microcentrifuge tubes. The cells were snap frozen on dry ice and stored at -80°C.

2-11.3. Plating M13 bacteriophage

Three mL of LB + tet (10 µg/mL) were inoculated with a loopful of SURE® cells from frozen glycerol stock and grown O/N in a shaking 37°C incubator. The next day, M13mp18 and M13mp19 plug stocks were diluted 1:1000 in LB broth. One, 10, and 100 µL of the diluted bacteriophage were mixed with 200 µL of the SURE® cells that had been incubated O/N. The cells were added to 3 mL of melted LB top agar (0.7% agar, 0.27 mg/mL X-gal, 1.3 mM IPTG) at 48°C and quickly poured over pre-warmed LB agar plates. The top agar was allowed to solidify for 10 min, and the plates were incubated at 37°C O/N.

2-11.4. Picking Bacteriophage M13 Plaques

Plaques were isolated by using a pasteur pipette to stab through the plaque into the underlying agar and expel the plug of agar into 1 mL LB. The plugs were incubated at room temperature for 1-2 hours to allow the bacteriophage to diffuse from the agar. The plugs were stored at –20°C.

2-11.5. Preparation of Infected Culture

SURE® cells were grown O/N as previously described. Four hundred µL of the O/N culture were used to inoculate 4 mL of LB + tet (10 µg/mL). The cells were grown at 37°C until they reached log phase (OD_{590} = 0.5 - 0.6). Twenty µL of the cells were infected with 100 µL of the bacteriophage plug stock. Cells were incubated at room

temperature for 5 min, then added to 2 mL of pre-warmed LB and incubated at 37°C for 5-6 hours. 1.5 mL of the infected cultures were centrifuged at 13 000 rpm for 5 min.

2-11.6. Small-scale Preparation of the Replicative Form of Bacteriophage M13 DNA

The M13 dsDNA, located in the pelleted cells, was isolated using a standard alkaline lysis treatment (Sambrook and Russell, 2001), and resuspended in 25 µL TE buffer.

2-11.7. Cloning CoxIV-1, CoxIV-2, and RPS27A into M13mp18 and M13mp19

Five µL of the isolated M13mp18 and M13mp19 dsDNA and 25 µL of the purified CoxIV-1, CoxIV-2, and RPS27A DNA (amplified under standard conditions, using the primers listed in table 2-11) was digested with *BamHI* and *EcoRI* (New England Biolabs) in 1x EcoRI buffer, 1x BSA for 2 hours at 37°C. The digested DNA was purified using the QIAquick PCR purification kit (Qiagen). Inserts and vectors were ligated in a 5:1 ratio, using 1x Ligase Reaction Buffer (Invitrogen), 1 mM ATP, and 0.05 units of T4 DNA ligase (Invitrogen) in a final volume of 20 µL. Ligations were allowed to proceed O/N at 16 °C.

2-11.8. Transformation of SURE cells with cloned M13 bacteriophage

SURE® cells were grown O/N as previously described. One µL of the ligation mixture was added to 40 µL of competent SURE cells and incubated on ice for 30 sec. The cells were transferred to pre-chilled Gene Pulser cuvettes (Bio-Rad) with 0.1 cm electrodes, and electroporated under the following conditions: 1.7 kV, 200 ohms, 25 µFD using a Gene Pulser system (Bio-Rad). The cells were immediately transferred to 175 µL of warmed LB buffer, then 1, 10 and 100 µL were mixed with 200 µL O/N SURE cells, and added to 3 mL of the previously described supplemented top agar at 47°C. The top agar was quickly mixed and poured onto pre-warmed LB agar plates. The top agar was

allowed to solidify for 10 min, and the plates were incubated O/N at 37°C. Plaques that contained recombinant bacteriophage were colourless, while plaques that contained the original vector were blue in colour.

2-11.9. Verification of Correct Cloning

Plug stocks were generated from the colourless plaques, and SURE® cells were infected with bacteriophage from the plaques, as described above. The RF M13 DNA was isolated and digested with restriction enzymes to verify the presence of the insert. M13mp18 was digested with *EcoR*I and *Bgl*II in 1x EcoRI buffer; M13mp19 was digested with *Hind*III and *Bgl*II in 1x buffer #2 (all from New England Biolabs) for 1-2 hours at 37°C. The DNA was separated on 0.7% agarose gels to visualize the presence of the insert. Once the CoxIV-1, CoxIV-2, and RPS27A inserts were shown to be present, large-scale preparations of ssDNA were generated to be used as probes.

2-11.10. Large-scale Preparations of ssDNA from M13 Bacteriophage

One hundred µL of plug stock were mixed with 500 µL of O/N SURE® cells and incubated at room temperature for 5 min. The cells were allowed to grow to log phase at 37°C in 50 mL LB in a shaking incubator, then the cells were pelleted for 20 min at 4000 rpm, 4°C, in a Beckman AccuSpin FR centrifuge. The supernatant was carefully transferred to a sterile beaker and stirred with 2 g PEG 8000 and 1.5 g NaCl for 1 hour at room temperature. The mixture was centrifuged for 20 min at 7850 rpm, 4°C, in snap cap tubes in a Sorvall RC 5C Plus centrifuge. The supernatant was discarded and the pellet resuspended in 2 mL TE. ssDNA was phenol:chloroform extracted twice, and precipitated O/N at -20°C with 1/10 volumes of 3 M sodium acetate and 2 volumes 100% ethanol. The ssDNA was pelleted for 10 min at 14 000 rpm, 4°C, air dried for 10 min,

and resuspended in 100 µL TE. The ssDNA was treated with 10 µg boiled RNAse A. Phenol:chloroform extraction and ethanol precipitation were performed as before, and the ssDNA was resuspended in 50 µL TE. Finally, the ssDNA was quantified and 1 µL was run on a 0.7% agarose gel to verify the quality of the sample.

2-11.11. Nuclei Isolation

M006x, M006xLo, and M010b nuclei were carefully isolated from cells that were grown under both normoxic and hypoxic (0.6% O_2) conditions. The nuclei were isolated on ice and kept at -80°C so that the transcriptional activity of the cells was suspended until radiolabeled nucleotides were available for incorporation into the nascent transcript. A total of $8x10^6$ cells were seeded and allowed to expand over 3 days. The media was removed and the cells were washed in a total of 20 mL ice-cold PBS. The cells were scraped into 50 mL tubes and pelleted for 4 min at 900 rpm, 4°C, in a Beckman AccuSpin FR centrifuge. The cells were resuspended in 20 mL ice-cold PBS; an aliquot of cells was removed for counting, and the remaining cells were pelleted. The samples were then washed in ice-cold RSB buffer (10 mM Tris, pH 7.4, 10 mM NaCl, 5 mM $MgCl_2$) and centrifuged. The cells were resuspended in 2 mL ice-cold RSB buffer, 18 mL RSB + 0.5% NP-40 buffer to lyse the cells hypotonically. Fifteen strokes of a type 'B' pestle broke the cells in ice-cold Dounce homogenizers. The nuclei were collected for 5 min at 2000 rpm, 4°C, resuspended in 210 µL Nuclear Freezing buffer (50 mM Tris pH 8.0, 5 mM $MgCl_2$, 40% glycerol, 0.5 mM DTT), and frozen at -80°C. Approximately 1-1.5 x 10^7 nuclei were collected from each cell line, for each condition.

2-11.12. Blotting ssDNA

One µg of each ssDNA probe was blotted onto Hybond XL membrane (Amersham Biosciences) that was stacked atop three pieces of Whatman filter paper in a bio-dot slot blotter (Bio-rad). The ssDNA was blotted onto the membrane in a final volume of 200 µL 1x SSC. Four hundred µL of 1x SSC were used to wash the membrane before the apparatus was disassembled. The DNA was covalently bound to the membrane by UV irradiation (Stratalinker) and by baking the membrane at 80°C for 2 hours.

2-11.13. Transcription Run-off Assay

The membranes were prehybridized at 65°C in 1 mL hybridization buffer (10 mM TES pH 7.4, 1% SDS, 10 mM EDTA, 0.3 M NaCl, 1x Denhardt solution, 0.25% skim milk, 250 µg/mL tRNA) for 2 hours. In the meantime, 1-1.5 x 10^7 nuclei were gently thawed on ice and mixed with 5x buffer (25 mM Tris, pH 8.0, 12 mM $MgCl_2$, 750 mM KCl, 1.2 mM ATP, CTP and GTP), and 30 µL [^{32}P] dUTP (300 µCi). The nuclei were incubated at 30°C for 30 min to allow transcription to continue. Every 10 min the contents of the tubes were mixed gently. The samples were then incubated for 10 min with 100 µg DNase I. Another 75 µg DNase I was added and the samples incubated an additional 10 min at 30°C. Samples were then incubated for 45 min at 50°C with 100 µg Proteinase K and 1x SET buffer (10% SDS, 100 mM Tris pH 7.5, 50 mM EDTA). Samples were cleaned by extraction with an equal volume of phenol/chloroform/isoamyl alcohol. Samples were vortexed for 1 min, then centrifuged for 5 min. The aqueous supernatant was carefully transferred to a fresh tube with 2 volumes of chloroform/isoamyl alcohol. Again the sample was vortexed for 1 min, and centrifuged for 5 min. The aqueous supernatant was transferred to a fresh tube and mixed with 200 µL of 7.5 M ammonium

acetate, 600 µL isopropanol and 1.25 µg *E. coli* tRNA. The RNA was allowed to precipitate on dry ice for 20 min, then it was pelleted for 20 min at room temperature. The pellet was carefully resuspended in 100 µL TE. Unincorporated nucleotides were removed by passing the samples through 1 mL G-50 spin columns. Briefly, the spin columns were assembled 15 min before use; the samples were added to the columns and centrifuged at 1350 rpm for 5 min at room temperature. Samples were transferred to fresh tubes and their final volume brought to 1 mL with the addition of hybridization buffer. The radioactivity of the samples was measured by counting 5 µL of the mixture using either the LS 6500 or LS 5801 scintillation counters (Beckman). The hybridization mixture was added to the blots and incubated for 48 hours at 65 °C in a hybridization oven. The blots were washed twice at room temperature for 5 min in blot wash I (0.1% SDS, 1x SSC). The RNA was degraded by washing the blots at room temperature for 20 min in an RNase A solution (2x SCC, 2 µg/mL RNase A). The blots were again washed twice for 5 min in blot wash I. The blots were then transferred to blot wash II (0.1% SDS, 0.1x SSC) and washed for 5 min at room temperature. The blots were washed two more times in blot wash II for 15 min at 65°C. Finally, the blots were sealed in polyethylene bags and exposed to XAR film for 9-10 days.

2-12 Cytochrome *c* oxidase activity assay

Cox enzyme activity was quantified spectrophotometrically by measuring the decrease in absorbance at 550 nm over time as Cox oxidized cytochrome *c*. A 1% cytochrome *c* solution was prepared in 20 mM Tris, pH 7.5. Half of the solution was reduced with approximately 2.0 mg sodium hydrosulfite. The reduced cytochrome *c* solution was

aerated by flicking the tube 10-12 times until foamy. Between 1.2 x 10^7 and 2.4 x 10^7 cells were scraped into 400 µL ice-cold PBS and sonicated in two 5 sec bursts. One hundred and fifty µL of the sonicated cells were added to 1 mL of 0.08% reduced cytochrome *c* in 20 mM potassium phosphate buffer, pH 7.0, immediately before absorbance was measured. Absorbance was recorded every 5 sec for a total of 60 sec. One mL of 0.08% oxidized cytochrome *c* was used to blank the spectrophotometer. The change in absorbance of 1 mL of 0.08% reduced cytochrome *c* was measured over 60 sec, and served as an internal control for auto-oxidation. Each experiment was performed in triplicate.

Cox activity was calculated using the equation $\Delta A = \varepsilon lc$, where $\varepsilon = 18.2\ mM^{-1}\ cm^{-1}$, $l = 1$ cm, so that $c = \Delta A/\varepsilon$. Cox activity was expressed as nmol/min/mg. The change in absorbance over 30 sec was plotted and the best-fit line was determined using statistical software from Graphpad Prism. ΔA was calculated as the slope of the best-fit line. Protein concentration was calculated as previously described.

Table 2-4. Primers used to amplify the human mtDNA genome

Fragment number	Primer Name	Sequence (5′ - 3′)	Product size (bp)
1	NDF	CCCATGGCCAACCTCCTACTC	1141
	NDR	CCAACATTTTCGGGGTATGGGC	
2a	F5	CCCATACCCCGAAAATGTTGG	1362
	F10-rev	CGAAGAAGCAGCTTCAAACCTG	
2b	F10	AGGTTTGAAGCTGCTTCTTCG	730
	R3	GAGAGTAGGAGAAGTAGGACTG	
3	CYTF	CAGTCCTACTTCTCCTATCTCTC	870
	CYTR	CTTTTCGCTTCGAAGCGAAGC	
4a	F1	TAACTAGTTTTGACAACATTC	1249
	F15-rev	GCCTAGGGTGTTGTGAGTGTA	
4b	F15	TACACTCACAACACCCTAGGC	1380
	R11	TGGACCATGTAACGAACAATGC	
8a	F18	TGGGGCTCACTCACCCACCAC	1432
	R8	GGTATGGTTTTGAGTAGTCC	
8b	R8-for	GGACTACTCAAAACCATACC	1284
	R1	GTCGTGGTTGTAGTCCGTGCGA	
9a	F19	GTTTATGTAGCTTACCTCCTC	1276
	F24-rev	GCAGAAGGTATAGGGGTTAGTC	
9b	F24	GACTAACCCCTATACCTTCTGC	1501
	R13	GGAGTAGGAGGTTGGCCATGG	
11a	F47	CGCACGGACTACAACCACGAC	1308
	F44-rev	GCTAATGGTGGAGTTAAAGAC	
11b	F44	GTCTTTAACTCCACCATTAGC	1180
	R15	CTGTGGGGGGTGTCTTTGGGG	
12a	F45	CCTAGGGTTTATCGTGTGAGC	1102
	F32-rev	CGTCTGTTATGTAAAGGATG	
12b	F32	CATCCTTTACATAACAGACG	1092
	R26	GCCTTGTGGTAAGAAGTGGGC	
12c	R26-for	GCCCACTTCTTACCACAAGGC	1132
	R14	CTAGTTAATTGGAAGTTAACGG	

Table 2-5. Primers used to sequence the human mtDNA genome

Fragment Number	Primer Name	Primer Sequence (5′ – 3′)
1	F2-rev	GGTTGGGTATGGGGAGGGGGG
	NDF	CCCATGGCCAACCTCCTACTC
	F2	CCCCCCTCCCCATACCCAACC
	F3	ACCTCTGATTACTCCTGCC
	NDR	CCAACATTTTCGGGGTATGGGC
2a	F6-rev	GTCCGGAGAGTATATTGTTG
	F5	CCCATACCCCGAAAATGTTGG
	F6	CAACAATATACTCTCCGGAC
	F7	CTTATCCATCATAGCAGGCAG
	F8	CAAGCTAACATGACTAACACCC
	F9	GGTTAAATACAGACCAAGAGCC
2b	SC-C-rev	GGTAAGAGTCAGAAGCTTATGT
	R3	GAGAGATAGGAGAAGTAGGACTG
	F11	CAACCTTCTAGGTAACGACC
3	CYTF	CAGTCCTACTTCTCCTATCTCTC
	F48	ATACATAGGTATGGTCTGAGC
	F46	CCTGACTGGCATTGTATTAGC
4a	F1	TAACTAGTTTTGACAACATTC
	F12	GCCCTCCTTTTACCCCTACC
	F13	TCTAGGAATACTAGTATATCG
	F14	CTCCAATGCTAAAACTAATCG
	F39	ATCCAGTGAACCACTATCACG
4b	F16-rev	GGCTATGTGTTTTGTCAGGGGG
	F15	TACACTCACAACACCCTAGGC
	F16	CCCCCTGACAAAACACATAGCC
	R12	TTAGGGAAGTCAGGGTTAGGGT
	R11	TGGACCATGTAACGAACAATGC
8a	F18	TGGGGCTCACTCACCCACCAC
	R10	GGATGAAACCGATATCGCCGATACGGT
	R9	GAGTGGTGATAGCGCCTAAGC
	R8	GGTATGGTTTTGAGTAGTCC
	R9-for	GCTTAGGCGCTATCACCACTC
8b	R7	GTAGGGTGGGGTTATTTTCGT
	R8-for	GGACTACTCAAAACCATACC
	R5	CTGGTTGAACATTGTTTGTTGG
	R4	TATTGAGGAGTATCCTGAGGC
	R1	GTCGTGGTTGTAGTCCGTGCGA
	R4-for	GCCTCAGGATACTCCTCAATA
9a	R21	GTATAGCTTAGTTAAACTTTCG
	F19	GTTTATGTAGCTTACCTCCTC
	R21-for	CGAAAGTTTAACTAAGCTATAC

	F24-rev	GACTAACCCCTATACCTTCTGC
	F23	ACTGGAAAGTGCACTTGGACG
9b	F24	GACTAACCCCTATACCTTCTGC
	F25	TTAGTTCAACTTTAAATTTGC
	F27	GCCGCGGTACCCTAACCGTG
	R13	GGAGTAGGAGGTTGGCCATGG
	F29	GACCGGAGTAATCCAGGTCGG
11a	R22	CGAGTGATGTGGGCGATTGATG
	F47	CGCACGGACTACAACCACGAC
	F40	CATCAATCGCCCACATCACTCG
	F41	ATCCGCCATCCCATACATTGG
	F42	ACATTAACACTATTCTCACC
11b	R20	AGGGTTGATTGCTGTACTTGC
	F44	GTCTTTAACTCCACCATTAGC
	R18	CCCAGACGAAAATACCAAATGCA
	R17	CCAGAAGCGGGGGAGGGGGGG
	R18-for	TGCATTTGGTATTTTCGTCTGGG
12a	R24	AAGATATATAGGATTTAGCC
	F30	GAAGCCTTCGCTTCGAAGCG
	F31	AATCCTATATATCTTAATGGC
12b	R30	TTGCTCCACAGATTTCAGAGC
	F33	CATTAGGCTTAAAAACAGATGC
	F34	CACCTCTTTACAGTGAAATGCC
	F35	CCCCCTCTATTGATCCCCACC
12c	F37-rev	CGATTTCTAGGATAGTCAGT
	R26-for	GCCCACTTCTTACCACAAGGC
	F38	ATGATGGCGCGATGTAACACG
	F49N	CCGAAACCAAATAATTCAAGCA

Table 2-6. Primers used for amplification of first strand cDNA during RT-PCR expression analysis

Gene	Primer Name	Primer sequence (5′ - 3′)	Product Size (bp)
Ngb	Ngb-3	ACAGCATGGAGCGCCCGG	466
	Ngb-4	CGCCTCTTACTCGCCATCC	
	Ngb-5	GTGTCTCCACCTACGACTGG	513
	Ngb-6	GAA GGAGCTGAGCTTCACAC	
RPS27A	RPS27A-1	TTTTCGATCCGCCATCTGCG	452
	RPS27A-2b	TGTCTGTCAAAGTGACTTGCC	

Table 2-7. Primers used for the amplification of Complex I and the melting temperatures used during WAVE analysis

Fragment	Primers	Melting Tm (°C)
1	NDF, NDR	59
2a 5′	F5, R34	59,
2a 3′	F7, F10-rev	59,
4a	F1, F15-rev	N/A
4b 5′	F15, R35	60, 61
4b 3′	F53, R11	59, 60
8a 5′	F18, R33	59,60
8a 3′	F52, R8	61
8b	R8-for, R1	59, 60
9b 5′	F24, R32	59, 60
9b 3′	F27, R13	61
12c	R26-for, R14	60, 61

Table 2-9. Taqman primers and probes used for the Cox subunit expression analysis. *Assays are further described at www.appliedbiosystems.com.

Subunit	Assay Identifier*
CoxIV-1	Hs00266371_m1
CoxIV-2	Hs00261747_m1
CoxVb	Hs00426948_m1
CoxVIa(L)	Hs01629071_s1
CoxVIa(H)	Hs00193226_g1
CoxVIIa(L)	Hs00190880_m1
CoxVIIa(H)	Hs00156989_m1
18S rRNA	Hs99999901_s1

Table 2-10. Primers for Northern Blot Probes. *The primer sequences for the β-actin probe were obtained from Horikoshi *et al.* (1992).

Probe	Primer Name	Primer Sequence (5′ – 3′)	Product Size (bp)
Ngb	Ngb-3	ACAGCATGGAGCGCCCGG	466
	Ngb-4	CGCCTCTTACTCGCCATCC	
CoxIV-1	CoxIV1-F	TAGCCTAGTTGGCAAGCGAG	426
	CoxIV1-R	CTTCATGTCCAGCATCCTCT	
CoxIV-2	CoxIV2-F	GATGCACAGCTCAGAAGGCA	250
	CoxIV2-R	CTTCCACTCATTGGAGCGAC	
RPS27A	RPS27A-1	TTTTCGATCCGCCATCTGCG	452
	RPS27A-2b	TGTCTGTCAAAGTGACTTGCC	
B-actin*	BA-67	GATGGAGTTGAAGGTAGTTTCGTG	282
	BA-68	GCGGGAAATCGTGCGTGACATT	

Table 2-11. Primers for Transcription run-off Probes

Probe	Primer Name	Primer Sequence (5′ – 3′)	Product Size (bp)
CoxIV-1	Cox4-1F(EcoRI)	CGGAATTCTAGCCTAGTTGGCAAG CGAG	426
	Cox4-2R(BamHI)	CGGGATCCCTTCATGTCCAGCATC CTCT	
CoxIV-2	Cox4-2F(EcoRI)	CGGAATTCGATGCACAGCTCAGAA GGCA	250
	Cox4-2R(BamHI)	CGGGATCCCTTCCACTCATTGGAG CGAC	
RPS27A	RPS27A-F(EcoRI)	CGGAATTCTTTTCGATCCGCCATCT GCG	452
	RPS27A-R(BamHI)	CGGGATCCTGTCTGTCAAAGTGAC TTGCC	

CHAPTER 3: RESULTS

3-1 WAVE Analysis of Complex I mtDNA Mutations

Many types of cancer, including ovarian, colon, and prostate, have increased numbers of somatic mtDNA mutations. These mutations are usually in the form of purine transitions, reflecting the high level of reactive oxidative species generated in the mitochondria. It has recently been demonstrated, in the case of colorectal cancer, that such mutations have prognostic significance (Lièvre *et al.,* 2005). Lièvre and colleagues (2005) reported that the three year survival rate for patients with mutations in the D-loop (the non-coding, regulatory region of mtDNA) was 53.5%, versus 62.1% for patients without mutations. Moreover, only 45.4% of patients with D-loop mutations benefited from adjuvant chemotherapy versus 78.3% of patients without such mutations (Lièvre *et al.,* 2005).

Initially there was speculation regarding the functional significance of mtDNA mutations. It was not known whether the mutations were contributing factors in carcinogenesis or whether they were only secondary effects of cancer progression. Recent studies using cybrids suggest that mtDNA mutations enhance tumor cell growth (Petros *et al.,* 2005). In their study, Petros and coworkers introduced mtDNA that harboured a mutation similar to one found in a prostate cancer biopsy, into a prostate cancer cell line whose own mtDNA had been destroyed with ethidium bromide (Petros *et al.,* 2005). The cybrids were then injected into nude mice and the rate of tumor growth was compared between mutant and wild-type cybrids (Petros *et al.,* 2005). The mutant cybrids produced tumors that were at least seven fold greater in volume than the wild-

type cybrid tumors (Petros *et al.*, 2005). Furthermore, when ROS production was compared between the mutant and wild-type cybrids, it was determined that the mutant tumor produced significantly more ROS (Petros *et al.*, 2005).

Our lab is interested in determining the prognostic significance of Complex I mtDNA mutations in cervical cancer. The WAVE DNA Fragment Analysis System is a fast, cost effective, and efficient high through-put system that to date has primarily been used for mutational screening of nuclear DNA. The WAVE is a DHPLC column that differentiates between hetero-duplexes, formed by combining normal and mutant DNA, and homo-duplexes, formed by matched normal or mutant DNA, based on their thermostability. Mutations are identified on the WAVE by the distinct patterns of peaks or 'waves' on a chromatograph which are the result of differences in elution time of the homo- and hetero-duplex DNA. The purpose of these experiments was to evaluate the sensitivity and reproducibility of the WAVE system for screening of Complex I mutations in mtDNA.

Before screening the cervical cancer samples, it was necessary to divide the regions of mtDNA encoding the Complex I subunits (more than 6 kb in total) into fragments that would be an appropriate size for WAVE analysis. Therefore, we amplified the Complex I subunits in 12 overlapping fragments, between 603 and 1283 bps in length. To make sure that the mtDNA primers amplified mtDNA specifically, we tested the primers using DNA isolated from cells lacking mtDNA (rho 0 cells) (kindly donated by Dr. Moira Glerum, Department of Medical Genetics, University of Alberta). The suggested fragment size for WAVE analysis is between 200-400 bp; however, the WAVE is able to detect sequence variations in fragments up to 1.5 kb in size. We also

had to test the fragments to ensure that the melting temperatures and denaturing conditions calculated by the WAVEMaker software were optimized for mutation detection. To test the accuracy of the WAVE, we extracted DNA from the whole blood of two normal donors (Sample 1 and Sample 2) and sequenced the mtDNA encoding the Complex I subunits (spanning bases 3307-5511 and 10059-14673) to determine the location of any DNA sequence variations. Sample 1 had several base substitutions that were not present in Sample 2. Table 3-1.1 lists these sequence variations. The vast majority of the base substitutions (15/16) were transitions, with 7/15 being A→G, 4/15 being G→A, 2/15 being C→T, and 2/15 being T→C. The lone transversion was C→A. Thirteen of the sixteen base substitutions occurred in codons that encoded an amino acid: 3/13 were mutations that resulted in an amino acid change, while the remaining ten substitutions were silent mutations. According to MitoAnalyzer (http://www.cstl.nist.gov/biotech/strbase/mitoanalyzer.html, 2000), the A→G4136 substitution is associated with Leber Hereditary Optic Neuropathy (LHON), and the A→G12308 substitution is associated with Chronic Progressive External Ophthalmoplegia (CPEO).

Table 3-1.1. Testing the accuracy of the WAVE for the screening of Complex I mtDNA mutations in pre-sequenced Sample 1 and Sample 2 mtDNA. Nucleotide changes were analyzed using MitoAnalyzer (http: //www.cstl.nist.gov/biotech/strbase/mitoanalyzer.html, 2000).
* The A→G12308 was detected by the WAVE in both fragments 4b3′ and 8a5′.

Complex I Fragment	Region (bps)	Nucleotide Change	Amino Acid Change	Subunit	Detected Correctly by WAVE
1	3309 – 4450	A → G3480 A → G4136	Lys → Lys Tyr → Cys	ND1 ND1	Yes
2a5′	4430 – 5033	None	-	-	Yes
2a3′	4946 – 5791	G → A5231	Leu → Leu	ND2	No
4a	10027 – 11275	A → G10550	Met → Met	ND4L	N/A
4b5′	11255 – 11980	A → G11467 G → A11719 C → A11869	Leu → Leu Gly → Gly Pro → Pro	ND4 ND4 ND4	Yes
4b3′	11891 – 12634	A → G12308* G → A12372	- Leu → Leu	$tRNA^{Leu}$ ND5	Yes
8a5′	12005 – 12837	A → G12308	-	$tRNA^{Leu}$	Yes
8a3′	12749 – 13436	C → T13135	Ala → Ser	ND5	Yes
8b	13417 – 14700	T → C14037 G → A14167	Ser → Ser Glu → Asp	ND5 ND6	Yes
9b5′	1831 – 2661	C → T2217	-	16S rRNA	Yes
9b3′	2568 – 3331	A → G2706	-	16S rRNA	Yes
12c	8902 – 10033	T → C9698 T → C9716	Leu → Leu Gly → Gly	CoxIII CoxIII	Yes

The presence of sequence variations in Sample 1 that were absent in Sample 2 allowed us to use these samples to test the accuracy of the WAVE mutation detection system. Each fragment was tested at two melting temperatures. Deviations from the wildtype or homo-duplex elution profile of Sample 2 signified the presence of a sequence variation in Sample 1. Figure 3-1.1 illustrates examples of two typical chromatographs derived from samples with known mtDNA sequence variations. For both examples, the single nucleotide change responsible for the differences in the elution profiles is shown below the chromatograph. No relationship was observed between the pattern of chromatograph peaks and the type or number of mutations detected. Out of the eleven fragments screened by the WAVE, ten were analysed correctly. The only sequence variation that was not detectable was a G→A5231 transition located in the ND2 subunit. Figure 3-1.2 shows the corresponding chromatograph for this false negative.

Although the WAVE was able to successfully identify the presence of a Complex I mutation 91% of the time, the high level of sequence variation in the mitochondria makes WAVE impractical as a screening method. The benefit of the WAVE screening system is in quickly pinpointing a mutation so that sequencing can be done selectively in a narrow region of interest. In our case, however, sequence variations were present in 11/12 of the fragments analyzed, which necessitated the sequencing of almost all of the fragments, regardless. Therefore, in this case, brute force sequencing is probably the most effective means of obtaining information on the prognostic significance of Complex I mutation in cervical cancer.

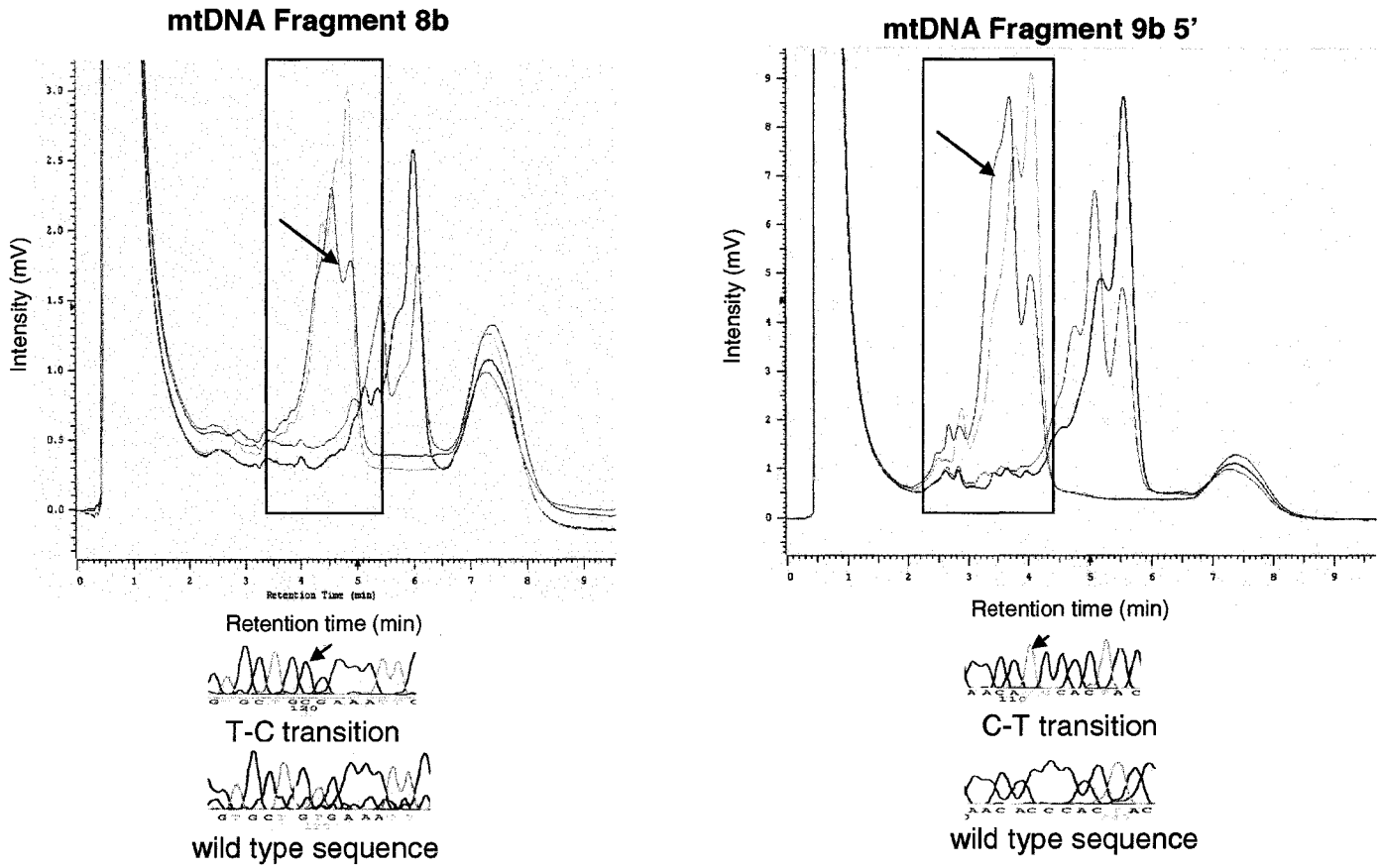

Figure 3-1.1. Successful WAVE analysis of Complex I mtDNA from the whole blood of two 'normal' donors. The red elution profiles are the Sample 2 homo-duplexes; the blue elution profiles are the Sample 1 and Sample 2 hetero-duplexes (arrow). Differences in the chromatograph peaks signal the presence of a sequence variation. The sequence variations were identified prior to WAVE analysis by sequencing the Complex I mtDNA of Sample 1 and Sample 2 (wildtype), and are shown below the corresponding chromatograph.

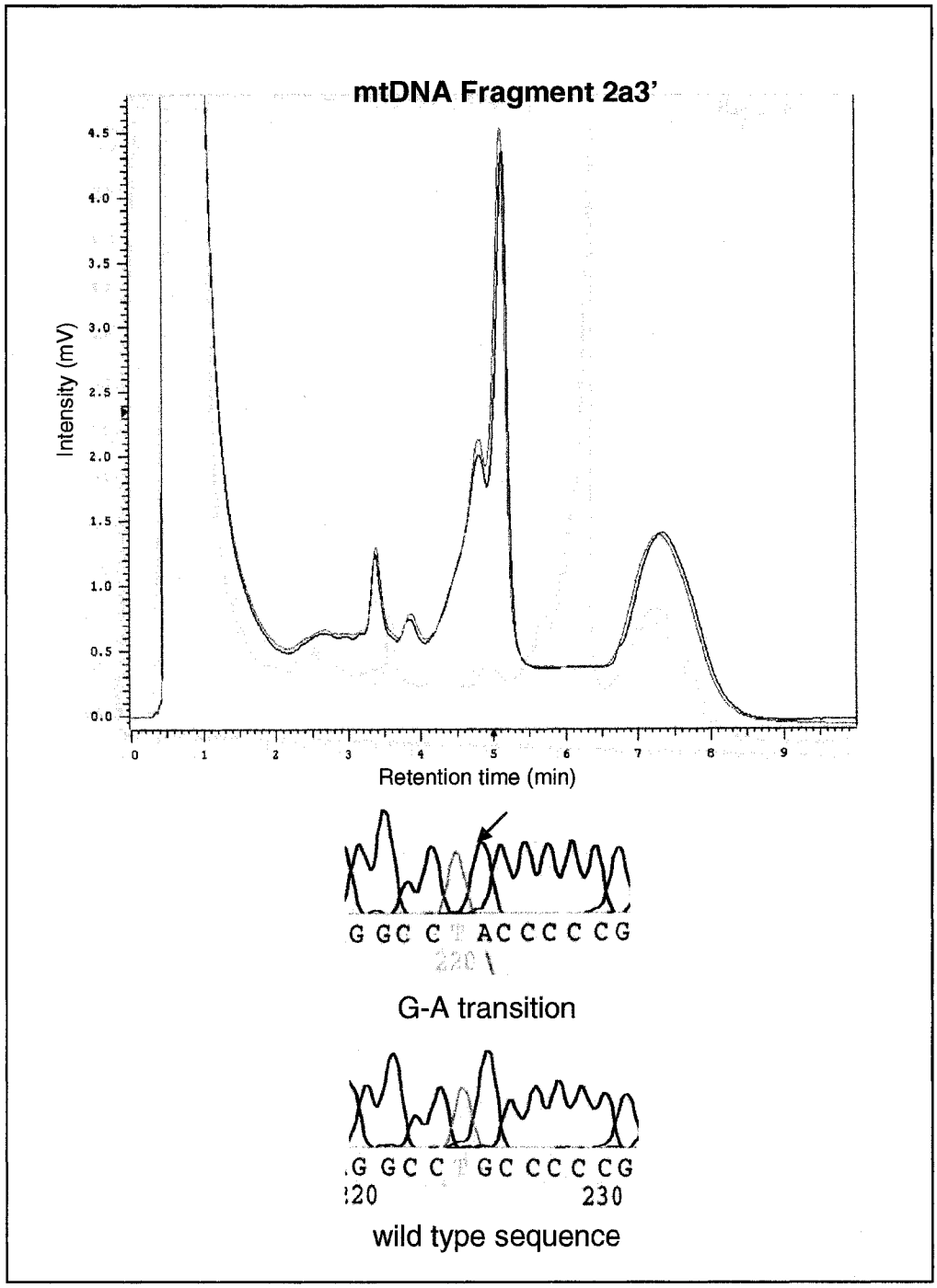

Figure 3-1.2. WAVE analysis failed to detect the presence of a G-A substitution in the Complex I fragment 2a3′ of mtDNA Sample 1, as seen by the identical pattern of peaks between the homo- and hetero-duplex DNA. The black elution profile is the Sample 2 homo-duplex; the blue elution profile is the Sample 1 and Sample 2 hetero-duplex.

3-2 The Role of Metabolic Adaptation in Establishing Hypoxia Tolerance

Metabolic adaptation is an important component of hypoxia adaptation in normal cells. Cytochrome *c* oxidase is a pivotal enzyme of oxidative phosphorylation, and may play a direct role in controlling respiration rate (Kadenbach *et al.,* 2000). Evidence suggests that Cox is responsive to changes in oxygen tension; for example, different Cox isozymes are expressed in tissues with differing oxygen demands. We hypothesized that the differential abundance and/or expression of Cox subunits and their isoforms is an adaptive mechanism used by tumors to respond to changes in oxygen supply. To test this hypothesis, we first determined if there was a difference in the Cox enzyme activity between hypoxia-tolerant and hypoxia-sensitive cell lines, and whether hypoxia was capable of inducing changes in the enzyme activity. We then studied the expression patterns of the nuclear-encoded Cox subunits from GBM cell lines cultured in atmospheric air, mild hypoxia (0.6% O_2), and severe hypoxia (0.01% O_2).

3-2.1. Comparison of cytochrome *c* oxidase enzyme activity in hypoxia-tolerant and hypoxia-sensitive GBM cell lines

As mentioned above, the presence of different Cox isozymes in normal tissues with different energy demands and substrate availabilities is consistent with the hypothesis that tissues capable of adapting to different environments do so in part by changing the catalytic properties of the Cox holoenzyme. We hypothesized that hypoxia-tolerant GBM cells might also be able to alter their catalytic properties to adapt to low oxygen conditions. To test this hypothesis, we compared the Cox enzyme activity of M006x, M006xLo, M010b, EcR293, and HepG2 cell lines cultured in atmospheric air, mild hypoxia (0.6% O_2, 12 hrs), and severe hypoxia (0.01% O_2, 6 hrs).

As the terminal electron acceptor of the ETC, Cox oxidizes cytochrome *c* and reduces O_2 to H_2O, while concomitantly pumping protons across the inner mitochondrial membrane. Cox activity can be quantified spectrophotometrically as a measure of the decrease in absorbance of cytochrome *c* as it is oxidized by Cox. The concentration of cytochrome *c* oxidized by Cox is calculated using Beer's Law, $A = \epsilon cl$, where A is the change in absorbance over time, ϵ is the extinction coefficient (18.2 $mM^{-1}cm^{-1}$) and l is the pathlength (cm). To determine ΔA, the change in absorbance over time was plotted and linear regression was used to determine the slope of the best fit line. Figure 3-2.1.1. shows representative plots of data obtained from cells cultured in atmospheric air, mild hypoxia, and severe hypoxia. It is important to note that the slopes of these lines cannot be compared directly as a measure of Cox activity because the protein concentration of each sample is not the same. Once the concentration of oxidized cytochrome *c* was calculated using Beer's law, Cox activity was expressed as nmol/min/mg protein.

Under conditions of atmospheric air, the enzyme activity of the hypoxia-sensitive M010b cell line was significantly greater ($p<0.05$) than that of the hypoxia-tolerant M006x and M006xLo cell lines (Figure 3-2.1.2). It was also significantly greater than the Cox activity of the HepG2 cell line. The M010b Cox activity was not significantly different from that of the EcR293 cell line.

Mild hypoxia (0.6% O_2, 12 hours) induced an increase in the Cox activity of the M006x cells (48% ± 13%) and M006xLo cells (64% ± 17%) (Figure 3-2.1.3). Although these increases were consistently observed, they were not statistically significant from the control values. On average, M010b Cox activity did not increase in response to mild hypoxia. As well, large inter-experimental variation was observed with M010b cells.

Severe hypoxia (0.01% O_2, 6 hours) induced a slight increase in the Cox activity of the M006x cells (5% ± 8%) and M006xLo cells (29% ± 5%) (Figure 3-2.1.3). Conversely, severe hypoxia resulted in a decrease in Cox activity (15% ± 4%) in the M010b cells. Again, the changes in Cox activity were not statistically significant.

The data from the HepG2 and EcR293 cell lines should be approached with some caution. A large degree of variation in the calculated Cox activity was observed in repeated experiments where HepG2 and EcR293 were incubated in mild and severe hypoxia. In many cases, the calculated activity was much higher than what is normally observed in cultured cells (Dr. Moria Glerum, personal communication). For example, in response to mild hypoxia HepG2 activity ranged from 40 nmol/min/mg to 119 nmol/min/mg. In response to severe hypoxia HepG2 activity ranged from 22 nmol/min/mg to 176 nmol/min/mg. The higher Cox activity levels that were calculated may have been the result of a decrease in cell viability in hypoxic conditions. Thus, we did not include the higher activity levels in the comparison of Cox activity.

Figure 3-2.1.1. Plotting the change in absorbance (550 nm) versus time as cytochrome *c* is oxidized by Cox in order to calculate Cox activity. Linear regression was used to calculate the slope of the best fit line. Each plot is representative of at least 3 independent experiments done in (**A**) atmospheric air, (**B**) 0.6% O_2 for 12 hours, (**C**) 0.01% O_2 for 6 hours.

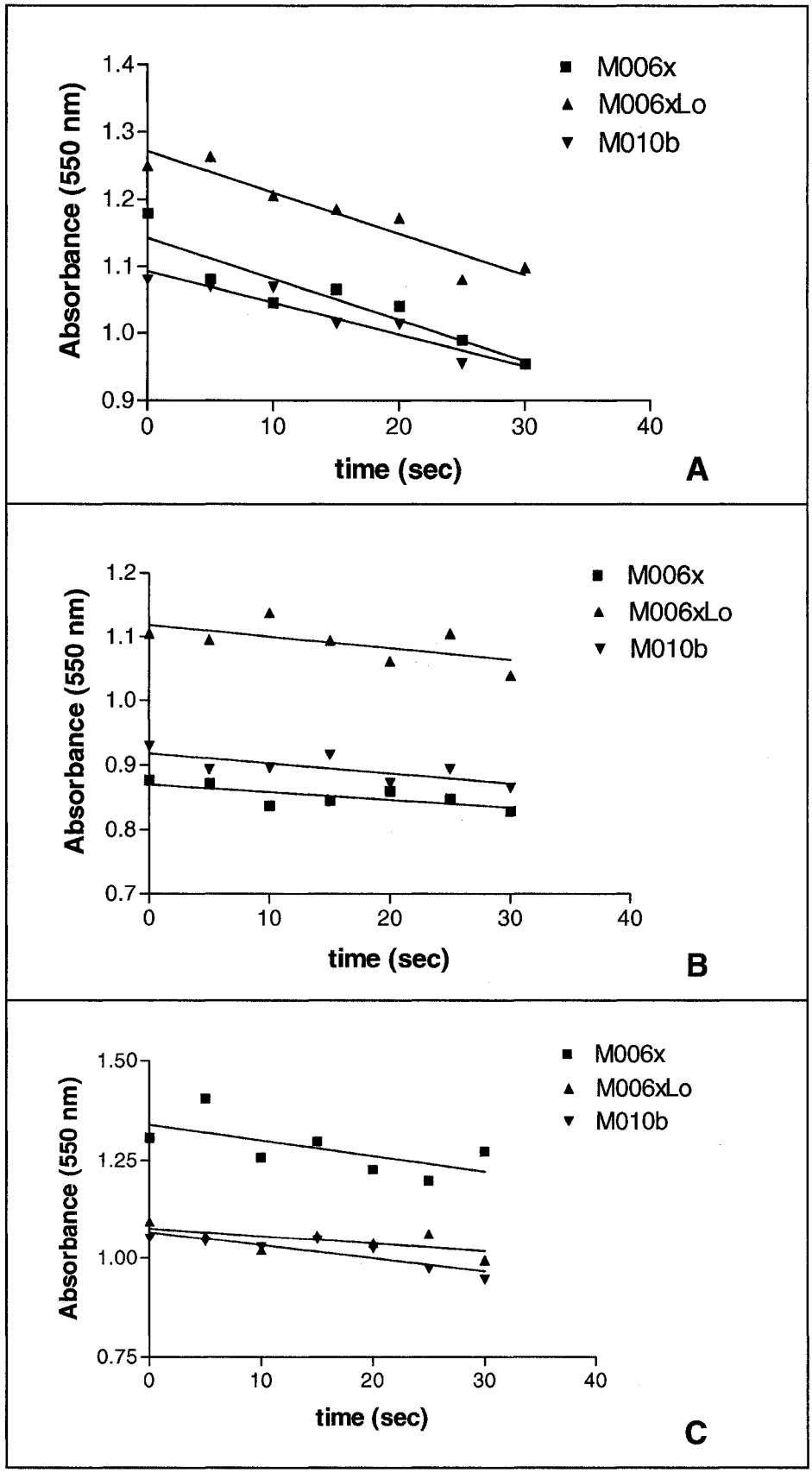

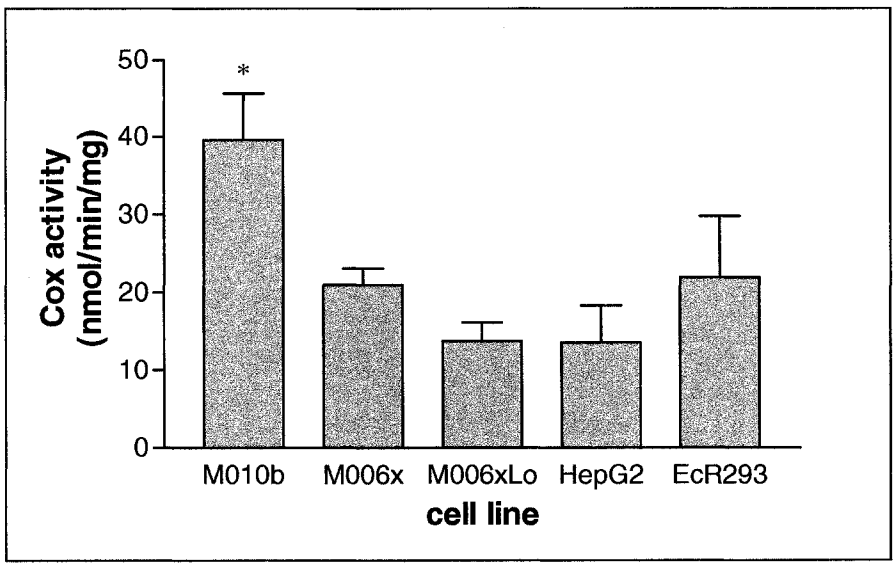

Figure 3-2.1.2. Comparison of the Cox enzyme activity between (hypoxia sensitive) M010b, and (hypoxia tolerant) M006x, M006xLo, HepG2, and EcR293 cell lines cultured in atmospheric air. Data are expressed as nmol/min/mg protein and represent the mean ± SD of triplicate experiments. * The M010b cell line has significantly higher activity ($p<0.05$) than M006x, M006xLo, and HepG2.

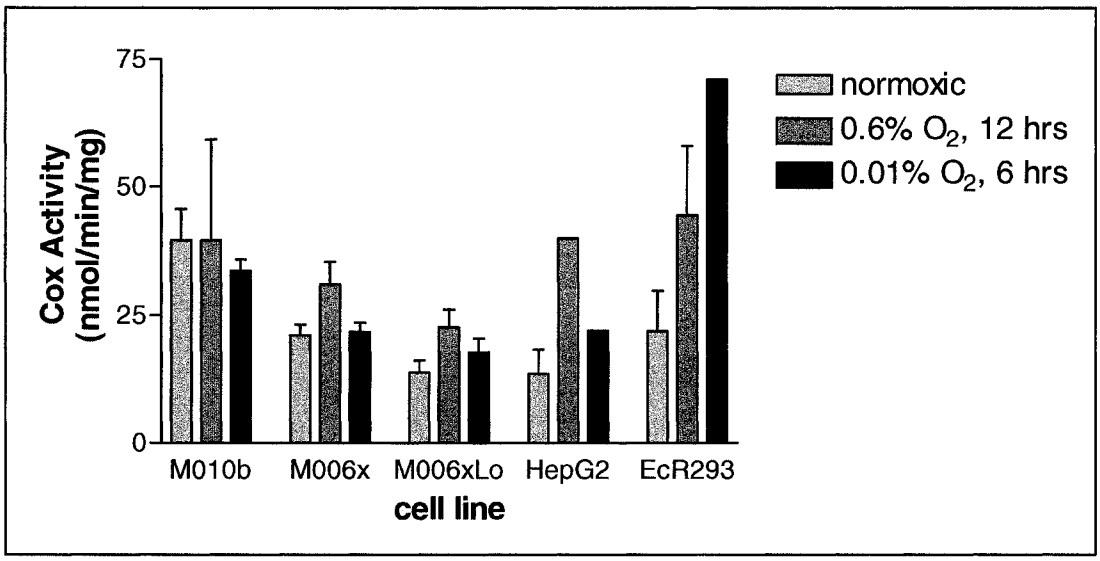

Figure 3-2.1.3. Comparison of the Cox enzyme activity between the (hypoxia sensitive) M010b, and (hypoxia tolerant) M006x, M006xLo, HepG2, and EcR293 cell lines cultured under conditions of mild (0.6% O_2 for 12 hours) and severe (0.01% O_2 for 6 hours) hypoxia. Data are expressed as nmol/min/mg protein, and for the M006x, M006xLo, and M010b cell lines represent the mean ±SD of triplicate experiments. The hypoxic data for HepG2 and EcR293 represent a single experiment, except for the Cox activity of EcR293 in mild hypoxia, which represents 2 experiments. Individual cell lines did not show statistically significant differences in Cox activity when cultured under different O_2 tensions.

3-2.2. Microarray analysis of hypoxia-tolerant and hypoxia-sensitive GBM cell line gene expression

cDNA microarray analysis was used to assess changes in gene expression induced in hypoxia-sensitive and hypoxia-tolerant GBM cell lines in response to hypoxic challenge. RNA from cells cultured in atmospheric air and mild hypoxia (0.6% O_2 for 12 hours) was isolated, reverse transcribed, and labeled with Cy5 and Cy3 fluorescent dyes, respectively. The labeled cDNA was mixed and allowed to hybridize to the microarray slide, which possessed over 13 000 genes spotted in duplicate. The ratio of Cy5 to Cy3

fluorescence was calculated for each spot. Ratios less than one indicated that the gene expression was higher in hypoxic (Cy3) samples, whereas ratios greater than one indicated that the gene expression was higher in atmospheric air (Cy5) samples. Changes in gene expression were considered to be significant if the Cy5/Cy3 ratio was less than 0.5 or greater than 1.5.

We first used the microarray results to compare global differences in gene expression in response to hypoxia among the hypoxia-tolerant and hypoxia-sensitive cell lines. Figure 3-2.2.1 illustrates the differences in the pattern of gene expression between the hypoxia-tolerant M006xLo and hypoxia-sensitive M010b cell lines. The hypoxia-tolerant M006xLo cell line showed greater responsiveness to hypoxia in terms of overall gene expression (Table 3-2.2.1). In M006xLo, 35% of the genes on the microarray showed relatively greater expression in atmospheric air (Cy5/Cy3 > 1.5), compared to only 5.5% of the genes in M010b. Under hypoxia, 10% of the genes in M006xLo showed relatively greater expression (Cy5/Cy3 < 0.5), as compared to only 1.5% in M010b. In M006xLo, 55% of the genes on the microarray did not change expression in response to hypoxia (0.5 < Cy5/Cy3 < 1.5), compared to 93% of the genes in M010b.

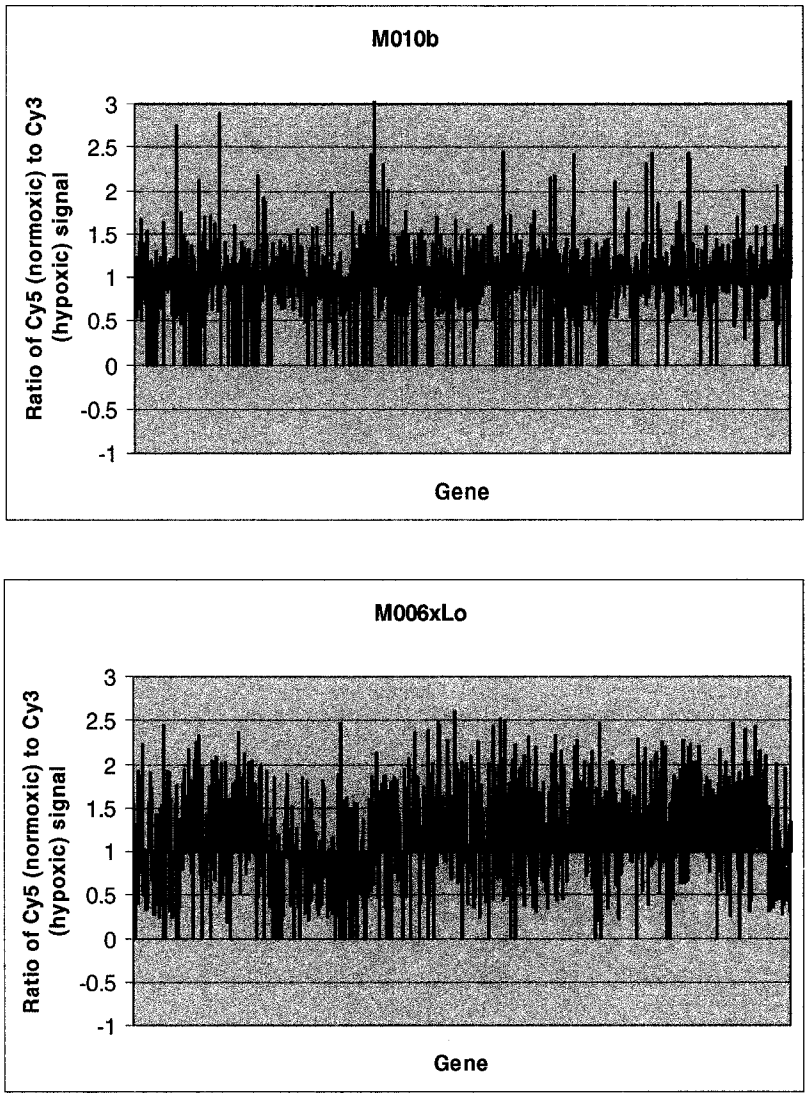

Figure 3-2.2.1. Microarray analysis: comparing the global changes in gene expression induced by hypoxia between hypoxia-sensitive M010b and hypoxia-tolerant M006xLo cell lines.

Table 3-2.2.1. Comparison of the hypoxia-induced global changes in gene expression between hypoxia-tolerant M006xLo and hypoxia-sensitive M010b.

Gene Expression	M006xLo	M010b
> in atmospheric air	35%	5.5%
> in hypoxia	10%	1.5%
No change	55%	93%

The data obtained from the microarray analysis was also used to screen the hypoxic response of clusters of genes involved in different biological pathways important to cancer development. Genes involved in cell adhesion, invasion, the cytoskeleton, and oxidative stress are listed in Table 3-2.2.2, along with genes that are commonly induced by hypoxia.

Finally, the microarray data were used to analyse the effect of hypoxia on the expression of genes involved in bioenergetics. The Operon Human 70-mer oligonucleotide microarray contained 54 genes involved in bioenergetics that yielded a signal in at least one of the cell lines (Table 3-2.2.3).

Table 3-2.2.2. Microarray analysis: hypoxia-induced gene expression in genes important to cancer development. Response is expressed as the ratio of normoxic/hypoxic signal, so that values less than 1.0 indicate greater expression in hypoxia, and values greater than 1.0 indicate expression greater in atmospheric air. Ratios coloured in red signify genes that have significantly higher expression in hypoxic conditions. Ratios coloured in blue signify genes that have significantly higher expression in normoxic conditions. A dashed line indicates that a signal was not detected for the gene of interest.

Gene Category	Gene	Unigene Code	Cell Line		
			M006x	M006xLo	M010b
Invasion, Cytoskeleton, Cell adhesion	Syndecan 4	Hs.252189	-	-	0.45
	Matrin 3	Hs.268939	-	0.46	0.83
	Tubulin α 1, testis specific	Hs.75318	-	-	1.1
	Tubulin α, brain-specific	Hs.524395	0.72	1.1	1.2
	Tubulin γ 1	Hs.279669	-	0.49	-
	Matrilin 3	Hs.6985	1.1	2.4	1.0
	Actin γ	Hs.514581	0.85	2.3	1.3
	Tropomyosin 1	Hs.133892	0.48	1.8	1.1
	Actin β	Hs.520640	1.2	1.7	0.75
	Neuritin	Hs.103291	0.43	-	-
	Endothelin 2	Hs.1407	0.45	-	-
	Matrix metalloproteinase 19	Hs.154057	1.0	1.8	1.2
	Amyloid β (A4) precursor-like protein 1	Hs.74565	-	-	1.5
	Cadherin 2, N-cadherin (neuronal)	Hs.464829	-	0.74	1.0
	Collagen type XVIII, α 1	Hs.517356	-	0.71	0.70
	Connective tissue growth factor	Hs.410037	-	-	1.8
	Catenin, α 1	Hs.445981	-	-	1.4
	Endoglin	Hs.76753	-	-	0.59
	FAT tumor suppressor homolog 1	Hs.481371	-	-	1.0
	Intercellular adhesion molecule 4	Hs.386467	1.1	1.3	1.0
	Laminin, β 1	Hs.489646	-	-	0.75
	Microfibrillar-associated protein 4	Hs.389137	0.56	-	-
	Myosin-binding protein C (cardiac)	Hs.524906	1.92	0.93	0.81
	Nephrosis 1, congenital	Hs.122186	1.1	1.7	0.91

Gene Category	Gene	Unigene Code	Cell Line		
			M006x	M006xLo	M010b
Oxidative Stress	Anti-oxidant protein 1	Hs.279910	1.1	-	-
	Dual specificity phosphatase	Hs.171695	-	-	2.2
	Glutathione peroxidase 1	Hs.76686	0.81	1.4	0.65
	Superoxide dismutase 1	Hs.443914	0.44	0.91	0.98
Hypoxia-responsive genes	Hypoxia inducible factor-1α	Hs.509554	-	-	1.1
	Jun D proto-oncogene	Hs.2780	0.95	0.68	0.91
	Vascular endothelial growth factor C	Hs.435215	-	0.82	0.72
	Vascular endothelial growth factor	Hs.73793	-	-	0.56

Table 3-2.2.3. Bioenergetic gene response to mild hypoxia. Response is expressed as the ratio of normoxic/hypoxic signal, so that values less than 1.0 indicate greater expression in hypoxia, and values greater than 1.0 indicate expression greater in atmospheric air. Ratios coloured in red signify genes that have significantly higher expression in hypoxic conditions. Ratios coloured in blue signify genes that have significantly higher expression in normoxic conditions. A dashed line indicates that a signal was not detected for the gene of interest.

Gene	UniGene Code	Cell Line		
		M006x	M006xLo	M010b
6-phosphofructo-2-kinase/fructose-2,6-biphosphatase 3	Hs.195471	0.44	-	0.30
Aldolase A, fructose-bisphosphate	Hs.513490	0.84	1.6	0.54
ATP synthase epsilon chain, mitochondrial	Hs.177530	1.2	-	-
ATP synthase, H+ transporting, mitochondrial F0 complex, subunit b, isoform 1	Hs.514870	0.70	-	0.74
ATP synthase, H+ transporting, mitochondrial F0 complex, subunit c isoform 3	Hs.429	0.93	-	1.3
ATP synthase, H+ transporting, mitochondrial F0 complex, subunit F6	Hs.246310	0.79	0.30	-
ATP synthase, H+ transporting, mitochondrial F0 complex, subunit d	Hs.514465	0.63	-	-
ATP synthase, H+ transporting, mitochondrial F1 complex, alpha subunit, isoform 1	Hs.298280	0.72	0.61	-
ATP synthase, H+ transporting, mitochondrial F1 complex, beta polypeptide	Hs.406510	0.82	0.65	0.83
ATPase inhibitory factor 1	Hs.241336	0.49	-	0.54
ATPase, Na+/K+ transporting, beta 3 polypeptide	Hs. 477789	-	-	0.56
Complex I Fe-S protein 4	Hs528222	0.91	-	0.92
Complex I Fe-S protein 5	Hs.472185	1.2	0.53	0.90
Complex I Fe-S protein 6	Hs.408257	-	-	1.1
Complex I flavoprotein 2	Hs.464572	0.79	-	-
Complex I subcomplex unknown, 1	Hs.84549	0.78	0.64	0.71
Complex I α subcomplex, 1	Hs.534168	0.67	0.86	1.0
Complex I α subcomplex, 5	Hs.83916	0.62	-	0.63
Complex I α subcomplex, 6	Hs.274416	0.81	0.53	1.0

Gene	UniGene Code	Cell Line		
		M006x	M006xLo	M010b
Complex I α subcomplex, 7	Hs.515122	0.84	0.5	0.70
Complex I β subcomplex, 1	Hs.183435	0.41	0.66	0.85
Complex I β subcomplex, 2	Hs.324250	0.67	0.41	0.66
Complex I β subcomplex, 3	Hs.109760	-	0.47	1.2
Complex I β subcomplex, 4	Hs.304613	1.0	0.66	1.0
Complex I β subcomplex, 5	Hs.518424	0.87	0.58	1.6
Complex II subunit D, integral membrane protein	Hs.356270	-	0.50	0.69
Complex II, subunit A, flavoprotein	Hs.440475	-	-	0.92
Complex II, subunit C, integral membrane protein	Hs.444472	0.91	1.4	1.2
Complex III binding protein	Hs.131255	0.85	0.97	-
Complex III hinge protein	Hs.449049	1.0	0.86	0.88
Cox 17 yeast homolog	Hs.534383	0.78	-	1.0
Cytochrome b5 reductase 3	Hs.517666	0.50	-	0.41
Cytochrome *c*	Hs.437060	1.0	-	1.5
Glyceraldehyde-3 phosphate dehydrogenase	Hs.479728	0.97	1.5	0.51
Isocitrate dehydrogenase 2, mitochondrial	Hs.513141	0.83	0.31	0.65
Isocitrate dehydrogenase 3 beta	Hs.436405	1.2	-	-
Lactate dehydrogenase A	Hs.2795	-	1.4	-
Lactate dehydrogenase B	Hs.446149	0.83	1.1	1.2
Nuclear respiratory factor 1	Hs.298069	-	1.2	-
Phosphofructokinase, platelet	Hs.26010	0.5	-	0.50
Phosphoglycerate kinase 1	Hs.78771	0.61	-	0.91
Phosphoglycerate mutase 1 (brain)	Hs.447492	0.64	1.1	0.47
Succinate-CoA ligase GDP forming α subunit	Hs.270428	1.9	-	1.4

When we looked more closely at the subset of genes involved in oxidative phosphorylation, we observed that several of the genes were expressed more under hypoxic conditions (Figure 3-2.2.2). For example, several Complex I subunits and ATPase subunits were expressed to a greater extent in hypoxic cells than in cells that had been cultured in atmospheric air (Figure 3-2.2.2). Consistent with other reports, hypoxic culture also induced an increase in the expression of glycolytic enzymes such as 6-phosphofructo-2-kinase.

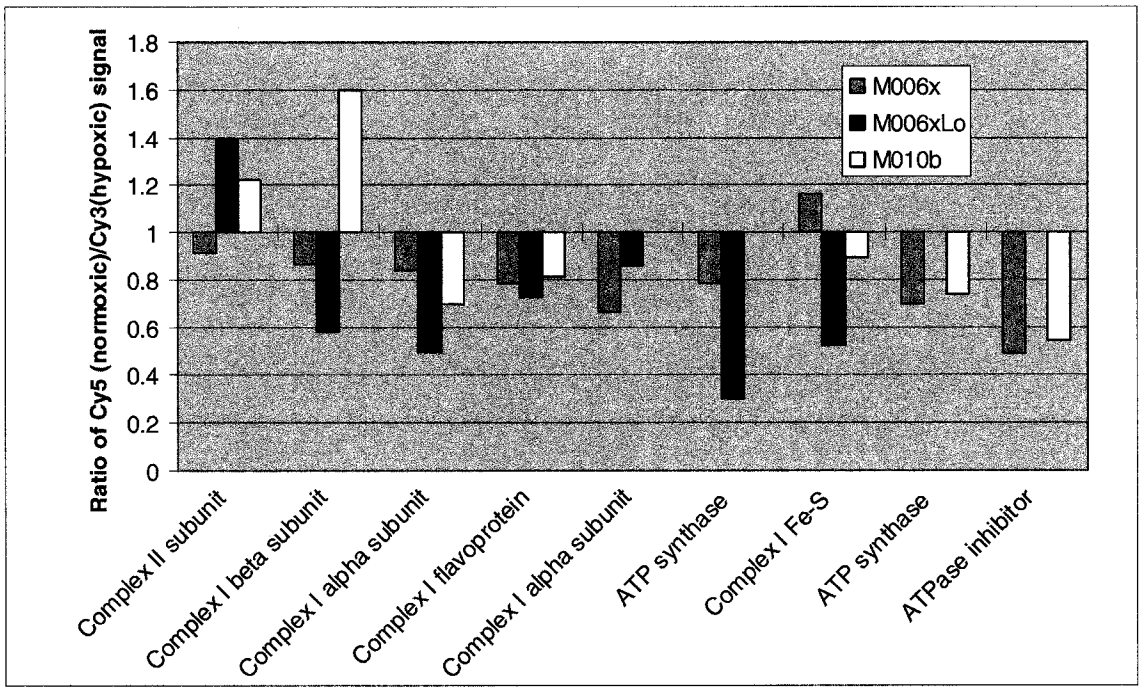

Figure 3-2.2.2. Microarray analysis: the effect of mild hypoxia (0.6% O_2 for 12 hours) on the expression of a selection of genes involved in oxidative phosphorylation in the M006x, M006xLo, and M010b cell lines. A ratio less than 1.0 indicates that expression was higher in the hypoxic cells, while a ratio greater than 1.0 indicates that expression was higher in the cells cultured in atmospheric air.

When we compared the expression of the nuclear-encoded Cox subunits in the hypoxia-tolerant and hypoxia-sensitive cell lines, we observed differential expression of subunits that was dependent on the cell line in question (Figure 3-2.2.3). All of the cell lines showed increased expression of CoxVIa(L), CoxVIIa(H), and CoxVIIb under hypoxic conditions. The hypoxia-sensitive cell line M010b also showed increased expression of several other Cox subunits, including CoxIV-1, CoxVa, CoxVb, CoxVIb, and CoxVIII under hypoxic conditions. M006x and M006xLo, the two hypoxia-tolerant cell lines, showed a similar pattern of expression: they both had decreased expression of CoxVb and CoxVIb, and increased expression of Cox7c.

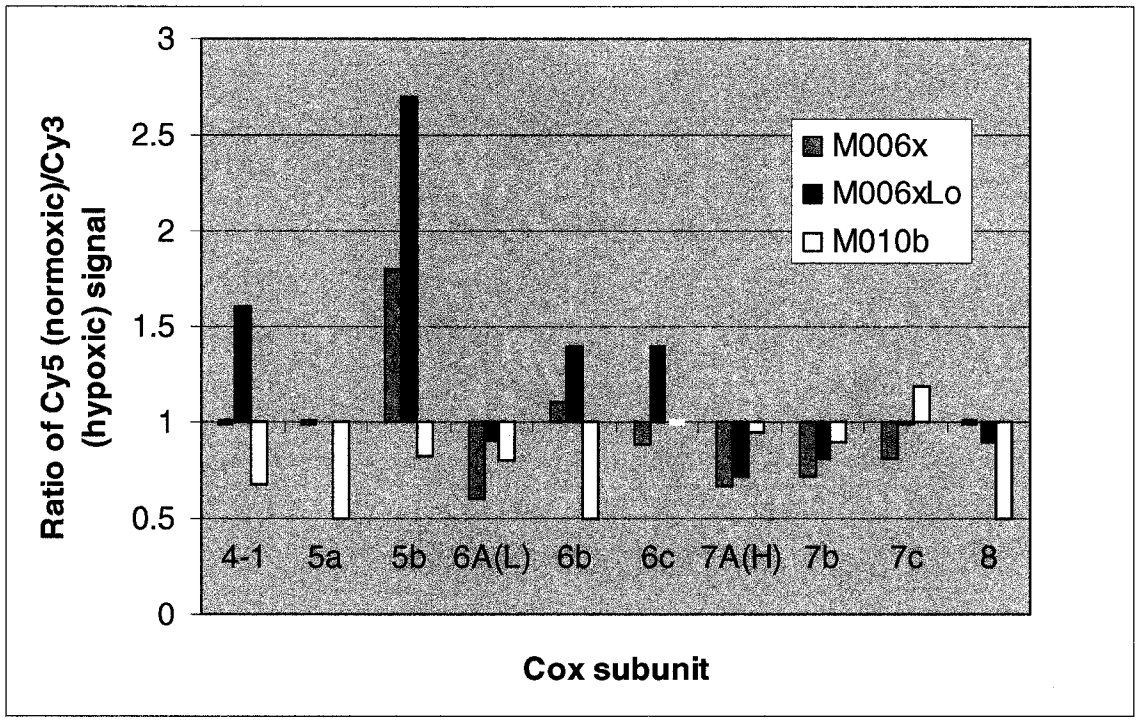

Figure 3-2.2.3. Microarray analysis: the effect of mild hypoxia (0.6% O_2 for 12 hours) on the expression of nuclear-encoded Cox subunits in the M006x, M006xLo, and M010b cell lines. A ratio less than 1.0 indicates that expression was higher in the hypoxic cells, while a ratio greater than 1.0 indicates that expression was higher in the cells cultured in atmospheric air.

3-2.3. Nuclear-encoded Cox Subunit Expression Analysis: Quantatative RT-PCR

The results of the microarray analysis suggested that there were some differences in the expression of the nuclear-encoded Cox subunits between hypoxia-tolerant and hypoxia-sensitive GBM cell lines. To validate these observations, we performed semi-quantitative real time RT-PCR, focusing particularly on the Cox subunits that were expressed as tissue-specific isoforms. Figure 3-2.3.1 summarizes the results of the expression analysis performed on cell lines cultured in atmospheric air. In this figure, the M006x, M006xLo, HepG2, and EcR293 subunit expression levels were made relative to the M010b levels, which were normalized to 1.0. The only exception was CoxIV-2, which was not expressed in M010b. In this case, CoxIV-2 expression in M006x was made relative to expression in M006xLo, whose CoxIV-2 expression was normalized to 1.0. The CoxVb and CoxVIa(L) subunits had similar levels of expression across all cell lines. The CoxVIIa(L) expression was at least 2 fold lower in M006x, M006xLo, HepG2, and EcR293 cell lines compared to M010b. The CoxVIIa(H) expression of M006x and M006xLo was 2.8 and 4.2 fold greater than M010b, respectively. Of particular interest is the fact that the CoxIV-2 isoform was expressed only in the hypoxia-tolerant M006x and M006xLo cell lines. The mammalian CoxIV subunit is homologous to the yeast subunit V, which is expressed as either Va or Vb in an oxygen-dependent way. This raises the possibility that the CoxIV isoforms might also be regulated in an oxygen-dependent manner, and that the incorporation of the different CoxIV isoforms into the holoenzyme may change the kinetic properties of the enzyme.

We next compared the levels of CoxIV-1 and CoxIV-2 isoform expression specifically, in the M006x, M006xLo, and M010b cell lines. Figure 3-2.3.2 shows the

relative amounts of CoxIV-2 isoform expressed relative to CoxIV-1 in atmospheric air. In M006x, CoxIV-2 expression occurred at the limit of detection, and was approximately 0.5% of CoxIV-1 expression. In M006xLo, the CoxIV-2 RNA expression was 12.5% of the CoxIV-1 expression. In M010b, CoxIV-2 RNA was not detected.

The effect of hypoxia on the expression of the CoxIV isoforms was then examined. M006x, M006xLo, and M010b cells were subjected to mild (0.6% O_2) or severe (0.01% O_2) hypoxia, or to 100 μM cobalt chloride (a hypoxia-mimetic compound) for 12 hours, and RNA was extracted for expression analysis. Importantly, in order to exclude the possibility that extracting the RNA in room air would affect the expression of the Cox subunits, we compared the expression levels of Cox RNA extracted in the glove box at 0.6% O_2 with RNA extracted in room air. There was no significant difference in the expression levels.

Neither hypoxia nor $CoCl_2$ caused significant changes to the ratio of CoxIV-1 to CoxIV-2 RNA expressed (Figure 3-2.3.3). Furthermore, when the expression of the CoxIV isoforms was compared in cells cultured in air with cells cultured under hypoxic conditions, we found that there was no significant change in expression (Figure 3-2.3.4.). Here, the isoform expression in hypoxia is compared to the isoform expression in atmospheric air, which has been normalized to 1.0. It should be noted that the CoxIV-2 expression in M006x cells appears to be at the limit of detection by real time RT-PCR, as it was not detected in all samples that were cultured in atmospheric air. Thus, the magnitude of change in expression shown in Panel A of Figure 3-2.3.4 may be less significant than is indicated.

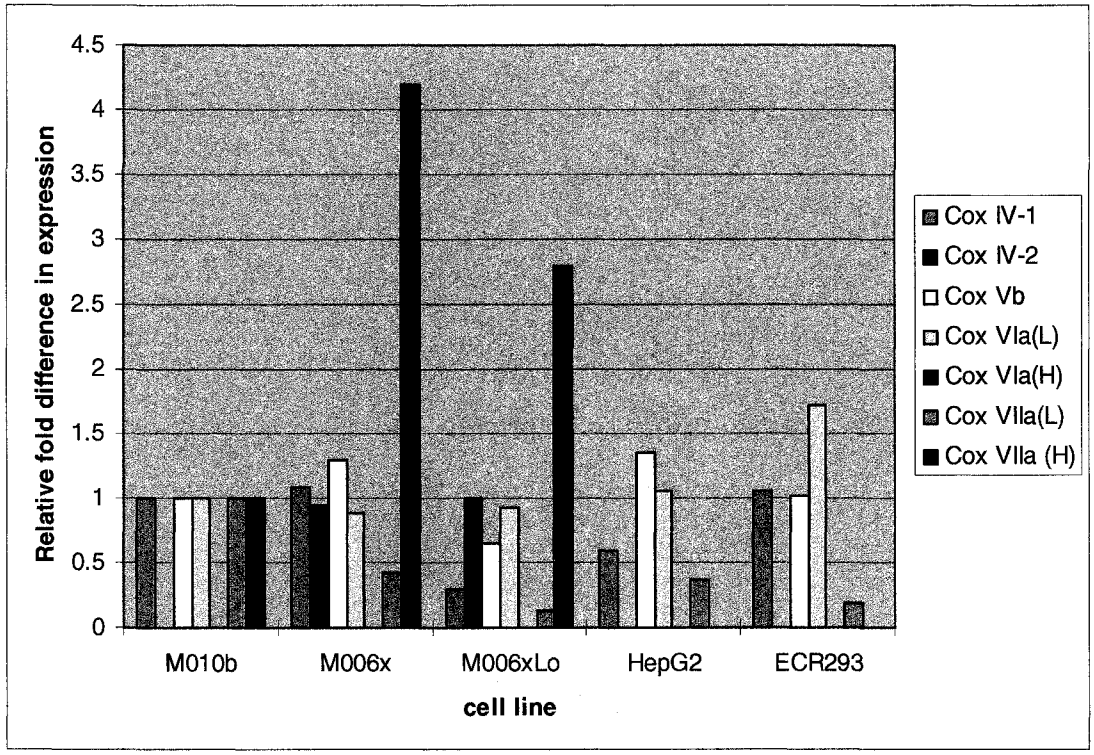

Figure 3-2.3.1. Semi-quantitative RT-PCR of nuclear-encoded Cox subunits from cell lines cultured under atmospheric air. All subunit expression levels, except CoxIV-2, were normalized to those of the M010b cell line. CoxIV-2 expression in M006x was normalized to CoxIV-2 expression in M006xLo.

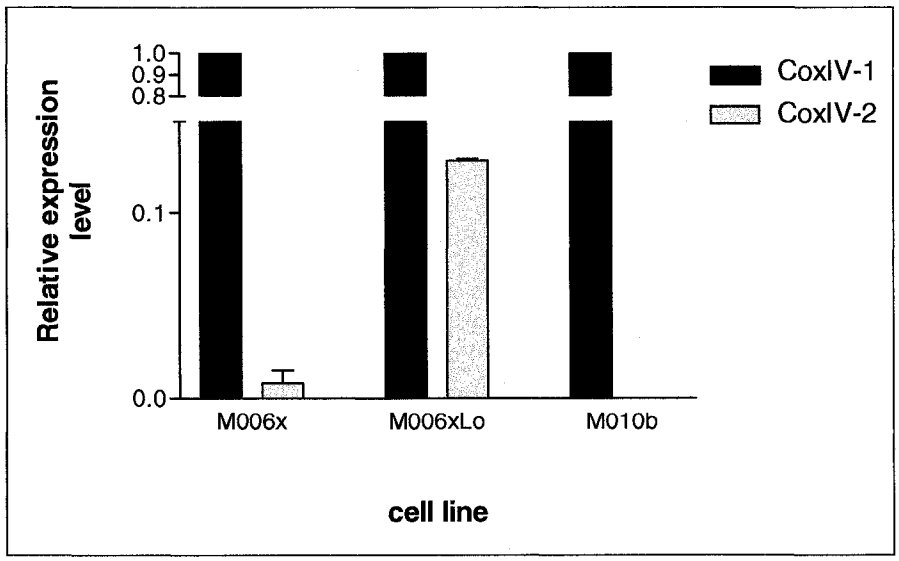

Figure 3-2.3.2. Semi-quantitative RT-PCR comparing the ratio of CoxIV-2 to CoxIV-1 expressed in cells cultured in atmospheric air.

Figure 3-2.3.3. Semi-quantitative RT-PCR comparing the effects of (**A**) mild hypoxia: 0.6% O_2 for 12 hours; (**B**) severe hypoxia: 0.01% O_2 for 12 hours; (**C**) 100 μM $CoCl_2$ for 12 hours on the ratio of CoxIV-2 to CoxIV-1 expression.

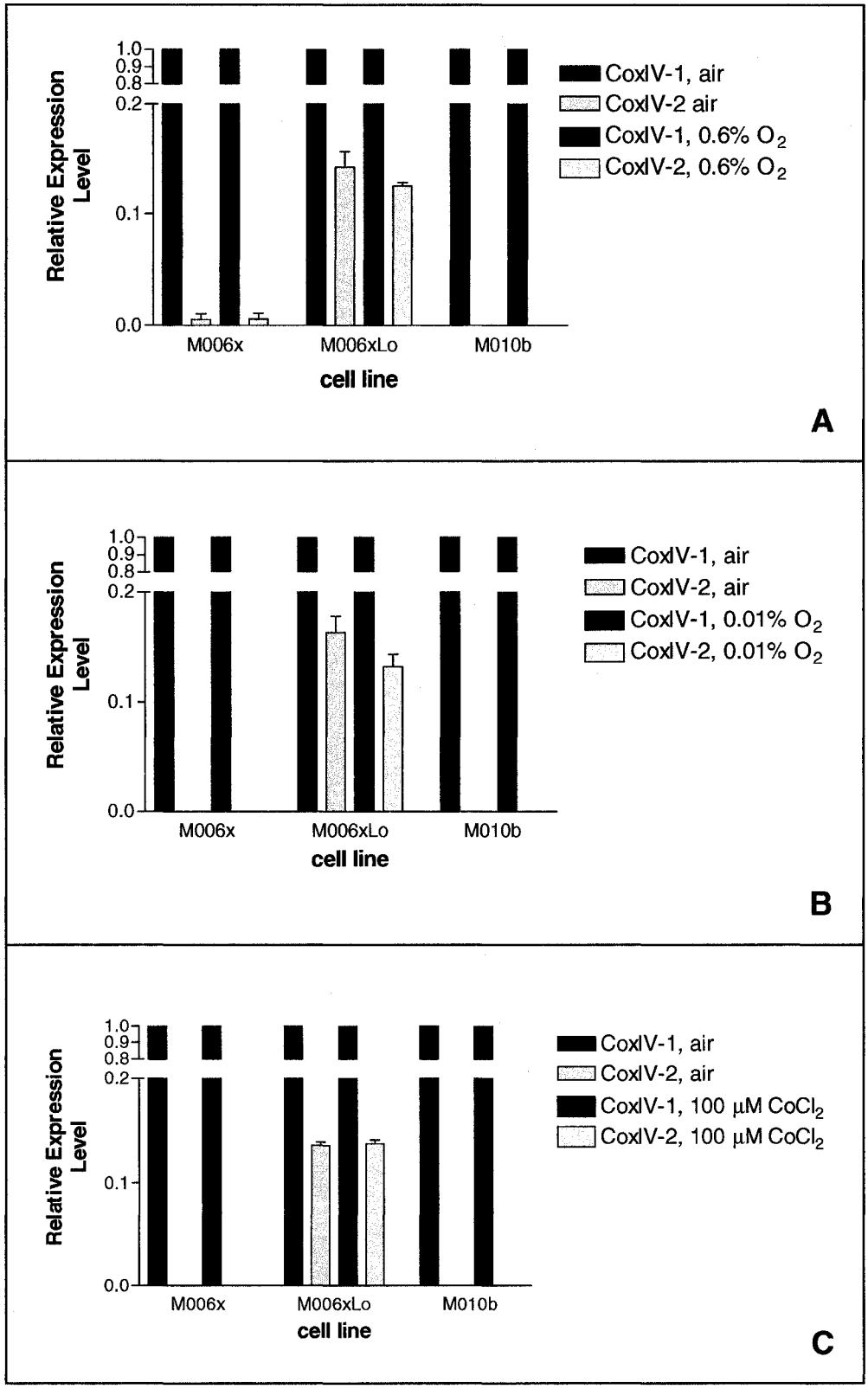

Figure 3-2.3.4. Semi-quantitative RT-PCR comparing the effects of (**A**) mild hypoxia, 0.6% O_2 for 12 hours; (**B**) severe hypoxia, 0.01% O_2 for 12 hours; (**C**) 100 μM $CoCl_2$ for 12 hours on CoxIV isoform expression. The CoxIV isoform expression under conditions of atmospheric air was normalized to 1.0 and hypoxic expression was made relative to this.

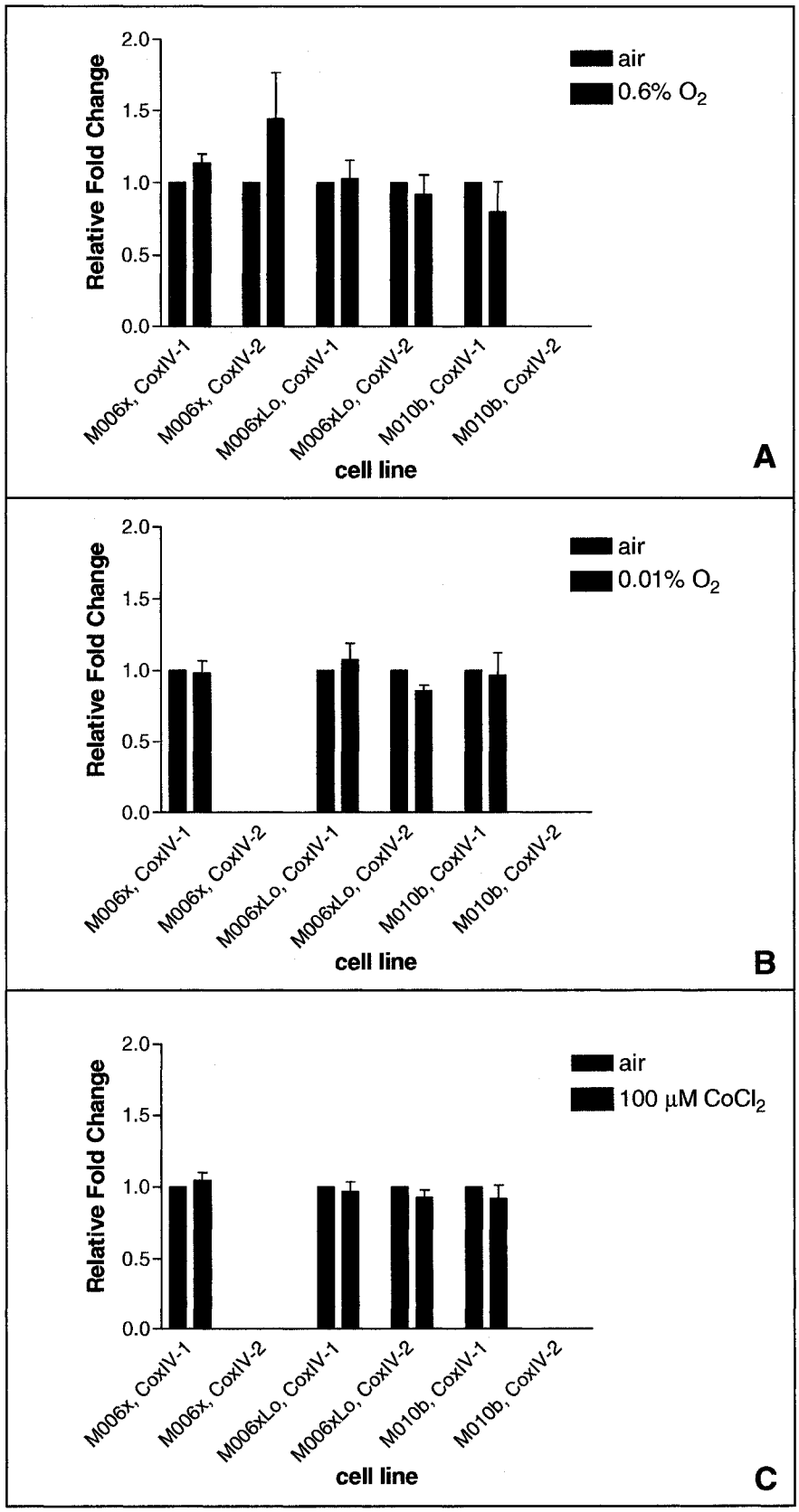

3-2.4. Transcriptional Run-off Experiments

Transcription run-off assays were used to analyze the transcription rates of the CoxIV isoforms in order to determine if the higher levels of CoxIV-1 mRNA expression observed in the M006x and M006xLo cells was due to higher rates of transcription. ssDNA probes against the genes of interest (CoxIV-1, CoxIV-2) and internal controls (RPS27A, GAPDH, H2B, and γ-actin 5′) were created using M13mp18 (expressing the sense strand) and M13mp19 bacteriophage (expressing the anti-sense strand) as cloning vectors (Figure 3-2.4.1). The GAPDH, H2b, and γ-actin 5′ constructs were kindly provided by Dr. Charlotte Spencer (Department of Experimental Oncology, University of Alberta). The nuclei of cells that had been subjected to atmospheric air or mild (0.6% O_2) hypoxia were harvested; the transcripts that had been initiated at the time of harvest were further elongated in the presence of ^{32}P ribonucleotides. Then, the labeled RNA was purified and allowed to hybridize to the membrane-bound ssDNA probes. HeLa S3 cells were used as a positive control for the assay, as GAPDH, H2B, and γ-actin 5′ RNA had been successfully detected in this cell line in other studies. RPS27A acted as a loading control, as microarray studies had previously established that its expression does not change under hypoxia. GAPDH was used as a positive control because published reports show that GAPDH expression increases 20-75% under hypoxic conditions, depending on the cell line (Zhong and Simons, 1999).

As seen in Figure 3-2.4.2, we were not able to obtain signals for the CoxIV-1 or CoxIV-2 RNA. This could be because the amount of transcript was too small to be detected by this assay. The fact that we were able to obtain signal from more abundant

housekeeping genes such as GAPDH, H2B, and γ-actin 5′ suggests that the assay was working, but further optimization may be necessary.

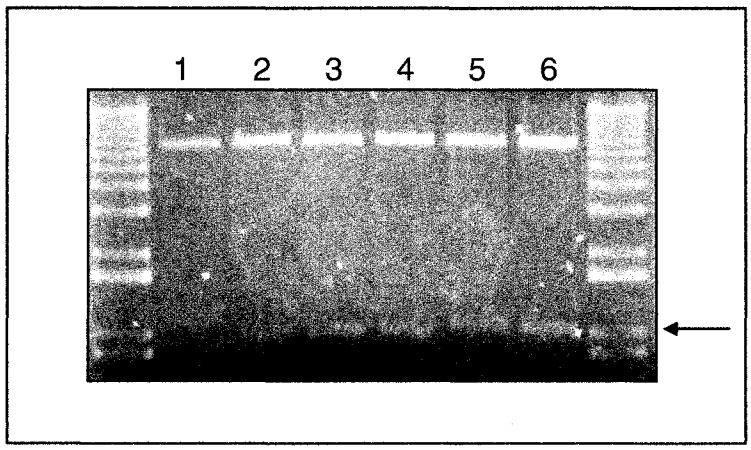

Figure 3-2.4.1. Verification of the cloning of CoxIV-1, CoxIV-2, and RPS27A into the M13mp18 and M13mp19 bacteriphage vectors. The replicative form of the cloned M13 bacteriophage were isolated and digested with *Bgl*II and *EcoR*I (M13mp18) and *Bgl*II and *Hind*III (M13mp19). (**1**) M13mp18/CoxIV-1, (**2**) M13mp19/CoxIV-1, (**3**) M13mp18/CoxIV-2, (**4**) M13mp19/CoxIV-2, (**5**) M13mp18/RPS27A, (**6**) M13mp19/RPS27A.

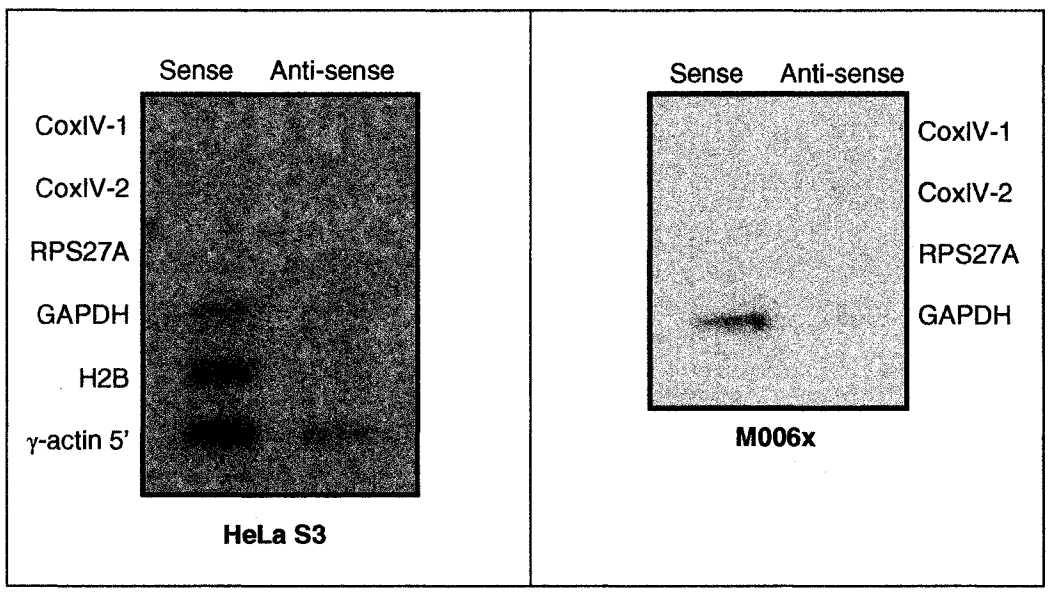

Figure 3-2.4.2. Transcription run-off analysis of CoxIV-1 and CoxIV-2 in HeLa S3 and M006x cells. RPS27A, GAPDH, H2B, and γ-actin 5′ are endogenous controls.

3-3 The Expression Pattern of Neuroglobin in Glioma Cell Lines

Neuroglobin is a newly discovered protein belonging to the globin superfamily. It is found primarily in the nerve cells of the vertebrate brain, and is thought to function as a neuroprotective agent during hypoxic stress. Because of the known ability of globin molecules (eg., hemoglobin) to transport molecular oxygen, we tested whether Ngb was expressed in glioblastoma cell lines, and whether its expression was affected by hypoxic conditions.

Initially, a panel of malignant glioma (A172, U87, CLA, M016, M0125) and neuroblastoma (UAN, SU-N-BE2C, GOTO, LAN-1, IMR32) cell lines was screened for Ngb expression. The RNA from these cells was kindly provided by Dr. Roseline Godbout (Department of Experimental Oncology, University of Alberta). Human cerebellum and medulla total RNA (Ambion) were used as positive controls. Although we used two different sets of primers, and a range of annealing temperatures, we were unable to amplify Ngb cDNA as a single, reproducible band. For example, Figure 3-3.1 shows three attempts at amplifying Ngb cDNA using human brain RNA (positive control) and the panel of malignant glioma and neuroblastoma cell lines with annealing temperatures of 59°C, 61°C and 63°C, and using the Ngb-3 and Ngb-4 primers. The PCR product obtained from the cerebellum RNA (lane 2) was the expected size for Ngb (466 bp), and its identity as Ngb was verified by sequencing. At 59°C, the SK-N-BE2C and LAN-1 cell lines appear to express Ngb (Figure 3-3.1., panel A). When the annealing temperature is raised to 61°C, only LAN-1 appears to express Ngb (Figure 3-3.1., panel B). And when the annealing temperature is raised again to 63°C, only the U87 cell line shows amplification of a band of the correct size (Figure 3-3.1, panel C).

As the RT-PCR analysis of Ngb expression in malignant glioma was inconclusive, Northern Blot analysis was used to establish its expression pattern. A probe, made using human cerebellum RNA, was used to detect Ngb in two malignant cell lines (M059K, and U87) that had been exposed to both atmospheric air and mild hypoxia (0.6% O_2, 12 hrs) (Figure 3-3.2). Ngb was detected in both the M059K and U87 cell lines cultured in room air. Mild hypoxia resulted in a decrease in Ngb expression in these cell lines.

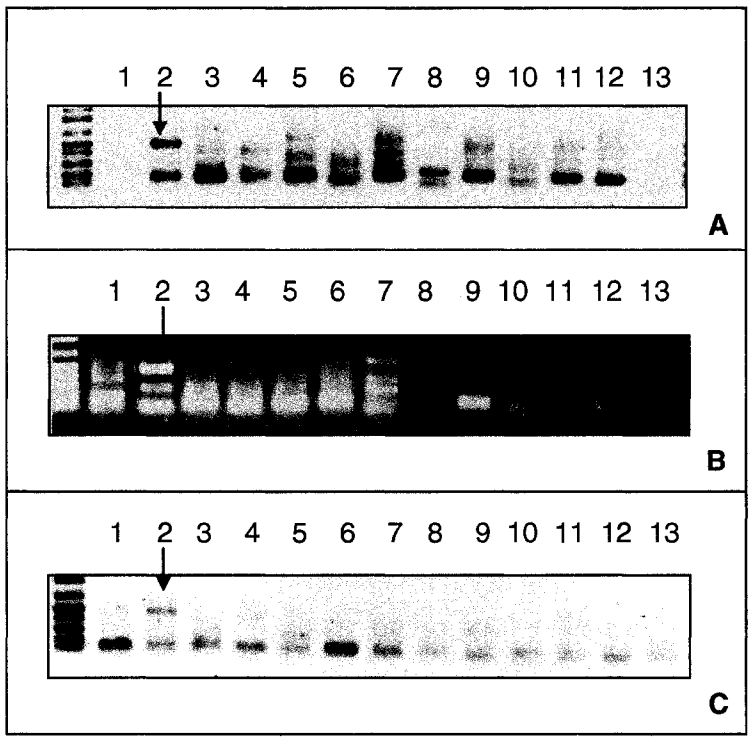

Figure 3-3.1. RT-PCR analysis of Ngb expression in (1) medulla, (2) cerebellum, (3) A172, (4) U87, (5) CLA, (6) M016, (7) M0125, (8) KAN, (9) SK-N-BE2C, (10) GOTO, (11) LAN-1, (12) IMR-32, (13) H_2O using primer annealing temperatures of (**A**) 59°C, (**B**) 61°C, and (**C**) 63°C.

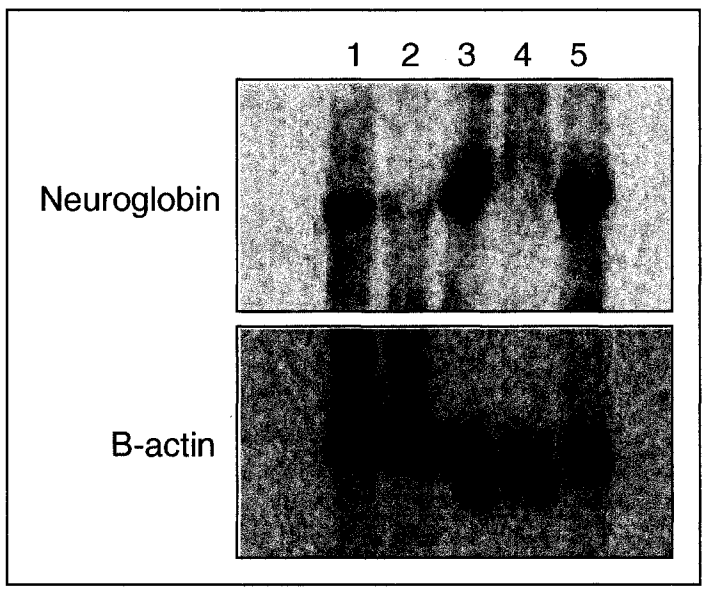

Figure 3-3.2. Northern Blot analysis of Ngb expression in malignant glioma cell lines exposed to mild hypoxia (0.6% O_2 for 12 hours) or to atmospheric air. (1) U87, atmospheric air; (2) U87, mild hypoxia; (3) M059K, atmospheric air; (4) M059K, mild hypoxia; (5) RNA from human cerebellum, used as a positive control.

CHAPTER 4: DISCUSSION

4-1 WAVE Analysis

WAVE analysis has been used successfully for the screening of germline mutations in cancer genes such as *BRCA 1*, *BRCA 2*, and the *MET* proto-oncogene (Klein *et al.*, 2001). There have also been several reports of WAVE analysis being used to screen for mtDNA mutations and mtDNA heteroplasmy (van den Bosch *et al.*, 2000; Liu *et al.*, 2002; Conley *et al.*, 2003; Biggin *et al.*, 2005). We wanted to take advantage of the efficiency and cost effectiveness of the WAVE system to screen for mutations in Complex I mtDNA from cervical cancer specimens in order to determine if there was a correlation between the presence of mtDNA mutations and prognosis.

We divided the region of mtDNA encoding the Complex I subunits into a set of smaller fragments that could be analyzed by WAVE and evaluated the sensitivity and reproducibility of the WAVE using previously sequenced mtDNA. The WAVE was successful at detecting the presence of mutations 91% of the time, a detection rate that is comparable to other published results [88% for mtDNA encoded mutations (Biggin *et al.*, 2005); 95% for nDNA-encoded VHL mutations (Klein *et al.*, 2001)]. Unfortunately, due to the nature of mtDNA, we were unable to take advantage of the WAVE's true benefit: the identification of mutations within a large region of interest, so that unnecessary sequencing is eliminated. The sequenced mtDNA we used to test the WAVE was isolated from two healthy, 'normal' donors, yet in one sample eleven out of the twelve fragments had sequence variations. This is not surprising considering that there are over 1000 known polymorphisms covering all regions of the mtDNA genome (Biggin *et al.*,

2005). Intrinsically, mtDNA has a much higher mutation rate than nuclear-encoded DNA; recent reports estimate that synonymous sites evolve twenty times more rapidly in mtDNA than in the nuclear DNA, while non-synonymous sites evolve at different rates, depending on the gene in question (Pesole *et al.,* 1999). There are several reasons for this increased mutation rate. First, mtDNA is not protected by histones. Second, mtDNA is subjected to a high level of ROS damage as a result of its association with the inner mitochondrial membrane; our sequencing results support this as 94% of the sequence variations were transitions, a mutations often arising as a result of oxidative damage. Third, the mitochondrial repair mechanisms are less effective than their nuclear counterparts (Fernandez-Silva, 2003).

In our experiment, we used blood samples from two unrelated individuals. If patient blood samples had been available, a better procedure might have been to compare the mtDNA from the matched blood and tumor material from a single patient. This way, we would have avoided the detection of so many polymorphisms. On the other hand, the functional significance of the polymorphisms in the coding regions of mtDNA is not known, and should probably not be disregarded. mtDNA polymorphisms have been associated with diseases as varied as Parkinson's disease (Tan *et al.,* 2000) and bi-polar disorder (Kato, 2001). One study also correlated the differentiation degree of gastric cancer with the frequency of polymorphisms in the 12S rRNA and $tRNA^{Phe}$ coding regions (Han *et al.,* 2003).

One possible benefit of using the WAVE to screen mtDNA mutations is the WAVE's ability to detect heteroplasmic mtDNA mutations. Since multiple copies of mtDNA are present in a single cell, mutations can arise and be maintained within a subset

of the mtDNA while other genomes remain wildtype (Fernandez-Silva, 2003). Heteroduplex analysis could be performed using a single sample. If different populations of mtDNA were present, they would be identified by the WAVE. Other studies have shown that DHPLC is capable of detecting heteroplasmy down to 1% (Meierhofer *et al.*, 2005), compared to 40% for conventional sequencing (Biggin *et al.*, 2005).

4-2 Hypoxia Adaptation

The oxygen tensions we used for all of our experiments (0.6% O_2 and 0.01% O_2) are oxygen levels that are commonly recorded in solid tumors (Brown, 1999; Vaupel and Harrison, 2004). Clinical investigations have shown that oxygen tensions of less than 0.35% O_2 are a common pathophysiological property of many solid tumors including cancers of the breast, prostate, uterine cervix, brain, and head and neck (Vaupel, 2004). Studies have shown that sustained hypoxia (1% O_2 for 6-8 hours) results in alterations of gene expression, as well as post-transcriptional and post-translational modifications in malignant tumors (Hockel and Vaupel, 2001).

When we examined the global changes in gene expression in GBM cells that had been exposed to mild hypoxia (0.6% O_2 for 12 hours), we immediately recognized a difference in the expression pattern between hypoxia-tolerant (M006xLo) and hypoxia-sensitive (M010b) cell lines. On a broad scale, it appeared that the hypoxia-tolerant M006xLo cell line was much more responsive to hypoxia than the hypoxia-sensitive M010b cell line. This is illustrated by the fact that 45% of the M006xLo genes identified on the microarray were transcriptionally responsive to hypoxia (with 35% of the genes

downregulated in hypoxia and 10% of the genes upregulated in hypoxia). This is in contrast to the M010b cell line: only 7% of its genes were hypoxia responsive.

Studies in comparative physiology have indicated that energy conservation is an important adaptive step towards hypoxia tolerance. It is part of an overall metabolic defense strategy that involves the consolidation of ATP supply and demand through the down-regulation of ATP-utilizing processes and the promotion of more efficient ATP production (Hochachka's Unifying Theory of Hypoxia Tolerance) (Hockachka *et al.,* 1996). For example, under normoxic conditions, protein turnover represents a major ATP sink, and it accounts for as much as 55% of total ATP consumption in hypoxia-tolerant organisms such as *Chrysemys picta* (a freshwater turtle) (Boutilier and St. Pierre, 2000). When these organisms are exposed to hypoxia, the demand for ATP for protein turnover drops to 10% of normoxic levels (Boutilier and St. Pierre, 2000). Indeed, the ability to down-regulate protein turnover is a hallmark of hypoxia adaptation (Guppy *et al.,* 2005). Our results suggest that tumor cell adaptation to hypoxia could follow a similar strategy of metabolic depression.

Previous experiments from our lab indicated that hypoxia-tolerant and hypoxia-sensitive GBM cell lines exhibit distinct patterns of mitochondrial function, in terms of the maintenance of mitochondrial membrane potential (MMP) and ATP concentrations, in response to hypoxic challenge (Turcotte *et al.,* 2002). These functional parameters are also commonly used to characterize the hypoxia-tolerance of normal tissues from different organisms. The MMP of the hypoxia-sensitive M010b cells increases in response to mild (0.6% O_2) hypoxia, while the MMP of the hypoxia-tolerant M006x and M006xLo remains constant (Turcotte *et al.,* 2002). Furthermore, in contrast to hypoxia-

tolerant cell lines, the hypoxia-sensitive cells are unable to maintain constant intracellular ATP concentrations during extended hypoxic incubation (Turcotte *et al.,* 2002). This makes sense in light of the microarray results, where 93% of the M010b genes were unresponsive to hypoxia compared to only 55% of the M006xLo genes, suggesting that the M010b cells attempt to maintain a constant ATP demand in the face of dwindling ATP supply, while the M006xLo cells reduce ATP demand by down-regulating gene expression to match ATP supply.

Most research on tumor cell adaptation to hypoxia focuses on HIF-1 and its downstream targets. And while HIF-1 activated pathways are undoubtedly an important component of hypoxia adaptation, evidence from our lab suggests that HIF-1 stabilization alone is not sufficient for hypoxia adaptation. Western blot analysis showed elevated levels of HIF-1 protein expression under hypoxic conditions in M010b cells, and yet this cell line is still not able to tolerate hypoxia (DeHaan *et al.,* 2004). In recent years, more attention has been focused on the importance of metabolic adaptation in tumor cell hypoxia adaptation. For example, a recent report from Guppy and colleagues (2005) suggested that MCF-7 breast cancer cells exhibited the classic hypoxia adaptive response of metabolic depression by decreasing their rate of protein synthesis in response to hypoxia. This response was not seen in non-transformed control cells (Guppy *et al.,* 2005).

Not only is the suppression of energy consuming pathways important to hypoxia adaptation, so is the promotion of more efficient energy production. The results of the microarray analysis provided a snapshot of the bioenergetic gene response to hypoxia in the hypoxia-tolerant and hypoxia-sensitive GBM cells lines. Interestingly, we did not

observe the same widespread upregulation of glycolytic genes in response to hypoxia that has been been reported elsewhere (Greijer *et al.,* 2005): only 3 of the 8 glycolytic genes on the microarray were significantly upregulated in any of the cell lines as a result of hypoxia. On the other hand, many of the genes involved in oxidative phosphorylation were shown to be upregulated in hypoxia (Figure 3-2.2.3). These results are consistent with other studies that examined hypoxia related gene changes in tumor tissue (Capuano *et al.,* 1997; Jung *et al.,* 2000).

The importance of oxidative phosphorylation to hypoxia adaptation has not been widely studied in either normal or cancer cells. The few available reports are often contradictory in their conclusions. For example, on the one hand, studies indicate that the oxidative capacity of muscles fibers from Sherpas living at high altitude is reduced compared with subjects living at low altitude (Hoppeler *et al.,* 2003). On the other hand, studies comparing the oxidative capacity in the muscles of athletes who train at high altitude for short periods with athletes who train at low altitude suggest that oxidative capacity is improved as a result of the high altitude training (Hoppeler *et al.,* 2003). Furthermore, many studies discount the importance of oxidative phosphorylation in tumor biology. Therefore, it is important to point out that studies in glioma cell lines show that when oxidative phosphorylation is blocked with rotenone, glycolysis alone is unable maintain intracellular [ATP] concentrations (Silver *et al.,* 1997).

We were particularly interested in studying the role of cytochrome *c* oxidase in cancer cell hypoxia adaptation as there is evidence to suggest that Cox may be responsive to changing oxygen availability. Using Hochachka's theory of hypoxia adaptation as a model, we postulated that the Cox activity of the hypoxia-tolerant GBM cell lines would

be different from the hypoxia-sensitive cell line, wherein the hypoxia-tolerant cell lines would be able to modify their Cox enzyme activity in response to changing oxygen availability as part of their adaptation strategy.

Under conditions of atmospheric air, the hypoxia-tolerant M006x and M006xLo cell lines had significantly lower Cox activity ($p<0.05$) than the hypoxia-sensitive M010b. Interestingly, HepG2, another cell line known to respond to hypoxia, also had significantly lower Cox activity. We thought that EcR293 might also show a similar pattern of Cox activity because it is derived from fetal embryonic kidney, a tissue that is tolerant of low oxygen conditions. However, extended *in vitro* culturing could have affected the EcR293 phenotype.

Interestingly, we were not able to detect a significant change in Cox activity in any of the cell lines in response to mild (0.6% O_2 for 12 hours) or severe (0.01% O_2 for 6 hours) hypoxia. There are many conflicting reports in the literature regarding the effect of hypoxia on the activity of Cox. Some reports suggest that Cox activity is reduced in response to hypoxia, while other reports indicate no change in Cox activity. The severity and duration of the hypoxic insult, as well as the type of cells and methodology used to determine Cox activity could all contribute to the variability of the results. For example, Schumacker and his colleagues (Budinger *et al.,* 1996) reported that the activity of cytochrome *c* oxidase from embryonic chick cardiac myocytes is reduced in response to hypoxia (3% O_2, for a few minutes). But, as they themselves point out, the pO_2 they termed hypoxia was still in the physiologically normal range for the tissue in question. Vijayasarathy *et al.* (2003) reported that the change in Cox activity in response to hypoxia (0.1% O_2 for 10 hours, followed by 6 hours of reoxygenation) varied depending

on the cell type. When the authors assayed the Cox activity of murine macrophage and adrenal pheochromocytoma cell lines they found that the macrophage Cox activity dropped by 52% compared to normoxic levels, while the adrenal pheochromocytoma Cox activity remained unchanged (Vijayasarathy *et al.,* 2003). Importantly, the authors chose to reoxygenate their cells for 6 hours after hypoxic exposure (Vijayasarathy *et al.,* 2003). Finally, a much earlier study using human tumor cell lines indicated that Cox activity did not change in response to hypoxia [2% O_2, for 96 hours (Simon *et al.,* 1981)]. To be confident that the M006x, M006xLo, and M010b Cox enzymes are truly unresponsive to hypoxia, the incubation timepoints should be extended. It will be important, however, to monitor the viability of the hypoxia-sensitive M010b cell line to avoid confounding effects from cell death. Finally, the brief reoxygenation of the cells in room air should be considered as a possible confounding effect since Chandel and co-workers (1996) have demonstrated that only five minutes of reoxygenation is enough to return Cox from a conformance state back to its native state.

Importantly, the Cox enzyme activity assay was performed using whole cell extracts. Emerging evidence indicates that Cox activity can be controlled by a second mechanism of respiratory control based on ATP or ADP binding to nuclear-encoded subunits. The ATP binding is regulated in part by signals originating in the cytoplasm, including cAMP dependent phosphorylation and Ca^{+}-activated dephosphorylation (Kadenbach, 2003). Such signals could potentially be lost if the Cox activity assay was performed on isolated mitochondria.

Our results suggest that the hypoxia-tolerant cell lines have intrinsically lower Cox activities compared to the hypoxia-sensitive cell line. This is reminiscent of the

"immediate adaptation" phenotype of several types of extremely hypoxia-tolerant organisms such as freshwater turtles and crucian carp, who are pre- or constitutively adapted to tolerate severe hypoxia (Bickler, 2004). According to the Hochachka model, having an intrinsically lower Cox activity would be beneficial to the cell because a coordinated suppression of ATP demand and supply pathways is required for the maintenance of cell viability.

While the Cox activity assay measures the rate of oxidization of cytochrome *c*, it would also be interesting to get a measure of the H^+/e^- ratio in order to more closely examine the efficiency of the proton pumping. Studies by Kadenbach and colleagues have demonstrated that the incorporation of the heart-specific isoform CoxVIa(H) into the holoenzyme decreases the H^+/e^- stoichiometry from 1.0 to 0.5 in the presence of increasing ATP/ADP; whereas holoenzymes that possess the CoxVIa(L) isoform maintain an H^+/e^- stoichiometry of 0.5, regardless of the ratio of ATP/ADP inside the mitochondrion (Kadenbach, 2003). It would be particularly interesting to study the catalytic efficiencies of the Cox enzymes among the different cell lines given that each cell line expresses different ratios of nuclear-encoded Cox subunits. It is not known how the CoxIV isoforms would affect the efficiency of proton pumping. In yeast, the homologous subunit V isoforms affect the efficiency of electron transfer within the holoenzyme. The incorporation of CoxVb results in more efficient electron transfer between heme a and the binuclear reaction center, and leads to 3-4 fold increase in the enzyme turnover rate. The presence of different isoforms within the different Cox isozymes of the hypoxia-tolerant and hypoxia-sensitive GBM cell lines could result in differences in enzyme efficiency, which are reflected by the H^+/e^- ratio.

As alluded to above, the microarray results indicated that each cell line had a unique pattern of nuclear-encoded Cox subunit expression in response to hypoxia. The changes in expression appeared to be subtle, and for the majority of the subunits, the change in expression was less than 2-fold. The biological significance of these changes in expression is not clear, since no statistically significant change in Cox enzyme activity was observed as a result of hypoxic incubation under similar conditions.

Q-RT-PCR was used to validate and expand upon the microarray results. The observation that CoxIV-2 was differentially expressed in hypoxia-tolerant and hypoxia-sensitive GBM cell lines generated much excitement. To our knowledge, this is the first study comparing the expression of nuclear-encoded Cox subunits in cancer cell lines. For many years, only one of the mammalian CoxIV subunits was identified in normal tissue, making it seem unlikely that the mammalian Cox could be responsive to changing oxygen availability in the same way as its yeast CoxV homolog. The recent discovery of the CoxIV-2 isoform in lung, heart, and brain tissue, however, has led to renewed interest in this possibility.

Although CoxIV-2 was detected in M006x in several independent Q-RT-PCR experiments, at 0.5% of the CoxIV-1 expression, CoxIV-2 isoform expression in M006x is extremely low. In fact, it seems that its expression is right at the limit of Q-RT-PCR detection, as we were not able to detect its presence in all of our experiments. Alternatively, the variation in M006x CoxIV-2 expression could be due to experimental stress. For example, the isolation of RNA from cells that have been incubated under hypoxic conditions in the aluminum canisters is performed one canister at a time to reduce the amount of time cells are exposed to atmospheric air. As a result, experimental

conditions are not identical for the cells between independent experiments. Such differences could potentially affect the expression of the CoxIV mRNA. The CoxIV-2 expression in M006xLo is much stronger (12.5% the expression of CoxIV-1). As a point of reference, it has been found that in the normal rat brain, CoxIV-2 expression is 4% of CoxIV-1 (Huttemann et al, 2001). The pattern of expression of CoxIV-2 in M006x and M006xLo is interesting because of the origins of these cell lines. M006xLo was derived from the same parental cell line as M006x, except that the M006xLo cells were derived to be adapted to hypoxic conditions: they were first grown as spheroids that were continuously exposed to 0.6% O_2 for thirteen days, before they were passaged through SCID mice and disaggregated to grow as monolayers in cell culture. Therefore, it is possible that increased CoxIV-2 expression could have been selected for during the creation of the M006xLo cell line, which would suggest that CoxIV-2 is beneficial for hypoxia-tolerance.

According to our results, the hypoxic conditions we used in our experiments (0.6% O_2 for 12 hours; 0.01% O_2 for 6 hours; 100 μM $CoCl_2$ for 12 hours) did not result in changes in the expression levels of the CoxIV isoforms in our cell lines. Our results suggest that the CoxIV isoforms in the GBM cell lines are not responsive to the changes in pO_2 at the transcriptional level in our experimental system. However, these are only preliminary results, and more work needs to be done before these results can be generalized. We chose our experimental time points for measuring changes in Cox subunit expression during hypoxic incubation based on the work done by Vijayasarathy and co-workers (2003). They determined that changes in the mRNA expression of nuclear encoded Cox subunits from murine cell lines occurred only after 10-12 hours of

incubation at a pO_2 of 0.1%. The hypoxic time points should be extended to ensure that sufficient time is allowed for a response to occur. Also, the pattern of CoxIV isoform expression should be examined in other cancer cell lines. It is note worthy to mention that CoxIV-2 was not found to be expressed in HepG2, a hypoxia-responsive hepatoma cell line.

We used transcription run-off assays to learn more about the regulation of CoxIV isoform expression among the different GBM cell lines. The run-off assays provide an indication of the rate of mRNA transcription for the genes of interest. These assays are technically demanding and require large amounts of radioactivity. Initially we had difficulty obtaining signal from even the more robustly expressed house-keeping genes, such as GAPDH and γ-actin. We decided to use HeLa S3 cells as a positive control, since we were following a protocol that had previously been shown to be successful with that cell line (Galloway *et al.*, 1999). We were able to get signal from the housekeeping genes, but not from the CoxIV isoforms. The CoxIV isoforms' mRNA is much less abundant than that of the housekeeping genes. For example, our Q-RT-PCR analysis indicated that it took, on average, 30 PCR cycles for the CoxIV-1 fluorescent signal to reach its threshold intensity, while it only took 17 PCR cycles for the endogenous control, 18S rRNA to reach the same fluorescent intensity. While there is limited information on mammalian CoxIV expression levels in the literature, a study evaluating the transcription rates for all yeast genes determined that the number of yeast subunit Va (homologous to CoxIV-1) transcripts per cell was 3.1 and the number of yeast subunit Vb (homologous to CoxIV-2) transcripts per cell was 1.3 (Garcia-Martinez *et al.*, 2004). The expression level of actin, on the other hand, was 21.1 copies per cell (Garcia-Martinez *et al.*, 2004).

The number of copies per cell was calculated by hybridizing labeled cDNA that had been reverse transcribed from yeast RNA to a macroarray that contained all of the yeast genes. The amount of signal was normalized to the total amount of poly(A) mRNA per cell. The low copy number of the CoxIV isoforms could be the reason we failed to detect them using transcription run-off analysis.

The next step after studying CoxIV mRNA expression must be to study the protein expression of the CoxIV isoforms. It will be necessary to develop an anti-CoxIV-2 antibody, as none are commercially available. It is imperative to perform these experiments because a recent report on the expression patterns of CoxIII and CoxIV-1 in the developing rat brain indicate that the levels of CoxIV protein and mRNA are not linearly related, suggesting a post-translational mode of regulation (Cannino *et al.,* 2004). In fact, it has been demonstrated that there is a protein in rat brain extracts that affects protein expression by binding specifically to the 3′ UTR region of CoxIV-1 RNA (Cannino *et al.,* 2004). The protein may play a role in positioning the CoxIV mRNA at the mitochondrial outer membrane to ensure that translation is coupled to mitochondrial import (Cannino *et al.,* 2004). It should be emphasized that non-transcriptional changes, in general, play an important role in hypoxia-induced gene expression. For example, in a study aimed at evaluating the contributions of mRNA transcription and mRNA translation to changes in gene expression induced by hypoxia, Koritzinsky *et al.* (2005) determined that CITED-2 (a negative regulator of HIF-1) had a 15-fold increase in translation and only a 5-fold increase in total mRNA.

The experiments that we performed with Cox led to a series of interesting observations regarding the differences in Cox activity and subunit expression between

hypoxia-tolerant and hypoxia-sensitive GBM cell lines. The next step is to begin to try to establish a correlation between decreased Cox activity, CoxIV isoform expression, and the ability to tolerate hypoxia. The first question that must be answered is: what is the functional significance of the CoxIV-2 subunit in terms of Cox activity? The best way to answer this question would be to knockdown the expression of CoxIV-2 in the hypoxia-tolerant M006x and M006xLo cell lines using RNA interference, and conversely to induce the expression of CoxIV-2 in the hypoxia-sensitive M010b cell line, and test for differences in Cox activity. Because the CoxIV subunit is vital for proper assembly of the holoenzyme, it is probably necessary to maintain the ubiquitously expressed CoxIV-1 at its physiological levels. Since the CoxIV isoforms are differentially expressed in tissues with different metabolic demands, it seems likely that the isoforms would contribute to different activity levels so that the enzyme could meet the metabolic needs of the given tissue. Of course, differences in CoxIV isoform expression are probably not the only factor affecting Cox activity. Multiple levels of regulation, including the coordinated expression of mitochondrial and nuclear Cox genes, mRNA stability, translational efficiency, mitochondrial importation, and the functioning of a myriad of assembly factors have an effect on the functioning of the mature holoenzyme. For example, patients with multiple mitochondrial disorder (MMD) have a 35% decrease in Cox activity that was attributed to reduced levels of protein translation, but not deficiencies in mRNA transcription or mitochondrial importation (Rungi *et al.,* 2002). Furthermore, we cannot assume that a subunit or isoform is necessarily incorporated into a functional holoenzyme just because it is expressed as a transcript. Mutations in assembly factors such as SURF1 and SCO1 result in the accumulation of non-functional

assembly intermediates (Stiburek *et al.*, 2005). Additional complexity arises from a recent discovery suggesting the existence of tissue-specific assembly proteins (Stiburek *et al.*, 2005).

An especially interesting question that needs to be addressed is: what is controlling the expression of the CoxIV isoforms? To date there is very limited information on the promoter region of CoxIV-2; in fact, the only transcription factor known to bind the CoxIV-2 gene is Sp1. There are almost certainly other elements that play a role in CoxIV-2 transcriptional regulation. In yeast, subunit Vb (homologous to mammalian CoxIV-2) expression is repressed by the Rox1p (*r*egulation by *ox*ygen) transcription factor, while subunit Va (homologous to mammalian CoxIV-1) expression is activated by the Hap2/3/4/5p transcription factor, in the presence of oxygen. Both Rox1p and Hap2/3/4/5p expression are regulated in part by heme and oxygen availability.

4-3 Neuroglobin

Although the precise function of Ngb is not known, the fact that its overexpression provides a neuro-protective effect in response to cerebral ischemia in rats (and conversely, its suppression causes increased neuronal cell death) suggests that Ngb protects cells against hypoxia. Ngb expression has been reported in the retina, brain, peripheral nervous system, endocrine system, and testis. Ngb expression has also been reported in both cultured neurons and astrocytes (Chen *et al.*, 2005). Our study is the first to examine Ngb expression in malignant glioma and neuroblastoma cell lines.

Preliminary results suggest that Ngb mRNA is expressed in at least two malignant glioma cell lines (M059K and U87). Hypoxic exposure resulted in a slight decrease in

Ngb expression; however, it is important to stress that these are very preliminary results, and the experiments have not yet been replicated. mRNA and protein expression analysis should be expanded to some of the other cell lines that showed ambiguous RT-PCR results. Future experiments should be performed to study the expression of Ngb in response to acute hypoxia. To exert a neuroprotective effect in response to hypoxia *in vivo* Ngb would have to respond almost immediately to prevent neuronal cell death. It would also be interesting to compare the level of Ngb expression between cultured astrocytes and malignant glioma cell lines.

Still, these results are intriguing: whether Ngb serves a similar role as Mb, whereby it facilitates the diffusion of O_2 and enhances its transport from the capillary to the mitochondria (Bentmann *et al.,* 2005), or whether it serves to neutralize reactive oxygen species and nitrogen species, such as NO (Brunori *et al.,* 2005), its presence in malignant glioma cells could provide another mechanism for the survival of the cells if they are challenged by hypoxia.

4-4 Conclusions

The mitochondria-cancer connection has long been under appreciated. In the last several years there has been a growing realization that mutations in the mtDNA genome, as in the nuclear genome, can affect tumorigenesis. Moreover, a shift in thinking has begun where experimental oncologists are starting to look at the metabolic mechanisms of vertebrate hypoxia tolerance, which were discovered by comparative physiologists, and apply those same mechanisms to tumor hypoxia tolerance. We are only at the beginning of this exciting new avenue of research, but it promises to shed new light on

our understanding of tumor development, and allow for the discovery of new therapeutic targets.

CHAPTER 5: BIBLIOGRAPHY

Acker, T. and Acker, H. (2004) Cellular oxygen sensing need in CNS function: physiological and pathological implications. The Journal of Experimental Biology, 207, 3171-3188.

Acker, T. and Plate, K.H. (2002) A role for hypoxia and hypoxia-inducible transcription factors in tumor physiology. Journal of Molecular Medicine, 80, 562-575.

Allalunis-Turner, M.J., Franko, A.J. and Parliament, M.B. (1999) Modulation of oxygen consumption rate and vascular endothelial growth factor mRNA expression in human malignant glioma cells by hypoxia. British Journal of Cancer, 80, 104-109.

Bachman, N.J., Riggs, P.K., Siddiqui, N., Makris, G.J., Womack, J.E. and Lomax, M.I. (1997) Structure of the human gene (Cox6A2) for the heart/muscle isoform of cytochrome *c* oxidase subunit VIa and its chromosomal location in humans, mice, and cattle. Genomics, 42, 146-151.

Bentmann, A., Schmidt, M., Reuss, S., Wolfrum, U., Hankeln, T. and Burmester, T. (2005) Divergent distribution in vascular and avascular mammalian retinae links neuroglobin to cellular respiration. Journal of Biological Chemistry, 280, 20660-20665.

Bickler, P.E. (2004) Clinical perspectives: neuroprotection lessons from hypoxia-tolerant organisms. Journal of Experimental Biology, 207, 3243-3249.

Biggin, A., Henke, R., Bennets, B., Thorburn, D.R. and Christodoulou, J. (2005)

Mutation screening of the mitochondrial genome using denaturing high-performance liquid chromatography. Molecular Genetics & Metabolism, 84, 61-74.

Bottaro, D.P. and Liotta, L.A. (2003) Out of air is not out of action. Nature, 423, 593-595.

Boutilier, R.G. and St-Pierre, J. (2000) Surviving hypoxia without really dying. Comparative Biochemistry and Physiology- Part A: Molecular & Integrative Physiology, 126, 481-490.

Brat, D.J. and Mapstone, T.B. (2003) Malignant glioma physiology: cellular response to hypoxia and its role in tumor progression. Annals of Internal Medicine, 138, 659-668.

Brown, J.M. (1999) The hypoxic cell: a target for selective cancer therapy- eighteenth Bruce F. Cain memorial award lecture. Cancer Research, 59, 5863-5870.

Brown, J.M. and Wilson, W.R. (2004) Exploiting tumor hypoxia in cancer treatment. Nature Reviews Cancer, 4, 437-447.

Brown, T. and Mackey, K. (1997) Analysis of RNA by Northern and Slot Blot Hybridization. John Wiley & Sons, Inc, Massachusetts.

Brunori, M., Giuffre, A., Nienhaus, K., Nienhaus, G.U., Scandurra, F.M. and Vallone, B. (2005) Neuroglobin, nitric oxide, and oxygen: functional pathways and conformational changes. Proc. Natl. Acad. Sci. USA, 102, 8483-8488.

Buck, L.T., Hochachka, P.W., Schon, E.A. and Gnaiger, E. (1993) Microcalorimetric measurment of reversible metabolic suppression induced by anoxia in isolated hepatocytes. American Journal of Physiology, 265, R1014-1019.

Budinger, G.R., Chandel, N.S., Shao, Z.H., Li, C.Q., Melmed, A., Becker, L.B. and Schumacker, P.T. (1996) Cellular energy utilization and supply during hypoxia in embryonic cardiac myocytes. American Journal of Physiology, 270, L44-53.

Burke, P.V. and Poyton, R.O. (1998) Structure/function of oxygen-regulated isoforms in cytochrome *c* oxidase. The Journal of Experimental Biology, 201, 1163-1175.

Burmester, T., Weich, B., Reinhardt, S. and Hankeln, T. (2000) A vertebrate globin expressed in the brain. Nature, 407, 520-523.

Bussink, J., Kaanders, J.H.A.M. and van der Kogel, A.J. (2003) Tumor hypoxia at the micro-regional level: clinical relevance and predictive value of exogenous and endogenous hypoxic cell markers. Radiotherapy and Oncology, 67, 3-15.

Cannino, G., Di Liegro, C.M., Di Liegro, I. and Rinaldi, A.M. (2004) Analysis of cytochrome *c* oxidase subunits III and IV expression in developing rat brain. Neuroscience, 128, 91-98.

Capuano, F., Guerrieri, F. and Papa, S. (1997) Oxidative phosphorylation enzymes in normal and neoplastic cell growth. Journal of Bioenergetics and Biomembranes, 29, 379-384.

Chandel, N.S., Budinger, G.R.S. and Schumacker, P.T. (1996) Molecular oxygen modulates cytochrome *c* oxidase function. The Journal of Biological Chemistry, 271, 18672-18677.

Chen, X.Q., Qin, L.Y., Zhang, C.G., Yang, L.T., Gao, Z., Liu, S., Lau, L.T., Fung, Y.W., Greenberg, D.A. and Yu, A.C. (2005) Presence of neuroglobin in cultured astrocytes. Glia, 50, 182-186.

Claxton, S. and Fruttiger, M. (2005) Oxygen modifies artery differentiation and network

morphogenesis in the retinal vasculature. Developmental Dynamics, 233, 822-828.

Conley, Y.P., Brockway, H., Beatty, M. and Kerr, M.E. (2003) Qualitative and quantitative detection of mitochondrial heteroplasmy in cerebrospinal fluid using denaturing high-performance liquid chromatography. Brain Reseach: Brain Research Protocols, 12, 99-103.

Copeland, W.C., Wachsman, J.T., Johnson, F.M. and Penta, J.S. (2002) Mitochondrial DNA alterations in cancer. Cancer Investigation, 20, 557-569.

Coutoure, M., Burmester, T., Hankeln, T. and Rousseau, D.L. (2001) The heme environment of mouse neuroglobin. Evidence for the presence of two conformations of the heme pocket. Journal of Biological Chemistry, 276, 36377-36382.

Cuezva, J.M., Krajewska, M., de Heredia, M.L., Krajewski, S., Santamaria, G., Kim, H., Zapata, J.M., Marusawa, H., Chamorro, M. and Reed, J.C. (2002) The bioenergetic signature of cancer: a marker of tumor progression. Cancer Research, 62, 6674-6681.

DeHaan, C., Habibi-Nazhad, B., Yan, E., Salloum, N., Parliament, M.B. and Allalunis-Turner, M.J. (2004) Mutation in mitochondrial complex I ND6 subunit is associated with defective response to hypoxia in human glioma cells. Molecular Cancer, 3, 19.

Erecinska, M. and Silver, I.A. (2001) Tissue oxygen tension and brain sensitivity to hypoxia. Respiration Physiology, 128, 263-276.

Evans, S.M., Judy, K.D., Dunphy, I., Jenkins, T., Hwang, W., Nelson, P.T., Lustig, R.A.,

Jenkins, K., Magarelli, D.P., Hahn, S.M., Collins, R.A., Grady, M.S. and Koch, C.J. (2004) Hypoxia is important in the biology and aggression of human glial brain tumors. Clinical Cancer Research, 10, 8177-8184.

Fabrizi, G.M., Sadlock, J., Hirano, M., Mita, S., Koga, Y., Rizzuto, R., Zeviani, M. and Schon, E.A. (1992) Differential expression of genes specifying two isoforms of subunit VIa of human cytochrome *c* oxidase. Gene, 119, 307-312.

Fernandez-Silva, P., Enriquez, J.A. and Montoya, J. (2003) Replication and transcription of mammalian mitochondrial DNA. Experimental Physiology, 88, 41-56.

Franko, A.J., Parliament, M.B., Allalunis-Turner, M.J. and Wolokoff, B.G. (1998) Variable presence of hypoxia in M006 human glioma spheroids and in spheroids and xenografts of clonally derived sublines. British Journal of Cancer, 78, 1261-1268.

Garcia-Martinez, J., Aranda, A. and Perez-Ortin, J.E. (2004) Genomic run-on evaluates transcription rates for all yeast genes and identifies gene regulatory mechanisms. Molecular Cell, 15, 303-313.

Geuens, E., Brouns, I., Flamez, D., Dewilde, S., Timmermans, J.P. and Moens, L. (2003) A globin in the nucleus! Journal of Biological Chemistry, 278, 30417-30420.

Graeber, T.G., Osmanian, C., Jacks, T., Housman, D.E., Koch, C.J., Lowe, S.W. and Giaccia, A.J. (1996) Hypoxia-mediated selection of cells with diminished apoptotic potential in solid tumors. Nature, 379, 88-91.

Graham, C.H., Postovit, L.M., Park, H., Canning, M.T. and Fitzpatrick, T.E. (2000) Adriana and Luisa Castellucci award lecture 1999: role of oxygen in the regulation of trophoblast gene expression and invasion. Placenta, 21, 443-450.

Greijer, A.E., van der Groep, P., Kemming, D., Shvarts, A., Semenza, G.L., Meijer, G.A., van de Wiel, M.A., Belien, J.A.M., van Diest, P.J., and van der Wall, E. (2005) Up-regulation of gene expression by hypoxia is mediated predominantly by hypoxia-inducible factor 1 (HIF-1). Journal of Pathology, 206, 291-304.

Grossman, L.I. and Lomax, M.I. (1997) Nuclear genes for cytochrome *c* oxidase. Biochimica et Biophysica Acta, 1352, 174-192.

Guppy, M., Brunner, S. and Buchanan, M. (2005) Metabolic depression: a response of cancer cells to hypoxia? Comparative Biochemistry and Physiology, Part B, 140, 233-239.

Guppy, M., Leedman, P., Zu, X.L. and Russell, V. (2002) Contribution by different fuels and metabolic pathways to the total ATP turnover of proliferating MCF-7 breast cancer cells. Biochemistry Journal, 364, 309-315.

Hamdane, D., Kiger, L., Dewilde, S., Green, B.N., Pesce, A., Uzan, J., Burmester, T., Hankeln, T., Bolognesi, M., Moens, L. and Marden, M.C. (2003) The redox state of the cell regulates the ligand binding affinity of human neuroglobin and cytoglobin. Journal of Biological Chemistry, 278, 51713-51721.

Han, C.B., Li, F., Zhao, Y.J., Ma, J.M., Wu, D.Y., Zhang, Y.K. and Xin, Y. (2003) Variations of mitochondrial D-loop region plus downstream gene 12S rRNA-tRNA(phe) and gastric carcinomas. World Journal of Gastroenterology, 9, 1925-1929.

Hermann, P.C., Gillespie, J.W., Charboneau, L., Bichsel, V.E., Paweletz, C.P., Calvert,

V.S., Kohn, E.C., Emmert-Buck, M.R., Liotta, L.A. and Petricoin, E.F. (2003) Mitochondrial proteome: altered cytochrome *c* oxidase subunit levels in prostate cancer. Proteomics, 3, 1801-1810.

Hochachka, P.W., Buck, L.T., Doll, C.J. and Land, S.C. (1996) Unifying theory of hypoxia tolerance: Molecular/metabolic defense and rescue mechanisms for surviving oxygen lack. Proc. Natl. Acad. Sci. USA, 93, 9493-9498.

Hockel, M., Schlenger, K., Mitze, M., Schaffer, U. and Vaupel, P. (1996) Hypoxia and radiation response in human tumors. Seminars in Radiation Oncology, 6, 3-9.

Hockel, M. and Vaupel, P. (2001) Tumor hypoxia: definitions and current clinical, biological, and molecular aspects. Journal of the National Cancer Institute, 93, 266-276.

Holland, E.C. (2001) Gliomagenesis: Genetic alterations and mouse models. Nature Reviews Genetics, 2, 120-129.

Hoppeler, H., Vogt, M., Weibel, E.R. and Fluck, M. (2003) Response of skeletal muscle mitochondria to hypoxia. Experimental Physiology, 88, 109-119.

Horikoshi, T., Danenberg, K.D., Stadlbauer, T.H., Volkenandt, M., Shea, L.C., Aigner, K., Gustavsson, B., Leichman, L., Frosing, R. and Ray, M. (1992) Quantitation of thymidylate synthase, dihydrofolate reductase, and DT-diaphorase gene expression in human tumors using the polymerase chain reaction. Cancer Research, 52, 108-116.

Huttemann, M., Kadenbach, B. and Grossman, L.I. (2001) Mammalian subunit IV isoforms of cytochrome *c* oxidase. Gene, 267, 111-123.

Huttemann, M., Muhlenbein, N., Schmidt, T.R., Grossman, L.I. and Kadenbach, B.

(2000) Isolation and sequence of the human cytochrome *c* oxidase subunit VIIaL gene. Biochimica et Biophysica Acta, 1492, 252-258.

Ichimura, K., Ohgaki, H., Kleihues, P. and Collins, V.P. (2004) Molecular pathogenesis of astrocytic tumours. Journal of Neuro-oncology, 70, 137-160.

Isidoro, A., Martinez, M., Fernandez, P.L., Ortega, A.D., Santamaria, G., Chamorro, M., Reed, J.C. and Cuezva, J.M. (2004) Alteration of the bioenergetic phenotype of mitochondria is a hallmark of breast, gastric, lung, and oesophageal cancer. Biochemistry Journal, 378, 17-20.

Jansen, M., de Witt Hamer, P.C., Witmer, A.N., Troost, D. and van Noorden, C.J.F. (2004) Current perspectives on antiangiogenesis strategies in the treatment of malignant gliomas. Brain Research Reviews, 45, 143-163.

Jung, M.H., Kim, S.C., Jeon, G.A., Kim, S.H., Kim, Y., Choi, K.S., Park, S.I., Joe, M.K. and Kimm, K. (2000) Identification of differentially expressed genes in normal and tumor human gastric tissue. Genomics, 69, 281-286.

Kadenbach, B. (2003) Intrinsic and extrinsic uncoupling of oxidative phosphorylation. Biochimica et Biophysica Acta, 1604, 77-94.

Kadenbach, B. and Arnold, S. (1999) A second mechanism of respiratory control. FEBS Letters, 447, 131-134.

Kadenbach, B., Huttemann, M., Arnold, S., Lee, I. and Bender, E. (2000) Mitochondrial energy metabolism is regulated via nuclear-coded subunits of cytochrome *c* oxidase. Free Radical Biology & Medicine, 29, 211-221.

Kato, T. (2001) The other, forgotten genome: mitochondrial DNA and mental disorders. Molecular Psychiatry, 6, 625-633.

Klein, B., Weirich, G. and Brauch, H. (2001) DHPLC-based germline mutation screening in the analysis of the VHL tumor suppressor gene: usefulness and limitations. Human Genetics, 108, 376-384.

Koch, C.J. (1984) A thin-film culturing technique allowing rapid gas-liquid equilibrium (6 sec) with no toxicity to mammalian cells. Radiation Research, 97, 434-442.

Koritzinsky, M., Seigneuric, R., Magagnin, M.G., Beucken, T.V., Lambin, P. and Wouters, B.G. (2005) They hypoxic proteome is influenced by gene-specific changes in mRNA translation. Radiotherapy and Oncology.

Kreig, R.C., Knuechel, R., Schiffmann, E., Liotta, L.A., Petricoin, E.F. and Hermann, P.C. (2004) Mitochondrial proteome: cancer-altered metabolism associated with cytochrome *c* oxidase subunit level variation. Proteomics, 4, 2789-2795.

Kwast, K.E., Burke, P.V., Staahl, B.T. and Poyton, R.O. (1999) Oxygen sensing in yeast: evidence for the involvement of the respiratory chain in regulating the transcription of a subset of hypoxic genes. Proc. Natl. Acad. Sci. USA, 96, 5446-5451.

Land, S.C. (2004) Hochachka's "Hypoxia Defense Strategies" and the development of the pathway for oxygen. Comparative Biochemistry and Physiology, Part B, 139, 415-433.

Lee, I., Bender, E. and Kadenbach, B. (2002) Control of mitochondrial membrane potential and ROS formation by reversible phosphorylation of cytochrome *c* oxidase. Molecular and Cellular Biochemistry, 234/235, 63-70.

Lenka, N., Vijayasarathy, C., Mullick, J. and Avadhani, N.G. (1998) Structural

organization and transcription regulation of nuclear genes encoding the mammalian cytochrome *c* oxidase complex. Progress in Nucleic Acid Research and Molecular Biology, 61, 309-344.

Leo, C., Giaccia, A.J. and Denko, N.C. (2004) The hypoxic tumor microenvironment and gene expression. Seminars in Radiation Oncology, 14, 207-214.

Lievre, A., Chapusot, C., Bouvier, A.M., Zinzindohoue, F., Piard, F., Roignot, P., Arnould, L., Beaune, P., Faivre, J. and Laurent-Puig, P. (2005) Clinical value of mitochondrial mutations in colorectal cancer. Journal of Clinical Oncology, 23, 3517-3525.

Liu, M.R., Pan, K.F., Li, Z.F., Wang, Y., Deng, D.J., Zhang, L. and Lu, Y.Y. (2002) Rapid screening mitochondrial DNA mutation by using denaturing high-performance liquid chromatography. World Journal of Gastroenterology, 8, 426-430.

Ludwig, B., Bender, E., Arnold, S., Huttemann, M., Lee, I. and Kadenbach, B. (2001) Cytochrome *c* oxidase and the regulation of oxidative phosphorylation. Chembiochem, 2, 392-403.

Meierhofer, D., Mayr, J.A., Ebner, S., Sperl, W. and Kofler, B. (2005) Rapid screening of the entire mitochondrial DNA for low-level heteroplasmic mutations. Mitochondrion, 5, 282-296.

Michiels, C. (2004) Physiological and pathological responses to hypoxia. American Journal of Pathology, 164, 1875-1882.

Miyazaki, T., Neff, L., Tanaka, S., Horne, W.C., Baron, R. (2003) Regulation of cytochrome *c* oxidase activity by c-Src in osteoclasts. Journal of Cell Biology, 160, 709-718.

Nijtmans, L.G.J., Taanman, J.-W., Muijsers, A.O., Speijer, D. and van den Bogert, C. (1998) Assembly of cytochrome *c* oxidase in cultured cells. European Journal of Biochemistry, 254, 389-394.

Papandreou, I., Powell, A., Lim, A.L. and Denko, N.C. (2005) Cellular reaction to hypoxia: sensing and responding to an adverse environment. Mutation Research, 569, 87-100.

Parliament, M.B., Franko, A.J., Allalunis-Turner, M.J., Mielke, B.W., Santos, C.L., Wolokoff, B.G. and Mercer, J.R. (1997) Anomalous patterns of nitroimidazole binding adjacent to necrosis in human glioma xenografts: possible role of decreased oxygen consumption. British Journal of Cancer, 75, 311-318.

Parsons, W.J., Williams, R.S., Shelton, J.M., Luo, Y., Kessler, D.J. and Richardson, J.A. (1996) Developmental regulation of cytochrome oxidase subunit VIa isoforms in cardiac and skeletal muscle. American Journal of Physiology, 270, H567-H574.

Pennacchietti, S., Michieli, P., Galluzzo, M., Mazzone, M., Giordano, S. and Comoglio, P.M. (2003) Hypoxia promotes invasive growth by transcriptional activation of the met proto-oncogene. Cancer Cell, 3, 347-361.

Pesce, A., Bolognesi, M., Bocedi, A., Ascenzi, P., Dewilde, S., Moens, L., Hankeln, T. and Burmester, T. (2002) Neuroglobin and cytoglobin. Fresh blood for the vertebrate globin family. EMBO Reports, 3, 1146-1151.

Pesce, A., Dewilde, S., Nardini, M., Moens, L., Ascenzi, P., Hankeln, T., Burmester, T.

and Bolognesi, M. (2003) Human brain neuroglobin structure reveals a distinct mode of controlling oxygen affinity. Structure, 11, 1087-1095.

Pesce, A., Dewilde, S., Nardini, M., Moens, L., Ascenzi, P., Hankeln, T., Burmester, T. and Bolognesi, M. (2004) The human brain hexacoordinated neuroglobin three-dimensional structure. Micron, 35, 63-65.

Pesole, G., Gissi, C., De Chirico, A. and Saccone, C. (1999) Nucleotide substitution rate of mammalian mitochondrial genomes. Journal of Molecular Evolution, 48, 427-434.

Petros, J.A., Baumann, A.K., Ruiz-Pesini, E., Amin, M.B., Sun, C.Q., Hall, J., Lim, S., Issa, M.M., Flanders, W.D., Hosseini, S.H., Marshall, F.F. and Wallace, D.C. (2005) mtDNA mutations increase tumorigenicity in prostate cancer. Proc. Natl. Acad. Sci. USA, 102, 719-724.

Poyton, R.O. (1999) Models for oxygen sensing in yeast: implications for oxygen-regulated gene expression in higher eukaryotes. Respiration Physiology, 115, 119-133.

Raghunand, N., Gatenby, R.A. and Gillies, R.J. (2003) Microenvironmental and cellular consequences of altered blood flow in tumours. The British Journal of Radiology, 76, S11-S22.

Ratcliffe, P.J., Pugh, C.W. and Maxwell, P.H. (2000) Targeting tumors through the HIF system. Nature Medicine, 6, 1315-1316.

Reynolds, T.Y., Rockwell, S. and Glazer, P.M. (1996) Genetic instability induced by the tumor microenvironment. Cancer Research, 56, 5754-5757.

Rice, G.C., Hoy, C. and Schimke, R.T. (1986) Transient hypoxia enhances the frequency

of dihydrofolate reductase gene amplification in Chinese hamster ovary cells. Proc. Natl. Acad. Sci. USA, 83, 5978-5982.

Rofstad, E.K., Mathiesen, B., Henriksen, K., Kindem, K. and Galappathi, K. (2005) The tumor bed effect: Increased metastatic dissemination from hypoxia-induced up-regulation of metastasis-promoting gene products. Cancer Research, 65, 2387-2396.

Rungi, A.A., Primeau, A., Nunes Christie, L., Gordon, J.W., Robinson, B.H. and Hood, D.A. (2002) Events upstream of mitochondrial protein import limit the oxidative capacity of fibroblasts in multiple mitochondrial disease. Biochimica et Biophysica Acta, 1586, 146-154.

Scarpulla, R.C. (1997) Nuclear control of respiratory chain expression in mammalian cells. Journal of Bioenergetics and Biomembranes, 29, 109-119.

Schmidt, M., Giessl, A., Laufs, T., Hankeln, T., Wolfrum, U. and Burmester, T. (2003) How does the eye breathe? Evidence for neuroglobin-mediated oxygen supply in the mammalian retina. Journal of Biological Chemistry, 278, 1932-1935.

Schulte, P.M. (2004) Changes in gene expression as biochemical adaptations to environmental change: a tribute to Peter Hochachka. Comparative Biochemistry and Physiology, Part B, 139, 519-529.

Shannon, A.M., Bouchier-Hayes, D.J., Condron, C.M. and Toomey, D. (2003) Tumor hypoxia, chemotherapeutic resistance and hypoxia-related therapies. Cancer Treatment Reviews, 29, 297-307.

Siemann, D.W. (1998) The tumor microenvironment: a double-edged sword. International Journal of Radiation Oncology, Biology, Physics, 42, 697-699.

Silver, I.A. and Erecinska, M. (1997) Energetic demands of the Na+/K+ ATPase in mammalian astrocytes. Glia, 21, 35-45.

Simon, L.M., Robin, E.D. and Theodore, J. (1981) Differences in oxygen-dependent regulation of enzymes between tumor and normal cell systems in culture. Journal of Cell Physiology, 108, 393-400.

Simonnet, H., Alazard, N., Pfeiffer, K., Gallou, C., Beroud, C., Demont, J., Bouvier, R., Schagger, H. and Godinot, C. (2002) Low mitochondrial respiratory chain content correlates with tumor aggressiveness in renal cell carcinoma. Carcinogenesis, 23, 759-768.

Sonoda, Y., Kanamori, M., Deen, D.F., Cheng, S., Berger, M.S. and Pieper, R.O. (2003) Overexpression of vascular endothelial growth factor isoforms drives oxygenation and growth but not progression to glioblastoma multiforme in a human model of gliomagenesis. Cancer Research, 63, 1962-1968.

Stiburek, L., Vesela, K., Hansikova, H., Pecina, P., Tesarova, M., Cerna, L., Houstek, J. and Zeman, J. (2005) Tissue-specific cytochrome *c* oxidase assembly defects due to mutations in *SCO2* and *SURF1*. Biochemical Journal.

St-Pierre, J., Brand, M.D. and Boutilier, R.G. (2000) The effect of metabolic depression on proton leak rate in mitochondria from hibernating frogs. Journal of Experimental Biology, 203, 1469-1476.

Suarez, R.K., Doll, C.J., Buie, A.E., West, T.G., Funk, G.D. and Hochachka, P.W. (1989) Turtles and rats: a biochemical comparison of anoxia-tolerant and anoxia-sensitive brains. American Journal of Physiology, 257, 1083-1088.

Subarsky, P. and Hill, R.P. (2003) The hypoxic tumor microenvironment and metastatic

progression. Clinical and Experimental Metastasis, 20, 237-250.

Sun, Y., Jin, K., Mao, X.O., Zhu, Y. and Greenberg, D.A. (2001) Neuroglobin is up-regulated by and protects neurons from hypoxic-ischemic injury. Proc. Natl. Acad. Sci. USA, 98, 15306-15311.

Sun, Y., Jin, K., Peel, A., Mao, X.O., Xie, L. and Greenberg, D.A. (2003) Neuroglobin protects the brain from experimental stroke in vivo. Proc. Natl. Acad. Sci. USA, 100, 3497-3500.

Swinnen, J.V., Beckers, A., Brusselmans, K., Organe, S., Segers, J., Timmermans, L., Vanderhoydone, F., Deboel, L., Derua, R., Waelkens, E., de Schrijver, E., van de Sande, T., Noel, A., Foufelle, F. and Verhoeven, G. (2005) Mimicry of a cellular low energy status blocks tumor cell anabolism and suppresses the malignant phenotype. Cancer Research, 65, 2441-2448.

Taanman, J-W., Capaldi, R.A. (1992) Purification of yeast cytochrome *c* oxidase with a subunit composition resembling the mammalian enzyme. Journal of Biological Chemistry, 267, 22481-22485.

Takano, S., Yoshii, Y., Kondo, S., Suzuki, H., Maruno, T., Shirai, S. and Nose, T. (1996) Concentration of vascular endothelial growth factor in the serum and tumor tissue of brain tumor patients. Cancer Research, 56, 2185-2190.

Tan, E.K., Khajavi, M., Thornby, J.I., Nagamitsu, S., Jankovic, J. and Ashizawa, T. (2000) Variability and validity of polymorphism association studies in Parkinson's disease. Neurology, 55, 533-538.

Thames, E.L., Newton, D.A., Black, S.A. and Bowman, L.H. (2000) Role of mRNA

stability and translation in the expression of cytochrome *c* oxidase during mouse myoblast differentiation: instability of the mRNA for the liver isoform of subunit VIa. Biochemistry Journal, 351, 133-142.

Turcotte, M.L., Parliament, M.B., Franko, A.J. and Allalunis-Turner, M.J. (2002) Variation in mitochondrial function in hypoxia-sensitive and hypoxia-tolerant human glioma cells. British Journal of Cancer, 86, 619-624.

Urtasun, R.C., Parliament, M.B., McEwan, A.J., Mercer, J.R., Mannan, R.H., Wiebe, L.I., Morin, C. and Chapman, J.D. (1996) Measurement of hypoxia in human tumours by non-invasive spect imaging of iodoazomycin arabinoside. British Journal of Cancer Supplement, 27, S209-212.

van Den Bosch, B.J., de Coo, R.F., Scholte, H.R., Nijland, J.G., van Den Bogaard, R., de Visser, M., de Die-Smulders, C.E. and Smeets, H.J. (2000) Mutation analysis of the entire mitochondrial genome using denaturing high performance liquid chromatography. Nucleic Acids Research, 28, E89.

Vaupel, P. and Harrison, L. (2004) Tumor hypoxia: causative factors, compensatory mechanisms, and cellular response. The Oncologist, 9, 4-9.

Vaupel, P., Kallinowski, F. and Okunieff, P. (1989) Blood flow, oxygen and nutrient supply, and metabolic microenvironment of human tumors: a review. Cancer Research, 49, 6449-6465.

Vijayasarathy, C., Biunno, I., Lenka, N., Yang, M., Basu, A., Hall, I.P. and Avadhani, N.G. (1998) Variations in the subunit content and catalytic activity of the cytochrome *c* oxidase complex from different tissues and different cardiac compartments. Biochimica et Biophysica Acta, 1371, 71-82.

Vijayasarathy, C., Damle, S., Prabu, S.K., Otto, C.M. and Avadhani, N.G. (2003) Adaptive changes in the expression of nuclear and mitochondrial encoded subunits of cytochrome *c* oxidase and the catalytic activity during hypoxia. European Journal of Biochemistry, 270, 871-879.

Villani, G. and Attardi, G. (2000) In vivo control of respiration by cytochrome *c* oxidase in human cells. Free Radical Biology & Medicine, 29, 202-210.

Warburg, G. (1956) On the origin of cancer cells. Science, 123, 309-314.

Waterland, R.A., Basu, A., Chance, B. and Poyton, R.O. (1991) The isoforms of yeast cytochrome *c* oxidase subunit V alter the in vivo kinetic properties of the holoenzyme. The Journal of Biological Chemistry, 266, 4180-4186.

Webb, T. (2005) Vascular normalization: study examines how antiangiogenesis therapies work. Journal of the National Cancer Institute, 97, 336-337.

Wolz, W., Kress, W. and Mueller, C.R. (1997) Genomic sequence and organization of the human gene for cytochrome *c* oxidase subunit (*COX7A1*)VIIa-M. Genomics, 45, 438-442.

Yu, M., Jaradat, S.A. and Grossman, L.I. (2002) Genomic organization and promoter regulation of human cytochrome *c* oxidase subunit VII heart/muscle isoform (*COX7AH*). Biochimica et Biophysica Acta, 1574, 345-353.

Zhang, C., Wang, C., Deng, M., Li, L., Wang, H., Fan, M., Xu, W., Meng, F., Qian, L. and He, F. (2002) Full-length cDNA cloning of human neuroglobin and tissue expression of rat neuroglobin. Biochemical and Biophysical Research Communications, 290, 1411-1419.

Zu, X.L. and Guppy, M. (2004) Cancer metabolism: facts, fantasy, and fiction.

Biochemical and Biophysical Research Communications, 299, 676-680.